INVESTIGATING THE BIOLOGICAL ROLE OF SIALIDASE NEU4 AND GALNAC-T ENZYMES IN A MOUSE MODEL OF TAY-SACHS DISEASE

A Thesis Submitted to
the Graduate School of Engineering and Sciences of
İzmir Institute of Technology
in Partial Fulfillment of the Requirements for the Degree of

MASTER OF SCIENCE

in Molecular Biology and Genetics

by
Edanur ATEŞ

November 2016
İZMİR

We approve the thesis of **Edanur ATEŞ**

Examining Committee Members

Prof.Dr.Volkan SEYRANTEPE
Department of Molecular Biology and Genetics, İzmir Institute of Technology

Assist.Prof.Dr.Çiğdem TOSUN
Department of Molecular Biology and Genetics, İzmir Institute of Technology

Assoc.Prof.Dr.Michelle M. ADAMS
Department of Psychology, Bilkent University

10 November 2016

Prof.Dr.Volkan SEYRANTEPE
Supervisor, Department of Molecular Biology and Genetics,
İzmir Institute of Technology

Prof. Dr.Volkan SEYRANTEPE
Head of Department of Molecular
Biology and Genetics

Prof. Dr. Bilge KARAÇALI
Dean of Garduate School of
Engineering and Sciences

ACKNOWLEDGMENTS

I would first like to thank my supervisor Prof. Dr. Volkan SEYRANTEPE, who expertly guided me through my master's education and who continuously conveyed the excitement and enthusiasm of carrying out research. His encouragement, understanding, patience, guidance and support immense knowledge helped me throughout my studies and my thesis writing.

I am thankful to Intensified Cooperation (IntenC) of German-Turkish Bilateral Agreement and TUBITAK (113T025) for financial support for this project and for my scholarship.

I would like to thank to Assoc. Prof. Dr. Michelle M. Adams and Assist. Prof. Dr. Çiğdem Tosun for being my committee members and for their suggestions valuable and contributions.

I am also grateful to my co-workers, Zehra K. Timur, Seçil Akyıldız Demir and Osman Yipkin Çalhan for their support and help during my thesis project. I would like to my special thanks to my co-worker Bora Taştan for his extra interest and help during behavioral experiments. I am also thankful to undergraduate members of Seyrantepe's Lab for their help and assistance during studies. Thanks to Özgür Okuş for his meticulous and disciplined work in the maintenance of my mice colonies.

My deepest gratitude belongs to my dearest family. I am grateful to my family, my lovely mother Fahriye Ateş, my father Barik Ateş and my little brother Kemal Furkan Ateş for their infinite love, motivation, belief, encouragement and support throughout my life. Without their support, I won't be able to here.

Lastly, I would like to express my special thanks to my love Yasin Öz, for his unfailing understanding, motivation, support and unending love.

ABSTRACT

INVESTIGATING THE BIOLOGICAL ROLE OF SIALIDASE NEU4 AND GALNAC-T ENZYMES IN A MOUSE MODEL OF TAY-SACHS DISEASE

Tay-Sachs disease is a lysosomal storage disorder that is caused by a mutation in the HexA gene coding for the alpha subunit of lysosomal B-hexosaminidase A. HexA is responsible for the removal of N-acetylglucosamine residue form GM2 ganglioside to convert it into GM3 in the ganglioside degradation pathway. Deficiency of HexA causes neuronal death with progressive neurological degeneration. Neu4 is a sialidese and found in lysosomes. Knock-out mice model of $Neu4^{-/-}$ show different ganglioside pattern than wild type mice and there is increased GD1a and decreased GM1 in brains of mice (Seyrantepe et al. 2008). As previously shown, Neu4 is a modifier gene of HexA. On a previous work (Seyrantepe et al. 2010) $Neu4^{-/-}HexA^{-/-}$ double deficient mouse showed more severe phenotype than $HexA^{-/-}$ deficiency alone. β1,4-N-acetylgalactosaminyltransferase; (Galgt1) is one of the key enzymes in the synthesis of complex gangliosides and it work in reverse direction of HexA. In the deficiency of Galgt1, there is only production of simple gangliosides occurs. Absence of complex gangliosides causes neurological degeneration. Mouse model of $Neu4^{-/-}HexA^{-/-}Galgt1^{-/-}$ was generated as a model of substrate deprivation therapy. That mouse has defects in both ganglioside synthesis and degradation mechanisms, so neither synthesis nor degradation of complex gangliosides will occur. By this mean, effects of Tay-Sachs disease were decreased. On previously shown Neu4 has role in the metabolism of GD1a into GM1. With this study, it was speculated that sialidase Neu4 may play a role in the metabolism of simple gangliosides.

Key Words: Lysosome, Sialidase, Mouse, Tay-Sachs

ÖZET

TAY-SACHS HASTALIĞI FARE MODELİNDE SIALIDAZ NEU4 VE GalNAC-T ENZİMLERİNİN BİYOLOJİK ROLÜNÜN ARAŞTIRILMASI

Bir lizozomal depo hastalığı olan Tay-Sachs hastalığı β-Hekzosaminidaz A enziminin α alt ünitesini kodlayan HEXA genindeki mutasyondan kaynaklanmaktadır. HexA, N-asetilglukozamin kalıntısını uzaklaştırarak GM2 ganglisitinin GM3'e dönüştürülmesinde görevlidir. HexA geninin eksikliği nöronal ölümlerle birlikte ilerleyen nörolojik dejenerasyona sebep olmaktadır. Sialidaz Neu4 lizozomlarda bulunur. Neu4 faresinin knock-out modeli control faresinden farklı bir ganglioisit modeli göstermektedir ve bu farelerin beyinlerinde GD1a ganglisit miktarı artarken GM1 miktarı azalmaktadır. Daha önce Neu4'ün HexA'nın bir tamamlayıcı geni olduğu gösterilmiştir. Daha önceki çalışmada $Neu4^{-/-}HexA^{-/-}$ ikili eksikliği bulunan farelerde GM2 birikiminin sebep olduğu nörolojik bozulmanın yalnızca HexA eksikliği bulunan farelerden daha fazla olduğu görülmüştür. B-1,4-N-asetilgalaktozaminiltransferaz (Galgt1) kompleks gangliositlerin sentezinde rol alan önemli bir enzimdir ve bu enzim HexA ile zıt yönde çalışmaktadır. Galgt1 eksikliğinde yalnızca basit ganliositler üretilmektedir. Kompleks gangliositlerin eksikliği nörolojik dejenerasyona sebep olmaktadır. $Neu4^{-/-}HexA^{-/-}Galgt1^{-/-}$ üçlü enzim eksikliği taşıyan fare ortam eksikliği terapisinin bir modeli olarak yaratılmıştır. Bu farede gangliosit yapım ve yıkım mekanizmalarından ikisi de hatalı olduğundan ganglioist üretimi ya da birikimi olmamaktadır. Bu yolla Tay-Sachs hastalığının etkileri azaltılmaktadır. Daha once Neu4 geninin GD1a gangliositini GM1'e çevirdiği gösterilmiştir. Bu çalışma ile Neu4'un bundan farklı olarak basit ganglioistlerinde yıkımında bir görevi daha olabileceği anlaşılmıştır.

Anahtar Kelimeler: Lizozom, Sialidaz, Fare, Tay-Sachs

To my precious family...

TABLE OF CONTENTS

LIST OF FIGURES

.

LIST OF TABLES

CHAPTER 1

INTRODUCTION

1.1.Glycolipids

Glycolipids contain one or more carbohydrate residues linked to a hydrophobic lipid moiety by glycosidic linkage (Yu et al. 2011). Glycolipids are mostly found in the extracellular part of the cell membrane and they have many functions including; recognition, cell differentiation, and signaling (Schengrund 2015). Other than those functions, glycolipids act as receptors to modulate function of membrane proteins. Glycolipids are primarily synthesized in cytoplasmic leaflet of the Endoplasmic Reticulum (ER) and transferred to Golgi apparatus. In Golgi apparatus, sequential addition of monosaccharides to ceramide backbone occurs (Jeyakumar et al. 2002). Degradation of these glycolipids occur in endosomes and lysosomes by removing monosaccharide residues (Kolter 2012).

1.2.Sphingolipids

Sphingolipids are a class of lipids that contain eighteen carbon amino-alcohol backbones. Sphingolipids are synthesized in ER and they are in the form of nonsphingolipids. They play role in membrane biology and regulate cell function. Sphingolipids are composed of three components: the sphingoid base, head group and a fatty acid (Lahiri and Futerman 2007). Sphingolipids are found in three structures: ceramide, sphingomyelin and glycosphingolipids. Their complexity is achieved by the sphingosine backbone and position and different combinations of bounded groups (Gault, Obeid, and Hannun 2010). Sphingolipids anchor lipid-bound carbohydrates to external layer of cell membrane and provide water permeability to skin (Kolter, Proia, and Sandhoff 2002).

1.2.1 Glycosphingolipids

Glycosphingolipids (GSLs) are glycolipids and they are found in the structure a sphingoid base and attached one or more sugar residues on it (Kolter 2012). GLSs are in a common structure that ceramide backbone is linked to either glucose or galactose. The ceramide moiety is embedded into the outer part of the plasma membrane and carbohydrate part faces the cell surface. Glucosylceramide (GlcCer) containing GSLs are mostly found throughout the body and Galactosylceramide (GalCer) derived GSLs takes role in the central nervous system that formation and stabilization of myelin (Jeyakumar et al. 2002). GSLs are found in cell membrane as clusters of "lipid rafts". They function as receptors, cell-cell recognition and protection from toxins (Schnaar, Suzuki, and Stanley 2009).

GSLs are in a heterogeneous structure and they diversify depending on their glycan part composition, ceramide part and lipid moieties. Fatty acids are found in ceramide part of the GSLs are mostly saturated and they have high melting point (Kolter 2012).

There are different ways to classify and name GSLs. Based on the carbohydrate structure glycosphingolipds are classified into series, that are; ganglio-, isoganglio-, lacto-, neolacto-, lactoganglio-, globo-, isoglobo-, muco-, gala-, and so on (Yu et al. 2011). GSLs can be subclassified as neutral (no charged sugars or sialic acid), sialylated (one or more sialic acid residue) or sulfated. Ceramide, glucosylceramide, galactosylceramide, galactocerebroside, lactosylceramide and globotriaosylceramide (Zhang and Kiechle 2004), cholesterol and sphingomyelin (Róg and Vattulainen 2014) are neutral gangliosides. Gangliosides, phosphatidylserine, phosphatidylinositol and sulfatides are sialylated gangliosides (Lloyd and Furukawa 1998). Sialylated GSLs are known as "gangliosides" (Schnaar, Suzuki, and Stanley 2009).

Table 1.1. Glycosphingolipid series with core structure (Kolter 2012)

Series	**Core structure**
Artho-	GlcNAcβ1,3Manβ1,4Glcβ1,1'Cer
Gala-	Galα1,4Galβ1,1'Cer
Neogala-	Galβ1,6Galβ1,6Galβ1,1'Cer
Ganglio-	Galβ1,3GalNAcβ1,4Galβ1,4Glcβ1,1'Cer
Globo-	GalNAcβ1,3Galα1,4Galβ1,4Glcβ1,1'Cer
Isoglobo-	GalNAcβ1,3Galα1,3Galβ1,4Glcβ1,1'Cer
Lacto-	Galβ1,3GalNAcβ1,3Galβ1,4Glcβ1,1'Cer
Neolacto-	Galβ1,4GalNAcβ1,3Galβ1,4Glcβ1,1'Cer
Muco-	Galβ1,3Galβ1,4Galβ1,4Glcβ1,1'Cer
Mollu-	Fucα,4GlcNAcβ1,2Manα1,3Manβ1,4Glcβ1,1'Cer
Schisto-	GalNAcβ1,4Glcβ1,1'Cer
Spirometo-	Galβ1,4Glcβ1,3Galβ1, 1'Cer

1.2.1.2.1. Gangliosides

Gangliosides are sialic acid containing glycosphingolipids and they constitute a significant part of the cell surface of neuron cells. Most gangliosides found in mammals are members of the ganglio-, gala-, lacto- and neolacto- series (Kolter 2012). Gangliosides can contain one or more sialic acid (N-acetlyneuraminic acid or N-glycolyneuraminic acid) residues in the carbohydrate moieties in mammals (Yu et al. 2011). Gangliosides are mostly found in brain and compose of about 10%-12% of total brain lipids. In the grey matter of the brain, concentration of gangliosides are about 5-fold higher than white matter. Gangliosides can affect neuronal function by modulating signaling events and its amount is correlated with neurogenesis, synaptogenesis and cell proliferation ((Kolter 2012), (Schengrund 2015)). Ganglioside composition in the brain is not stable. They can be affected from physiological and pathophysiological conditions such as oncogenesis, tumor formation, cell growth or lactation. On the other hand, the ganglioside content and the composition of brain also changes with aging. In

earlier ages the amount of lipid-bound sialic acid amount is higher and it decreases in older ages (Kolter 2012).

During brain development, gangliosides are expressed at different levels and they take role in brain function. Individual gangliosides and complex of gangliosides are important for the continuity of life. During post-natal period of embryogenesis GM3, GD3 and 9-O-acetyl GD3 are highly expressed in brain. On the other hand, in adult brains GM1, GD1a, GD1b, and GT1b become predominant (Lahiri and Futerman 2007).

Even though most of the gangliosides are found in the brain; they can also be found in other regions of the body. Gangliosides are found in serum; especially GM3, GD3, GD1a, GM2 GT1b, GD1b and GQ1b. Those gangliosides transport via serum lipoproteins; LDL and HDL to target tissue and/or organ (Senn et al. 1989). Gangliosides are also found in bone marrow, erythrocytes, intestine, liver, spleen, kidney, and testis. In each of those organs the intensity and amount of gangliosides show different pattern.

In the cellular level, gangliosides are mostly found in the plasma membrane. Also, those gangliosides are found in mitochondria and nuclear membranes. In the mitochondria, gangliosides regulate apoptosis (Kolter 2012). Endoplasmic reticulum and nucleus have continuous Ca^{2+} pumping between nuclear envelope and cytoplasm. In the nucleus GM1 and GD1a gangliosides take role in Ca^{2+} homeostasis (Ledeen and Wu 2011).

Gangliosides in the body have several functions and are related to several diseases. GSLs take role in apoptosis, endocytosis, cell proliferation, intracellular transport, cell migration and senescence and inflammation. Differences in GSL expression and alterations are related to tumor formation in cancer cells. Gangliosides GT1b, GD1a, GM3 and GM1 inhibit cell proliferation and epidermal growth factor receptor tyrosine kinase phosphorylation. Other GSLs globoside GB4 and Gb5 enhance cell proliferation and motility. Again, ganglioside GD2 enhances tumor growth and ganglioside GD3 enhances invasiveness of malignant melanoma by modulating Src kinase and focal adhesion kinase activity. Also there is a relationship between gangliosides and other cancer types such as osteocarcinoma, lung and breast cancers (D'Angelo et al. 2013).

Gangliosides function as viral receptors on cell membranes. Binding of pathogens and toxins to human cells occur by the interaction of cell surface GSLs. One

of the infectious dieses, influenza A viruses recognize sialic acid residues of gangliosides on cell surfaces as receptor to invade host cells (Yu et al. 2011). Also different components of HIV interact with cell surface GSLs and invasion of HIV components occur (Lahiri and Futerman 2007).

Alzheimer's disease (AD) is a cognitive neurodegenerative disease and is caused by the aggregation of β-amyloid peptides in the brain. Recently, it was found that ganglioside GM1 bound β-amyloid plaques in the brains of Alzheimer's disease patients and GM1 to be considered as critical in the AD pathology (Manna, Róg, and Vattulainen 2014). Also it is found that other gangliosides GD1b and GT1b may be related with AD. In the learning and memory center of the brain, hippocampal grey matter, amounts of GD1b and GT1b show reduction when compared with controls (Schengrund 2015).

Huntington's disease (HD) is an autosomal dominant disorder that is caused by the trinucleotide repeat in huntingtin gene. People with HD show problems coordination in muscles and mental decline. Experiments with HD transgenic mice show decreased amounts of GM1 and GD1a in the cortex. In the cortex of HD mice expression of GM1/GD1b synthase gene is down regulated. With addition of GM1 ganglioside to HD cell line shows restoration in ganglioside levels and reducing toxicity of trinucleotide repeat increases cell survival. It shows that in HD, GM1 can be a therapeutic (Schengrund 2015).

1.2.1.2.1.1. Biosynthesis of Gangliosides

Ganglioside synthesis starts in the Endoplasmic reticulum by the condensation of L-serine with the coenzyme-A activated fatty acid to form ceramide. Later, ceramide backbone transported to cytoplasmic face of the Golgi apparatus by the transfer protein CERT (Hanada et al. 2003). Then GSL synthesis continues by serial addition of monosaccharide units on ceramide backbone by glucosyltransferase activity. The first step in the synthesis of gangliosides is the transfer of a glucose residue from UDP-glucose to ceramide backbone. GlcCer is transported across Golgi apparatus and addition of monosaccharides continues. LacCer forms by transfer of a galactose residue by galactosyltransferase I activity. Further, carbohydrate residues added on LacCer to

form simple gangliosides: GM3, GD3 and GT3. Those simple gangliosides are precursors of complex ganglio- series of o-, a-, b- and c- series. Those series are defined by the number of sialic acid residues attached. If there is no sialic acid residue it is O-series ganglioside. At the same way, one sialic acid (a- series), two sialic acid (b- series) and three sialic acid (c- series) attached to 3-position of inner galactose form different series (Kolter 2012). After biosynthesis, glycosphingolipids are delivered to the plasma membrane by vesicular transport (Kolter and Sandhoff 2006).

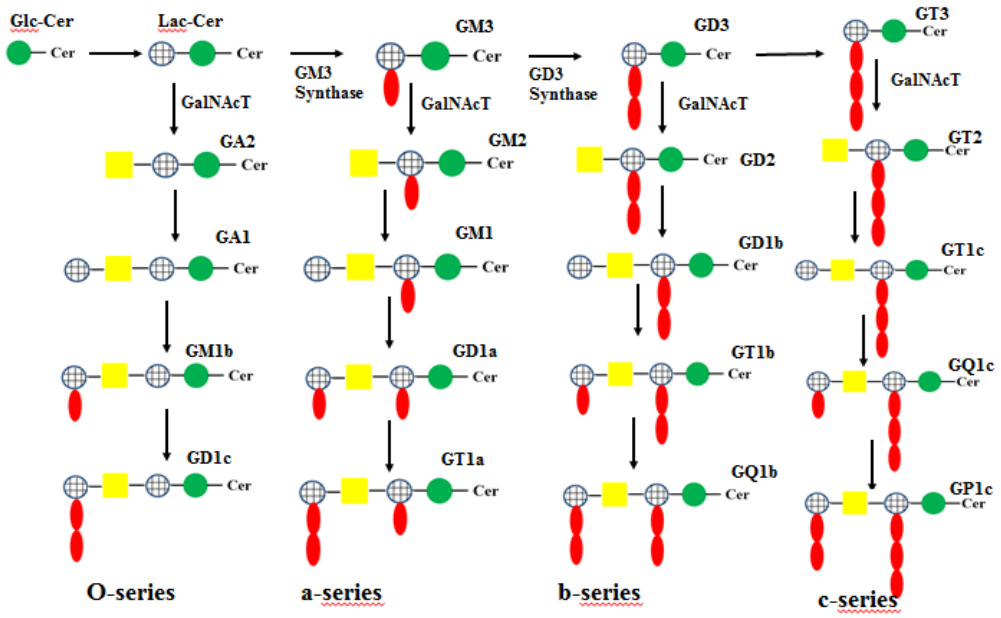

Figure 1.1. Biosynthesis pathway of gangliosides. (Blue circles with black vertical and horizontal lines represent galactose, red and green spheres represent sialic acids and glucose, respectively and yellow squares represents N-acetylgalactoseamine residues)

1.2.1.2.1.1.1 β1,4-N-Acetylgalactosaminyltransferase

GalNAcT (β1,4-N-acetylgalactosaminyltransferase; (GM2/GD2 synthase)) is one of the key enzymes in the synthesis of complex gangliosides. It controls the expression of most of the complex gangliosides along with the synthesis pathways (Yu, Tsai, and Ariga 2012). GalNAcT deficient mice have been created by two different

groups in 1996 (Takamiya et al. 1996) and 1998 (Liu et al. 1999). GalNAcT deficient mice are unable to synthesize GM2, GD2 and other complex gangliosides derived from LacCer, GM3, GD3 and GT3. Only simple gangliosides are synthesized. Even though those mice lack complex gangliosides, they show normal lifespan. On the other hand, examination of brain tissues show multiple defects in brain function such as axonal degeneration (Yamashita et al. 2005) , demyelination and reduced central conduction velocity (Sheikh et al. 1999) ,defects in motor function (Chiavegatto et al. 2000), impaired immunological response (Zhao et al. 1999) and Parkinson type symptoms (Wu et al. 2011). There is Wallerian degeneration (the crushing of a nerve cell axons in the nerve fiber break or located outside the body is a result of the degeneracy of the developing process of expressing and damage) in GalNAcT$^{-/-}$ mice (referred to as Galgt1$^{-/-}$ in this thesis) and it shows complex gangliosides which are important for axonal integrity for continuity of both the Central Nervous System and Peripheral Nervous Systems (Sheikh et al. 1999). Behavioral analysis shows that, those mice have deficiencies in balance, reflexes, strength and coordination (Yao et al. 2014).

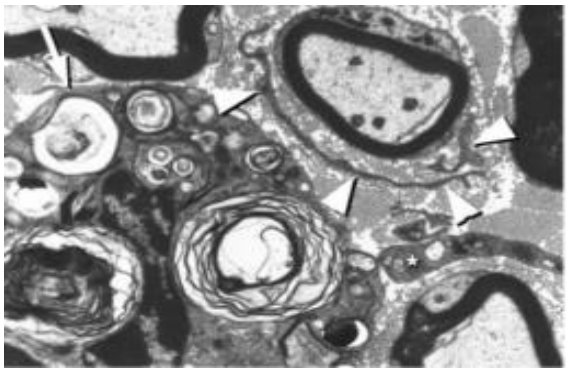

Figure 1.2. Electron microscopy image of Galgt1-/- mice brain. That shows macrophage containing myelin debris (arrow) and a minor onion bulb around a myelinated fiber (arrowheads) Source: (Sheikh et al. 1999).

Also, Galgt1$^{-/-}$ mice showed defects in expression of gangliosides in T-cells. Gangliosides bind to interleukin-2 and inhibit T cell proliferation. In the deficiency of GM1, GD1b and GA1 structural defects in interleukin 2 receptors were seen. Those results show that gangliosides regulate signal proliferation and activation of T-cells (Zhao et al. 1999) . Galgt1 female mice are fertile. However, Galgt1 male mice are sterile (Liu et al. 1999). Because circular spermatids are not elongated and do not

change their shape. The amount of testosterone hormone in blood decreases in non-fertile Galgt1 male mice (Sandhoff et al. 2005).

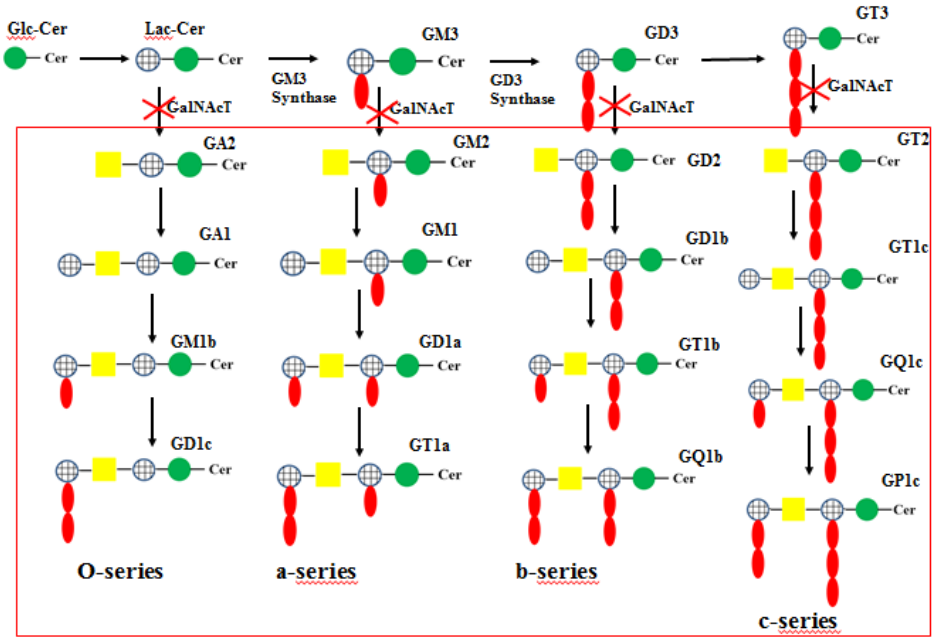

Figure 1.3. Deficiency of Galgt1 in metabolic pathway. There is no production of complex gangliosides indicated in red box. (Blue circles with black vertical and horizontal lines represent galactose, red and green spheres represent sialic acids and glucose and yellow squares represents N-acetylgalactosamine residues)

Parkinson disease is the second most common late-onset neurodegenerative disorder that affects people with the age of 65 and older. Lacking of GM1 complex ganglioside in Galgt1$^{-/-}$ mice causes Parkinson-like disease symptoms. As a progressive neurodegenerative disease, symptoms of disease are characterized by resting tremor, postural rigidity, neuropathies, autonomic instability and cognitive and emotional problems. L-DOPA and membrane-soluble GM1 analog Liga20 are drugs that are used for the treatment of Parkinson's disease. According to experiments made on Galgt1$^{-/-}$ mice with L-DOPA and Liga20, it was seen that symptoms of mice can be reversible (Wu et al. 2011). With this study, it was seen that GM1 prevents α-synnuclein to be aggregated as cytotoxic fibrils. By this mean symptoms of Parkinson's Disease became milder (Martinez et al. 2007).

1.2.1.2.1.2. Glycosphingolipid Metabolism

Digestion of glycosphingolipids occurs in endosomes and lysosome (Kolter 2012). Lysosomes are cellular organelles that are small, membranous, enriched in transmembrane proteins and hydrolytic enzymes and play role in the degradation of biomolecules in the cell. Lysosomes are acidic organelles and they contain enzymes that are required for degradation of biomolecules and permits the movement of small molecules inside-out movement of small molecules (Platt, Boland, and van der Spoel 2012).

Ganglioside degradation starts with the glycosylation of monosaccharide parts of GSLs. Glycosidases are soluble endosomal and lysosomal enzymes and trim monosaccharides at each step of catabolism pathway (Jeyakumar et al. 2003). At the beginning multiple sialic acid containing gangliosides are transformed by sialidase to only one sialic acid containing gangliosides: GM1, GM2 and LacCer. From GM1 galactose is removed and GM2 production occurs and the N-acetylgalactosamine residue removal turns ganglioside into GM3. Those degradations are achieved by different enzymes: β-galactosidase, β-Hexosaminidase A and β-glucosidase. This procedure continues the conversion into LacCer, GlcCer and ceramide by sequential action of β-galactosidase and β-glucosidase (Tettamanti et al. 2003).

In vivo, GSL with less than four sugar residues are degraded with sphingolipid activator proteins (SAPs or saposins). In vitro, these sphingolipid activator proteins can be replaced by detergents. Sphingolipid activator proteins mediate the interaction between the membrane bound lipid gangliosides and the water-soluble enzyme, or they can activate the enzyme directly (Saposins A-D and GM2 Activator Protein) (Schulze, Kolter, and Sandhoff 2009). The GM2-AP is an essential cofactor in the in vivo degradation of ganglioside GM2 by β- hexosaminidase A (Bernardo et al. 1995).

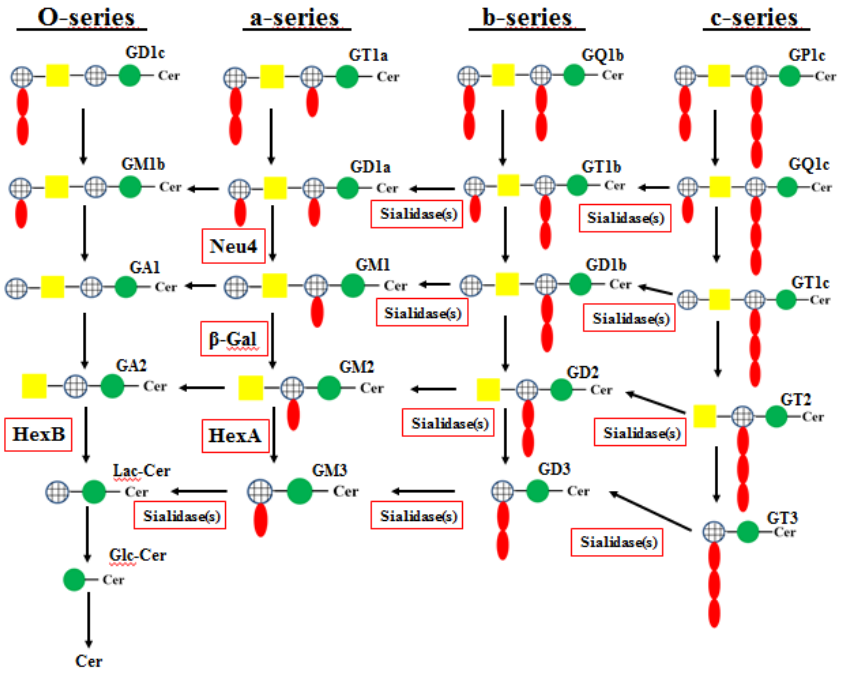

Figure 1.4. Degradation pathway of gangliosides. (Blue circles with black vertical and horizontal lines represent galactose, red and green spheres represent sialic acids and glucose and yellow squares represents N-acetylgalactosamine residues)

If lysosomal enzymes or lysosomal membrane proteins and soluble lysosomal proteins are deficient in lysosomes, accumulation of nondegraded biomolecules inside or monomers of nondegraded biomolecules occur (Platt, Boland, and van der Spoel 2012). When the amount of those uncatabolised products levels increase in lysosomes and it leads to inherited disease, the lysosomal storage diseases (Kolter 2012).

1. 3. Sialidases

Sialidases, also known as neuraminidases, are members of glycosidases and are responsible for the removal of α-glycosidic linked sialic acid residues from sugar groups of glycoproteins and/or glycolipids (Taeko Miyagi and Yamaguchi 2012). There are four types of mammalian sialidases and they are different from each other by subcellular localizations and enzymatic properties (T Miyagi and Tsuiki 1984). All sialidases have common primary sequence. All contain common Asp boxes (-Ser-X-Asp-X-Gly-X-Thr-Trp-) and the RIP (-Phe (Tyr)-Arg-Ile-Pro-) sequence. NEU1 shows less homology (19- 24%) among other human sialidases, whereas NEU2, NEU3 and NEU4 show 34-40% homology to each other (Taeko Miyagi and Yamaguchi 2012). Among human sialidases, NEU1 generally shows 10–20 times greater expression than NEU3 and NEU4. Expression of NEU2 is extremely low as it is only 4000 to 10,000th of the NEU1 expression in a range of tissues, according to a quantitative real-time RT–PCR using a standard curve for each cDNA (Hata et al. 2008).

Table 1.2. Sialidases

Sialidase	Location in cell	Substrates	Proposed major function	Disease
Neu1	Lysosome makes complex with β-GAL and CathA Plasma Membrane	Sialylated oligosaccharides Glycopeptides	Degradation in lysosomes Exocytosis Immune function Phagocytosis Elastic fiber assembly	Lysosomal storage disease Sialidosis (mucolipidosis I) accumulation of undegraded sialylated oligosaccharides, and glycoproteins, G_{M3} and G_{D3}
Neu2	Cytosol	Oligosaccharides Glycoproteins Gangliosides	Myoblast differentiation Neural differentiation	No known disease

(Cont on next page)

Table 1.2. (cont).

Neu3	Plasma membrane	Gangliosides- G_{M1},$G_{D1a,}$ G_{M2} and G_{M3}	Neuronal differentiation Apoptosis Adhesion	No known disease
Neu4	Lysosome Mitochondria Endoplasmic Reticulum	Glycoproteins, Oligosaccharides and Glycolipid	Neuronal differentiation Apoptosis Adhesion	No known disease

Sialidase NEU1 is located mostly in lysosomes and it is associated with a carboxypeptidase protective protein Cathepsin A (CathA) and β-galactosidase enzyme. CathA stabilizes active form of sialidase and protects it against rapid proteolytic degradation in the lysosome (D'Azzo et al. 1982). Deficiency and/or malfunction of NEU1 is linked to sialidosis and galactosialidosis which are lysosomal storage diseases with skeletal abnormalities and neurological degeneration (Dridi et al. 2013). Sialidase NEU1 takes role during immune response that is expression levels of sialidase increases in activation of T cells, B cells, macrophages and neutrophils (Seyrantepe et al. 2003).

Sialidase NEU2 is located in the cytoplasm of cells. Lysosomal sialidase NEU2 takes role in degradation of complex type N-glycans in some cancer cells and it takes role in cellular differentiation and tumor malignancy. Experiments showed NEU2 has role in cell growth and apoptosis in some cancer cell lines (Stamatos et al. 2010). NEU2 is able to hydrolyze glycoproteins, oligosaccharides and gangliosides. Also, sialidase NEU2 is found in muscle cells and takes role in muscle differentiation. Also, it takes role in neuronal differentiation (Taeko Miyagi and Yamaguchi 2012).

Sialidase NEU3 is located on the plasma membranes of cells and removes sialic acid residues from gangliosides by the means of modulating cellular activation, differentiation and transformation (Stamatos et al. 2010). Sialidase NEU3 is active towards gangliosides including GM1 and GD1a (Seyrantepe et al. 2008). NEU3 can regulate apoptosis in human fibroblast cells by producing ceramide from GM3 in plasma membrane by removing monosaccharide part (Valaperta et al. 2006). As like sialidase NEU1, NEU3 also contributes to immune response. NEU3 levels are up

regulated at the RNA, protein and enzyme levels during differentiation of monocytes into dendritic cells (Stamatos et al. 2010). Also, NEU3 is up regulated in many cancer types including colon, ovarian and prostate cancers and down regulated in lymphoblastic leukemia (Takahashi et al. 2015).

Sialidase NEU4 is mostly located in the lysosomes of cells. There are two forms of NEU4 found; short form and long form. Long form has extra 12 amino acid sequence at the N-terminus. In mice both forms of NEU4 are present. NEU4 expression level is highest in the brain and it is also found in less amounts in muscle, kidney, colon and liver (Taeko Miyagi and Yamaguchi 2012). Expression level of NEU4 gene increases 3 to 14 days after birth. This suggests that Neu4 has a role in brain development (Shiozaki et al. 2009). Knock-out mice model of $Neu4^{-/-}$ shows different ganglioside pattern than wild type mice and there is increased GD1a and decreased GM1 in brains of mice. $Neu4^{-/-}$ mice showed lysosomal storage bodies in macrophage cells in lung, spleen and lymphocytes. There is an increase in gangliosides, ceramide, cholesterol and fatty acids in brain, lung and spleen (Seyrantepe et al. 2008). Also according to cell line experiments, it is shown that Neu4 is active against majority of NEU2 substrates and has therapeutic potential (Seyrantepe et al. 2004).

1.4. Lysosomal Storage Diseases

Lysosomal storage disorders can be defined as rare, genetic, autosomal (except Fabry's disease) biochemical diseases. There are over 40 different lysosomal disorders and incidence of disease is 1:5000 to 1:7000 person in population (Kaye 2001). This ratio can be increased or decreased in some populations. Common feature of those diseases is the deficiency of one or more catabolic enzymes in lysosomes. Even in the deficiency of a single enzyme, entire pathway becomes blocked and it inhibits the further actions of other enzymes and the rest of the pathways become nonfunctional. These defects may occur in hydrolases or cofactors that are responsible for the degradation of macromolecules or transporters that deliver the monomers into the cytosol (Gieselmann 1995). In any condition, accumulation of substrates occurs in lysosomes.

Lysosomal storage disorders show clinical variability depending on the age of onset and progression of symptoms. Generally, LSDs are separated into three groups: infantile, juvenile and adult. Those classifications are important to differentiation of disease severity (Gieselmann 1995).

Table 1.3. Major lysosomal storage diseases and their accumulated substrates.

Source: (Schultz et al. 2011)

Disease	**Protein Deficiency**	**Accumulated Substrate**
Fabry	α-Galactosidase A	Trihexosylceramide Digalactosylceramide
Gaucher disease (Types I,II,III)	β-glucosidase	Glucosylceramide Glucosylsphingosine
GM1 gangliosidosis	β-galactosidase	GM1 ganglioside
GM2 gangliosidosis (Tay-sachs)	β-Hexosaminidase A	GM2 ganglioside
Sialidosis (Mucolipidosis I)	α-acetly Neuraminidase	Sialic acid
Mucopolisacchoridosis I (Hurler Syndrome)	α-L-iduronidase	Glycosaminoglycan (GAG)
Sandhoffs Disease	β- Hexosaminidase A and B	GM2 ganglioside Asialo-GM2 ganglioside Globoside

1.4.1. Tay-Sachs Disease

Tay-Sachs disease, also known as GM2 gangliosidosis, is an autosomal recessive neurodegenerative disorder that is caused by mutation in HEXA gene that is found in long arm of 15^{th} chromosome. That mutation results in block in the hydrolysis of ganglioside GM2 to GM3 by β-Hexosaminidase enzyme and causes accumulation of GM2 ganglioside in lysosomes (Miklyaeva et al. 2004). There are 3 forms of β-Hexosaminidase that are HexS (α+α) composed of two α subunits; HexA (α+β) composed of α and β subunits and HexB (β+β) composed of two β subunits. HexA and HexB remove terminal N-acetyl glucosamine (GlcNAc) and/or N-acetylgalactosamine (GalNAc) residues from GM2 ganglioside (Phaneuf et al. 1996). If the mutation occurs in α- subunit of β-Hexosaminidase it causes Tay-Sachs disease and if the mutation

occurs in β subunit of β-Hexosaminidase it causes Sandhoff's disease (Huang et al. 1997). In both diseases, GM2 ganglioside is found as the storage material (Gieselmann 1995).

In classical Tay-Sachs disease, symptoms start to show between three to five months of age with progressive weakness and hyperirritability. Severity of the diseases changes among patients. Tay-Sachs patients can be grouped into three classes. The most severe form is infantile acute form is also known as classical Tay-Sachs. Disease symptoms start in between three to five months of age and generally end with death in two to five years of life. Juvenile (subacute) and adult (chronic) forms may progress slower and milder clinical signs that starts in the 2rd and 3nd decade of life (Miklyaeva et al. 2004), Gieselmann 1995). Currently, there is no treatment for GM2 gangliosidosis.

Cherry red spots in eyes are seen in all patients. Accumulation of GM2 gangliosides in the brain causes neuronal cell death and progressive neurodegeneration. Clinical features of Tay-Sachs include ataxia, muscle weakening with motor degeneration, spasticity, convulsions, deafness and blindness (Chen et al. 2014).

1.4.1.1. Mouse Model of Tay - Sachs disease

The first, mouse model of GM2 gangliosidosis were created in 1996 in Roy A. Gravel's laboratory by homologous recombination to enlighten metabolic pathway of Tay-Sachs disease. The mutant mice were accumulating GM2 ganglioside in neuron cells and they have characteristic features of Tay-Sachs disease as inclusion bodies in lysosomes. However, unlike human patients, mice had no obvious behavioral phenotype. Examinations of brain and liver gangliosides revealed below threshold amounts of GM2 that was not toxic. On the other hand, different from human patients, GM2 derived ganglioside GA2 was present in $HexA^{-/-}$ mice and this ganglioside can be further metabolized into ceramide by HexB (Phaneuf et al. 1996). Because of the metabolic bypass, those mice can escape disease over one years of life (Igdoura et al. 1999).

Normally, in Tay-Sachs patients there are high levels of neuronal death. On the other hand apoptotic cells in $HexA^{-/-}$ mice are not increased when compared to control

mice. The brain and spinal cord shows decreased histopathology and lower amount of GM2 accumulation (Huang et al. 1997).

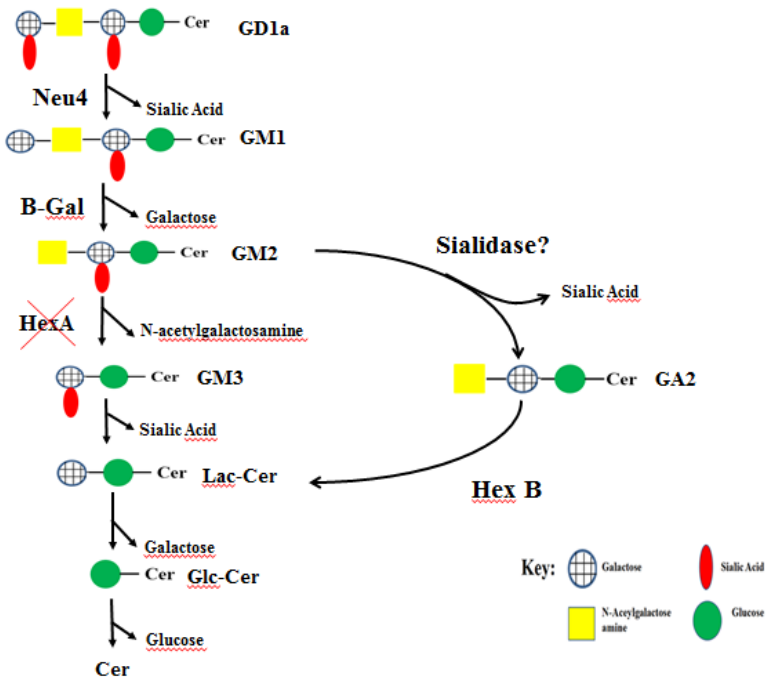

Figure 1.5. Metabolic by-pass mechanism in ganglioside degradation pathway in HexA deficient Tay-Sachs mouse model

Transfection of cultured neuroglia cells from Tay-Sachs patients with Neu4 expressing plasmid showed normal morphology and GM2 accumulation decreased by the metabolic bypass. In this cultured cell experiment, GM2 ganglioside metabolized via GA2 ganglioside to ceramide and HexA deficiency fully corrected (Seyrantepe et al. 2008). Mice with double deficiency of Neu4 and HexA created by Dr. Seyrantepe in 2010 $Neu4^{-/-}HexA^{-/-}$ double deficient mice show much more severe phenotype either than $Neu4^{-/-}$ and $HexA^{-/-}$ single knock-out mice alone. $Neu4^{-/-}HexA^{-/-}$ double deficient mice show motor impairment, tremor, weakness and spacity and in 40% of mice show seizures which are characteristic features of Tay-Sachs disease. Double deficient mice were showed seizures starting at 3 months age. Those double deficient mice have accumulation of GM2 ganglioside in brain. Electron microscopy images of double deficient mice show large irregular lysosomes and whorls as in Tay-Sachs patients (Seyrantepe et al. 2010). In brains of double knockout mice, there are multiple

degenerated neurons in the cortex and hippocampus regions and there is accumulation of GM2 ganglioside as multiple layers (Timur et al. 2015). It is suggested that Neu4 is a modifier gene in mouse model of Tay-Sachs disease.

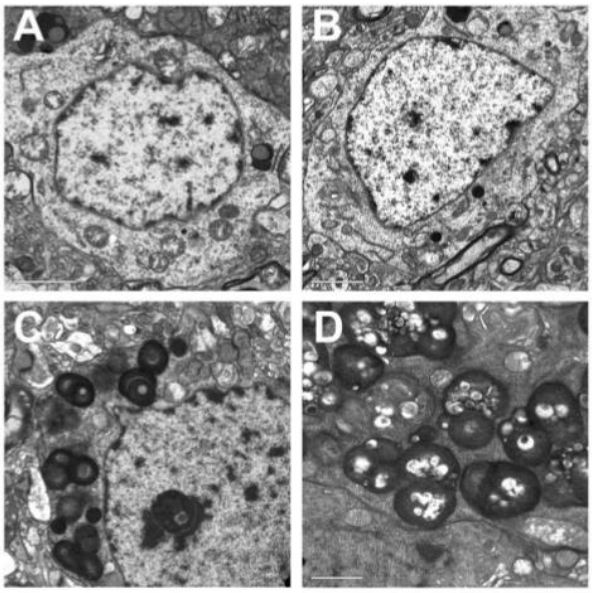

Figure 1.6. Electron micrographs of hippocampus region of mouse brain tissues. A) Cortical neurons from wild type mouse, B) $Neu4^{-/-}$ mouse C) $Hexa^{-/-}$ mouse, D) $Neu4^{-/-}HexA^{-/-}$ double knockout mouse (Seyrantepe et al. 2010)

1.5. Behavioral Tests

With the increasing manipulation technologies of transgenic and knock-out mice many functional genes were identified in brain. Biochemical, anatomical, molecular biological, physiological and behavioral examinations enabled us to see consequences of mutations. Behavioral tasks show us how brain affected from mutations. Changes in the nervous system can be observed as behavioral change. With the behavioral tests sensory abilities, motor coordination, memory-learning, feeding habits, social interactions, anxiety related behaviors and sexual relations of mice can be evaluated (Crawley 2008). In this thesis, motor coordination was examined using Rotarod Test and memory-learning abilities were examined using Passive Avoidance Test.

1.5.1. Rotarod Test

Rotarod test is designed to evaluate motor coordination of mice. Increased time on rod over repeated testing sessions show cerebellar learning of mice (Crawley 1999). Among many motor coordination tests, rotarod test is suitable for identification of cerebellar deficits in mice and rats (Shiotsuki et al. 2010). In the test, mice stay balanced on a rotating rod and time of fall off the rod is recorded. By adding constant acceleration to rod (accelerate-rod) does not allow to the mice walk at the same pace. At the end of several training days, it is expected that the mice stay longer on the rod when compared to the first training (Buitrago et al. 2004).

1.5.2. Passive Avoidance Task

Passive avoidance test is a fear motivated test and used to detect short term or long term memory in mice. Test box is composed of two areas which are one big bright area and small dark area that are separated by a sliding door. Normally mice prefer to stay in small dark areas rather than bright areas.

The experiments were composed of three day procedure: habituation, training and test. In habituation, mice are placed in facing the light compartment and after the door is opened mice can explore both light and dark environments. Intrinsically, mice will prefer to enter dark box. In training day, when mice enter the dark compartment with four paws, the door is closed and electric shock is given to foot of mice. Test day, mice are placed into the light box and the door is kept open to allow the mice to move between the light and dark boxes (Yamanaka et al. 1994) (Liu et al. 1997). In the experiment, mice has to make a decision between safe (light box) and unsafe (dark box) places (Stiedl and Ögren 2014).

1.6. Aim of the Study

In this thesis, it was aimed to understand the effect of sialidase Neu4 in glycosphingolipid metabolism. Therefore, we used three different mice strain lack of HexA, Neu4 and Galgt1 respectively. We generated $Neu4^{-/-}$, $HexA^{-/-}$, $Galgt1^{-/-}$, $Neu4^{-/-}$ $HexA^{-/-}$, $HexA^{-/-}Galgt1^{-/-}$, $Neu4^{-/-}Galgt1^{-/-}$, $Neu4^{-/-}HexA^{-/-}Galgt1^{-/-}$ to see how ganglioside contents were affected from the absence of each enzyme responsible for the biosynthesis and biodegradation of brain gangliosides. To understand changes in ganglioside composition biochemical, molecular biological and immunohistochemical analyses were performed. Additionally, the effect of alterations in ganglioside levels on behavior was assessed.

CHAPTER 2

MATERIALS AND METHODS

2.1. Animals

Mice with two enzyme deficiencies ($HexA^{-/-}Neu4^{-/-}$) were previously generated by Prof. Dr. Volkan Seyrantepe, in Montreal, Canada. $HexA^{-/-}Neu4^{-/-}$ was a generous gift by Prof. Alexey V. Pshezhetsky (Centre Hospitaliere Universitaire Sainte-Justine, University of Montreal, Montreal, Quebec, Canada). Galgt1-/- mice were provided by our collaborator Prof. Roger Sandhoff (Hochschule Mannheim - Mannheim University of Applied Sciences, Institut für Instrumentelle Analytik und Bioanalytik, Germany) along the project "Intensified Cooperation (IntenC): Promotion of German-Turkish Higher Education Research" (Project number: 113T025). Triply deficient mice were generated in our laboratory with proper breedings. In this study, breeding and crossing have made between brothers and sisters to get the same genetic background.

All animals were bred and maintained in the Turkish Council on Animal Care accredited animal facility of İzmir Institute of Technology according to all ethical concerns. Mice were housed 12h dark/light cycle under constant temperature and humidity. Mice were fed as *ad libitum*.The animal care and the use in experiments were granted by the Animal Care and Use Committee of İzmir Institute of Technology, İzmir, Turkey.

From Prof. Roger Sandhoff's Laboratory, two female (8517 and 8518) $Galgt1^{-/-}$ mice and two male (8512 and 8513) $Galgt1^{+/-}$ mice were provided. Breedings of $Galgt1^{+/-}$ and $Galgt1^{-/-}$ mice with $Neu4^{-/-}HexA^{-/-}$ mice gave two times birth (1st newborns cannibalized 2nd newborns 3 female 1 male $Neu4^{+/-}HexA^{+/-}$ $Galgt1^{+/-}$). Then in F_2 and later generations, desired genotypes were obtained. At the end of a year, eight different genotypes mice were obtained.

Table 2.1. Breeding Pairs

Breeding pairs	**Expected genotypes in F1 generation**
$Neu4^{-/-}HexA^{-/-}Galgt1^{+/+}$	$Neu4^{+/-}HexA^{+/+}Galgt1^{+/-}$
$Neu4^{+/+}HexA^{+/+}Galgt1^{-/-}$	
Breeding pairs	**Expected genotypes in F2 genaration**
$Neu4^{+/-}HexA^{+/-}Galgt1^{+/-}$ $Neu4^{+/-}HexA^{+/-}Galgt1^{+/-}$	$Neu4^{+/-}HexA^{+/+}Galgt1^{+/+}$
	$Neu4^{+/-}HexA^{+/-}Galgt1^{+/-}$
	$Neu4^{+/+}HexA^{+/+}Galgt1^{+/-}$
	$Neu4^{+/+}HexA^{+/-}Galgt1^{+/+}$
	$Neu4^{+/+}HexA^{+/-}Galgt1^{+/-}$
	$Neu4^{+/-}HexA^{+/+}Galgt1^{+/+}$
	$Neu4^{+/-}HexA^{+/+}Galgt1^{+/+}$
	$Neu4^{+/-}HexA^{+/-}Galgt1^{+/+}$
	$Neu4^{+/+}HexA^{+/+}Galgt1^{-/-}$
	$Neu4^{+/+}HexA^{+/-}Galgt1^{-/-}$
	$Neu4^{+/-}HexA^{+/+}Galgt1^{-/-}$
	$Neu4^{+/-}HexA^{+/-}Galgt1^{-/-}$
	$Neu4^{+/+}HexA^{-/-}Galgt1^{+/+}$
	$Neu4^{+/+}HexA^{-/-}Galgt1^{+/-}$
	$Neu4^{+/-}HexA^{-/-}Galgt1^{+/+}$
	$Neu4^{+/-}HexA^{-/-}Galgt1^{+/-}$
	$Neu4^{+/+}HexA^{-/-}Galgt1^{-/-}$
	$Neu4^{+/-}HexA^{-/-}Galgt1^{-/-}$
	$Neu4^{-/-}HexA^{+/+}Galgt1^{+/+}$
	$Neu4^{-/-}HexA^{+/+}Galgt1^{+/-}$
	$Neu4^{-/-}HexA^{+/-}Galgt1^{+/+}$
	$Neu4^{-/-}HexA^{+/-}Galgt1^{+/-}$
	$Neu4^{-/-}HexA^{+/+}Galgt1^{-/-}$
	$Neu4^{-/-}HexA^{+/-}Galgt1^{-/-}$
	$Neu4^{-/-}HexA^{-/-}Galgt1^{+/+}$
	$Neu4^{-/-}HexA^{-/-}Galgt1^{+/-}$
	$Neu4^{-/-}HexA^{-/-}Galgt1^{-/-}$

2.2. Mouse Genotyping

Mouse genotypes were determined by the DNA isolation protocol already optimized in Dr. Seyrantepe's lab (Seyrantepe et al. 2010). DNA extraction was made from mouse tail. DNA isolation was performed in two days. In the first day, mouse tail were put into 1,5ml eppendorf tube with 500 µl of lysis buffer (contains 10% 1M Tris pH 7.6, 2.5% 0.2M EDTA, 20% SDS, 4% 5M NaCl) and 12 ul of proteinase K (25 mg/ml solution). Samples were incubated overnight in a shaking incubator 55^{o}C at 70

rpm. Second day, samples were centrifuged at 13000 rpm for 10 minutes at room temperature. Supernatant were transferred into new 1,5ml eppendorf tube and 1 volume of 100% isopropanol were added on each tube. Tubes were inversed gently until DNA is seen. DNA was collected and transferred into new eppendorf tube that contains 500 µl of 70% ethanol. Centrifugation was performed at 15000 rpm for 1 min. Later, supernatant were discarded and the pellet was air dried. DNA were dissolved in 100ul of dH2O and incubated for 1 hour at 55^{o}C and later stored at -20 ^{o}C.

The PCR for Neu4 and HexA were conducted with 100ng genomic DNA. Total 25 µl of reaction mixture was prepared for each mice containing, 0.4 µM of forward primer, 0.8 µM of reverse primer, 0.4 mM of each dNTPs, 1X reaction buffer without $MgCl_2$, 1.5 mM $MgCl_2$, 1.75 unit Taq polymerase (Invitrogen) and 4% DMSO. Allele specific primers were used to identify wild type and knock-out alleles. PCR was done in the condition of 1 cycle 3 minutes at 94˚C; 30 cycles 45 seconds at 94˚C, 45 seconds at 60˚C, 50 seconds at 72˚C; and 1 cycle 10 minutes at 72˚C.

The PCR for Galgt1 were performed with 100 ng genomic DNA. Total 50 µl of reaction mixture prepared for each mouse that contains 0.4 mM of each primer, 0.5 mM of each dNTPs, 1 X reaction buffer without $MgCl_2$, 3mM $MgCl_2$ and 2.5 units Taq polymerase (Invitrogen). Allele specific primers were used to identify wild type and knock-out alleles. For wild type and knock out alleles two different PCR reactions were prepared. PCR was done in the condition of 1 cycle 1 minute at 94˚C; 30 cycles 45 seconds at 94˚C, 30 seconds at 58˚C, 3 minute at 72˚C; and 1 cycle 10 minutes at 72˚C.

Table 2.2. Primer pairs for genotyping of mice

Gene	Primer	Primer Sequence
Neu4	Neu4 Forward	CTCTTCTTCATTGCCGTGCT
	Neo Forward	GCCGAATATCATGGTGGAAA
	Neu4 Reverse	GACAAGGAGAGCCTCTGGTG
HexA	HexA Forward	GGCCAGATACAATCATACAG
	PKG Forward	CACCAAAGAAGGGAGCCGGT
	HexA Reverse	CTGTCCACATACTCTCCCCACAT
Galgt1	Galgt1-WT-Forward	CGTGGAGCACTACTTCATGC
	Galgt1-WT-Reverse	CTCTCCTCCCCTACCAGGTC
	Galgt1-KO-Forward	TCGTCCTGCAGTTCATTCAG
	Galgt1-KO-Reverse	ATATGGCTCCATGGGCCTC

After PCR reaction, HexA and Neu4 PCR products were run on 1% agarose gel at 90 volt for 30 minutes. Galgt1 PCR products were run on 1% agarose gel at 100 volt for 30 minutes.

2.3. Tissue Handling

Age matched single, double and triple knock-out mice (three- and six-month-old) were sacrificed in a CO_2 cabinet. Full brains were removed and right and left hemispheres were separated from each other, brains were immediately frozen on dry ice and kept in -80 ˚C until needed. Liver, lung, heart, spleen, kidney and (for males) testis were removed and washed in 0.9% saline solution. Those organs were immediately frozen in liquid nitrogen and kept in -80 ˚C until needed.

2.4. Lipid Isolation

25 mg of tissue were homogenized in 1.5 ml of dH_2O using IKA T10 basic-ultra turax homogenizer for 30 seconds in borosilicate glass tube. After that, samples were sonicated (with Bandelin-sonoplus) for 2 times for 30 seconds. After that, samples were lyophilized with N_2 gas flow in 55 ˚C water bath to speed up evaporation. Then, two times extraction were performed with 3 ml of 100% acetone. Samples were vortexed and centrifuged at 2000 rpm for 5 minutes. Each time supernatants were removed containing phospholipids and other small membrane lipids. Then, 1.5 ml of chloroform: methanol: water (10:10:1) solution added on tubes and vortexed. Extraction was performed at 2000 rpm for 5 minutes and supernatant collected in new glass tube with glass Pasteur pipette. This step repeated for two times and each time supernatant added on the same glass tube. After that, 2 ml of chloroform: methanol: water (30:60:8) solution was added to tubes and vortexed. Extraction was performed at 2000 rpm for 5 minutes and supernatant collected in the same tube on the previous step and that step were repeated for two times. At the end of this step, there were both acidic and neutral gangliosides found in the glass tube. To separate neutral and acidic gangliosides DEAE

A-25 columns were used. DEAE A-25 ion exchange columns were prepared in laboratory freshly each time (Yu and Ledeen 1972). For this purpose 10 ml chloroform: methanol: 0.8M sodium acetate (30:60:8) was added to 1.0 gr DEAE Sephadex A-25 resin (GE Health Care). After incubation at room temperature for 5 minutes, centrifugation was done at 2000rpm for 1 minute. Solution was removed and resin was washed with same solution for three times. Then, resin was incubated overnight with 10 ml chloroform: methanol: 0.8M sodium acetate (30:60:8). The next day supernatant was removed and resin was washed with 10 ml chloroform: methanol: water (30:60:8) for three times and it were become ready to use. Before loading resin to column for acidic and neutral ganglioside separation, Pasteur pipettes' ends were closed with glass wool. Resin was loaded to Pasteur pipettes and length of column was equalized to 2cm. Columns were washed with 1 ml chloroform: methanol: water (10:10:1) solution, 1 ml chloroform: methanol: water (30:60:8) solution.

To clean up the columns 1ml of chloroform: methanol: water (10:10:1) solution was flushed inside the column. Then obtained total gangliosides were added to the column. Washed out solution contained neutral gangliosides and they were collected into a glass tube. To be sure all neutral gangliosides were washed away; columns were washed with 2 ml of 100% methanol. Eluted samples were evaporated with N_2 gas flow in 55 ˚C water bath before loading to thin layer chromatography plate.

Acidic gangliosides were bounded to a column. To collect acidic gangliosides new glass tubes were put under the columns and columns were washed with 4 ml of 500 mM potassium acetate solution in methanol. Acidic gangliosides were collected in new tube.

For desalting of acidic gangliosides, Supelclean LC-18 column (Supelco) was used. Columns were placed on the Chromabond Vacuum manifold (MachereyNagel) and vacuum was fixed to 5 Hg. For equilibration, each column was washed with firstly 2ml methanol, then with 2ml 500 mM potassium acetate in methanol solution. Collected acidic gangliosides were loaded on columns and after flowed through the columns were washed with 10 ml distilled water. Samples were then eluted with 4 ml methanol and 4 ml methanol: chloroform (1:1) in low vacuum (<5 Hg). Eluted samples were evaporated with N_2 gas flow in 55 ˚C water bath before loading to thin layer chromatography plate.

2.5. Thin Layer Chromatography

Thin Layer Chromatography (TLC) method is used to separate lipids based on their structures and weights. TLC plates were incubated at 100 ˚C oven for 30 minutes to evaporate humidity and make plates dry.

Thin Layer Chromatography tank (Camag) was prepared 2 hour 15 min before running. As solvent mixture to develop tank chloroform: methanol: water (60: 35: 8) were used. Both neutral and acidic gangliosides developed in the same conditions. To load samples on to Silica plates (Merck), Camag Linomat automated machine were used. Nitrogen dried samples resolved in 100 µl of tank chloroform: methanol: water (10:10:1) and from each sample 30 µl sample were loaded on the TLC plate. Plate were put into TLC tank and were run for 10 cm (1 to 1.5 hours)

2.6. Staining With Orcinol

Orcinol (Sigma) was freshly prepared. For 10 ml of orcinol solution 0.04 g orcinol was solved in 10 ml 25% sulphuric acid in 50 ml TLC sprayer (Sigma). Orcinol is a colorless solution and to make colder the solution 5 minutes waited. Dye was sprayed on air dried dry plates. Then plates were incubated TLC plate heater (Camag) at 120 ˚C until all bands become visible. After staining, lipids were identified by comparing with brain ganglioside standards (Avanti Polar Lipids). Plates were scanned (Hp scanner system) and photographs were saved.

2.7. RNA Isolation

50 mg of the left hemisphere of mice brain was put into 500 µl of Genezol reagent (GeneAid). Tissue samples were homogenized in 2 ml eppendorf tube with RNAse free beads using tissue homegenizator (Retsch MM100). Homogenized samples were incubated for 5 minutes at room temperature and were transferred into new 1.5 ml of microcentrifuge tube. Then, 100 µl of chloroform were added to the sample and microcentrifuge tubes were shaken vigorously for 10 seconds. Samples were centrifuged 15000 x g for 15 minutes at +4 ˚C to separate phases. Upper aqueous phase were transferred into new 1.5 ml microcentrifuge tube. Then, 1 volume of isopropanol was added to the aqueous phase and tubes were mixed by inverting several times. Samples were incubated at room temperature for 10 minutes. Samples were centrifuged at 15000 x g for 5 minutes at +4˚C to form RNA pellet. Supernatant were removed and discarded carefully. As the next step, 1ml of 70% ethanol was added on RNA pellet to wash and they were vortexed briefly. Samples were centrifuged at 16000 x g for 5 minutes at +4˚C. Supernatant were discarded and RNA pellet were dried 5-10 min at 55 ˚C. To suspend RNA, 40 µl of nuclease free water were added on samples and incubated at 50 ˚C water bath for 10 minutes. RNA concentrations were measured with Nanodrop spectrophotometer (ND-1000).

2.8. cDNA Synthesis

Isolated RNA was converted into cDNA. cDNA was synthesized by High-Capacity cDNA Reverse Transcription Kit (Applied Biosystems). Reaction conditions were arranged for 50 ng/µl total cDNA product. For each reaction; 1 X RT buffer, 4 mM dNTP mix, 1X RT Random primers, 50 units MultiScribe Reverse Transcriptase were mixed with water and RNA dependent on RNA concentration that was measured in NanoDrop. Total mixtures were in 20 µl volumes. Conditions of PCR were optimized to; 1 cycle 10 minutes at 25˚C; 1 cycles 120 minutes at 37˚C, 1 cycle 5 minutes at 85˚C.

cDNAs were controlled by normal PCR using GAPDH gene primers. PCR were conducted with 75 ng cDNA. Total 25 µl of reaction mixture was prepared for each cDNA that contains, 0.8 mM of each primer, 10 mM of each dNTPs, 1X reaction buffer with MgCl2 and 1.75 units AmpONE Taq DNA polymerase (GeneAll). PCR was done in the condition of 1 cycle 2 minutes at 95˚C; 30 cycles 20 seconds at 95˚C, 15 seconds at 65˚C, 22 seconds at 72˚C; and 1 cycle 3 minutes at 72˚C. After PCR reaction, PCR products were run on 1% agarose gel at 90 volt for 30 minutes.

2.9. Real-Time PCR

Expression analyses of genes given in the Table.2.3 were done with age matched mice brains for 8 genotypes. Roche LightCycler 96 system with Roche LightCycler 480 SYBR Green I Master Mix was used. Real-Time PCR were optimized with 75 ng cDNA in the 20µl reaction mix containing 0.4 uM each primer and 1X Roche LightCycler 480 SYBR Green I Master Mix. Conditions of PCR was optimized to; 1 cycle 10 minutes seconds at 95˚C; 45 cycles 20 seconds at 95˚C, 15 seconds at 61˚C, 22 seconds at 72˚C, reading was done after each cycle. In the end 1 cycle 30 seconds at 95˚C, 10 seconds at 60˚C then continuous reading was applied while temperature increases to 99˚C to detect primer dimers if exist.

Table 2.3. Genes that will be analyzed by Real-Time PCR and their specific primers

Gene	**Primer**	**Primer Sequence**	**PCR product length**
Sialidase Neu1	Forward	TCATCGCCATGAGGAGGTCCA	431bp
	Reverse	AAAGGGAATGCCGCTCACTCCA	
Sialidase Neu2	Forward	CGCAGAGTTGATTGTCCTGA	429bp
	Reverse	TTCTGAGCAGGGTGCAGTTTCC	
Sialidase Neu3	Forward	CTCAGTCAGAGATGAGGATGCT	416bp
	Reverse	GTGAGACATAGTAGGCATAGGC	
Sialidase Neu4	Forward	AGGAGAACGGTGCTCTTCCAGA	339bp
	Reverse	GTTCTTGCCAGTGGCGATTTGC	
Hexosaminidase B	Forward	AGTGCGAGTCCTTCCCTAGT	412bp
	Reverse	ATCCGGACATCGTTTGGTGT	

(Cont. on next page)

Cont. Table 2.3

G_{M2} Activator Protein	Forward	GCTGGCTTCTGGGTCAAGAT	193bp
	Reverse	GCACTGTGAAGTTGCTCGTG	
G_{M3} Synthase	Forward	AATGCACTATGTGGACCCTG	133bp
	Reverse	GTTGATGCTGTACCTGTCCTC	
G_{D3} Synthase	Forward	CGATAATTCCACGTACTCCCTC	193bp
	Reverse	TTTGGAACCGACATCTCTGG	
N-acetyl-Galactosaminyl Transferase 1 (Galgt1)	Forward	TCAGGATCAAGGAGCAAGTG	124bp
	Reverse	AAGGCTTTAGTGAGGTCAACC	
B-Galactosidase	Forward	TTTCTGGGGACCGTGATGTG	432bp
	Reverse	AATCCACTGTGGCGTACAGG	
Galactosyl Transferase (B3Galt4)	Forward	GGCAGTGCCCCTTCTGTATT	407bp
	Reverse	GTGCAGTCCTCTCCCCATTC	
LacCer Synthase (B4Galt6)	Forward	CACCTGATTCCGATGCTCCA	410bp
	Reverse	CCTTCTGGCCGGGTTACATT	
Glyceraldehyde-3-Phosphate Dehydrogenase (GAPDH)	Forward	CCCCTTCATTGACCTCAACTAC	347bp
	Reverse	ATGCATTGCTGACAATCTTGAG	

2.10. Enzyme Activity Assay

25 mg of the brain tissue was homogenized in 100 ul of dH_2O using IKA T10 basic- ultra turax homogenizer for 30 seconds in test tube. Samples were sonicated with Bandelin-sonoplus 2 times for 45 seconds in cold- water bath. Specific activities of sialidase Neu1, β-Hexosaminidase B and β-Galactosidase and β-Glucosidase enzymes were measured. Substrates for these enzymes (Table 2.4) were fluorescently tagged with 4-Methylumbelliferyl (4-MU). 4-MU was digested by substrate, released 4-MU concentration were calculated depending on the standard curve by spectrofluorophotometer (Shimadzu RF5301 PC) in emission wavelength 365 nanometer and excision wavelength of 445 nanometer.

Table 2.4. Substrates used for enzyme activity assay

Enzyme	Substrate
Sialidase	2′-(4-Methylumbelliferyl)-α-D-N-acetylneuraminic acid
β-Hexosaminidase	4-Methylumbelliferyl N-acetyl-β-D-glucosaminide
β-galactosidase	4-Methylumbelliferyl β-D-galactopyranoside
β-glucosidase	4-Methylumbelliferyl β-D-glucopyranoside

For β-Hexosaminidase B enzyme reaction 20µl of the homogenate were diluted in 1/5 ratio with 0,1M sodium citrate pH 4.3. To measure β-Hexosaminidase B enzyme activity these diluted homogenates were incubated at 55°C for three hours before setting reaction. For other enzymes reaction 20µl of the homogenate were diluted in 1/10 ratio with 0.5M sodium acetate pH 4.5 and used directly. Reactions were prepared as given in the Table2.5.

Table 2.5. Reaction ingredients for enzyme activity assay

Sialidase (Sigma 96587)	
Blank	**Sample**
50µl substrate	50µl substrate
40µl 0.5M sodium acetate buffer (pH4.5)	40µl 0.5M sodium acetate buffer (pH4.5)
10µl dH_2O	10µl sample
30 minutes incubation at 37°C 3.9ml 0.2M glycine buffer (pH10.8) to stop reaction	
β-Galactosidase (Sigma M1633)	
Blank	**Sample**
25µl substrate	25µl substrate
50µl 0.1M NaCl	50µl 0.1M NaCl
25µl dH_2O	25µl sample
10 minutes incubation at 37°C 3.9ml 0.2M glycine buffer (pH10.8) to stop reaction	
β-Glucosidase (Sigma M3633)	
Blank	**Sample**
50µl substrate	50µl substrate
40µl 0.5M sodium acetate buffer (pH4.3)	40µl 0.5M sodium acetate buffer (pH4.3)
10µl dH_2O	10µl sample
30 minutes incubation at 37°C 3.9ml 0.2M glycine buffer (pH10.8) to stop reaction	
β-Hexosaminidase (Sigma M2133)	
Blank	**Sample**
75µl substrate	75µl substrate
25µl dH_2O	25µl sample
30 minutes incubation at 37°C 3.9ml 0.2M glycine buffer (pH10.8) to stop reaction	

Protein concentrations of samples were measured by Bradford Reagent (Sigma B6916). For this purpose, 5µl of homogenates were diluted with their buffer in 1/4 ratio. 5µl of sample were incubated for 10 minutes at room temperature in dark with 250µl Bradford reagent and absorbance of each were measured in microplate reader (i-Mark Biorad) at 595nanometer. Protein concentration was calculated depending on the BSA standard curved created from known concentrated bovine serum albumin protein. To calculate specific enzyme activity following calculation was used for each sample.

Enzyme Activity (nmol/hour/ml) = Concentration of 4-MU x (Last volume/Sample volume) x (1/time in hour)

Specific Enzyme Activity (nmol/mg protein/hour) = Enzyme activity / protein concentration

Relative enzyme activity= (Specific Enzyme Activity/ Specific Enzyme Activity of control littermate)*100

2.11. Behavioral Analysis

Two different behavioral tasks were performed. Roratod test was performed to evaluate motor coordination of mice. Passive avoidance task were performed to evaluate changes in memory-learning abilities of mice.

2.11.1. Rotarod Experiment

Mice separated into eight groups (control, $Neu4^{-/-}$, $HexA^{-/-}$, $Galgt1^{-/-}$, $Neu4^{-/-}$ $HexA^{-/-}$, $HexA^{-/-}Galgt1^{-/-}$, $Neu4^{-/-}Galgt1^{-/-}$, $Neu4^{-/-}HexA^{-/-}Galgt1^{-/-}$) of three- and six-month-old. The latency to fall off rotarod was measured. First, all mice were trained to walk and to be stable on rotating rod (Harvard Apparatus) (3 cm diameter and 30 cm above the base) at constant speed (5 minutes) prior to the experiment started. Then, mice were tested on accelerating rod three times for a day. Speed of rotarod started at 4 rpm and gradually increased up to 40 rpm in a 5 minutes period. The speed and

acceleration that mice felt was recorded (Sedacomv2.0, Harvard Apparatus), data saved and comparison were done (Miklyaeva et al. 2004).

2.11.2. Passive Avoidance Task

In passive avoidance task, mice were separated into eight groups (WT, $Neu4^{-/-}$, $HexA^{-/-}$, $Galgt1^{-/-}$, $Neu4^{-/-}HexA^{-/-}$, $HexA^{-/-}Galgt1^{-/-}$, $Neu4^{-/-}Galgt1^{-/-}$, $Neu4^{-/-}HexA^{-/-}Galgt1^{-/-}$) of three- and six-month-old. Passive avoidance box has two distinct compartments; one big light box and one small dark box and those two boxes were separated by a sliding door. Experiment was composed of three day procedure: habituation, training and test. Time interval between each experiment was 24-hours. After each subject removed, passive avoidance cages were cleaned with 70% ethanol solution.

In habituation day, mice were placed in the light compartment facing the door for 30 seconds and after the door was opened the mice was able to explore both the light and dark environments. When mice entered the dark environment the door was closed. After 10 seconds mice were removed and placed back in their home cage.

In training day, after mouse entered the dark compartment with four paws, door was closed and 0.2 mA electric shock was given to foot of mouse for 2 seconds. After 10 seconds mice were removed and placed in its home cage.

In test day, mouse was placed into light box facing with door and door was kept open to allow mouse to move into dark box. Latency time for stepping through the door was recorded with ShutAvoidv1.8 (Harvard Apparatus) and data was saved. If mouse were not moved between dark and light boxes, the experiment finished in 500 seconds after the start of each trial (Yamanaka et al. 1994) (Liu et al. 1997).

2.12. Immunohistochemistry

Mouse brains were prepared for immunohistochemical analysis by transcardiac perfusion. Ksilazol and basilazin were used as anesthetic agents (20 µl basilazin + 64 µl ksilazol + 66 µl 0.9% NaCl solution) for each animal. After mouse was fading off, tail and hand reflexes were controlled. Mouse was immobilized lying on their backward and their faces were upward. Incision was made through with surgical scissors and their diaphragm was separated from chest. Using forceps mouse chest was secured. The needle was inserted in the left-down part of ventricle. Right atrium was cut by scissor and 0.9% NaCl solution (pH 7.4) was infused to organs. 10-15 ml NaCl was circulated into body until blood was completely thrown upon the body. Later, NaCl switched to 4% freshly prepared formaldehyde fixation solution. 15-20 ml of formaldehyde circulation was enough to fix all organs. Later, mouse was decapitated by surgical scissors and the brain tissues were carefully collected. Collected brain samples were incubated in 4% paraformaldehyde solution at 4^{o}C for overnight. Samples were incubated in 10% and 20% sucrose in 0.2 M Phosphate Buffer Saline (PBS, pH 7, 6) at 4^{o}C for 2 hours, and incubated in 30% sucrose in 0.2 M Phosphate Buffer Saline (PBS, pH 7, 6) at 4^{o}C for overnight. Brain samples were then embedded with OCT (optimal cutting temperature) into cryomolds in the position with olfactory bulbs facing upwards. Cryomolds were slowly frozen in dry-CO_2 buckets filled with dry ice for 30 minutes. Tissues were kept into -80^{o}C for later use. The temperature of the cryostat chamber (Leica CM1850UV) was set to - 22^{o}C. The tissue was placed in the chamber of the cryostat and the temperature allowed equilibrating for at least 30 minutes. Ten micron thick sections were coronally sectioned and collected onto adhesive-coated slides at -20^{o}C. Tissue sections were stored at -80^{o}C, unless they immediately were used for further immunostaining procedure (Schneider Gasser et al. 2006; Risher et al. 2014).

2.12.1. GM2 Antibody Staining

Slides were chosen according to size of hippocampus region. Slides were incubated on ice for 15-20 minutes and sections with similar sizes of the hippocampal region were washed for 10 minutes in PBS one time at room temperature. Then, sections were incubated in ice-cold acetone for 15 minutes to open pores on the brain tissues. Later, sections were washed in PBS 5 minutes for two times at room temperature. Sections were blocked in 10% Normal Goat Serum in PBS containing %1 glycine for 1 hour at room temperature Primary GM2 antibody (KM966, Hakko-Kırın, Japan) were diluted in blocking solution. 1:500 diluted GM2 antibody was applied on the slides. Sections were incubated overnight at 4°C with primary antibodies. The other day, slides were washed in PBS 5 minutes for three times at room temperature. Secondary Pierce Goat anti-Human Cross Adsorbe antibody (DyLight488) (Thermo) was added (1:500 in blocking solution) for 1 hour at room temperature at dark. Then, slides were washed in PBS 5 minutes for four times at room temperature. Slides were mounted with DAPI (ab104139, ABCAM) and images were acquired and quantified on the OLYMPUS BX53 fluorescence microscope.

2.13. Statistical Analysis

All data were processed and analyzed using Excel (Microsoft software). All expression experiments and behavioral analyses statistical differences between animals were tested by two-tailed student's t-test. Densitometry analyses of Thin Layer Chromatography for band size were performed using Image J 1.49v.

CHAPTER 3

RESULTS

3.1. Genotyping of Mice

The genotypes of mice for Neu4, HexA and Galgt1 alleles were determined by the PCR with allele specific primers as mentioned in Material and Methods Chapter.

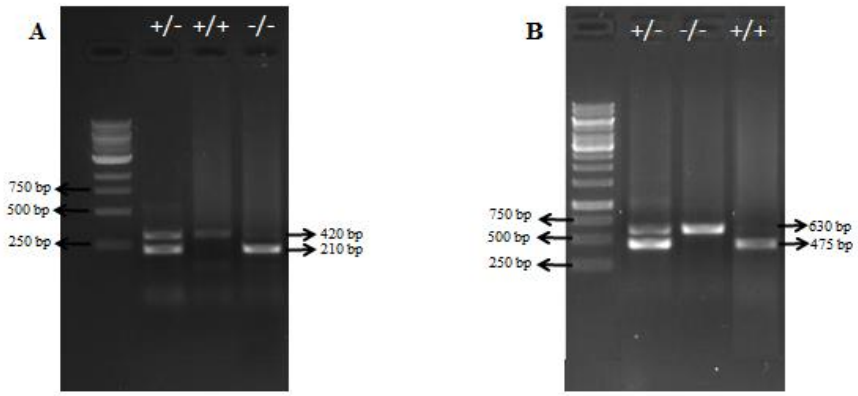

Figure 3.1. Gel images of HexA and Neu4 mice. A. HexA PCR products (wild type allele: 400bp, knock-out allele: 200bp) and B. Neu4 PCR products (wild type allele: 400bp, knock-out allele: 600bp)

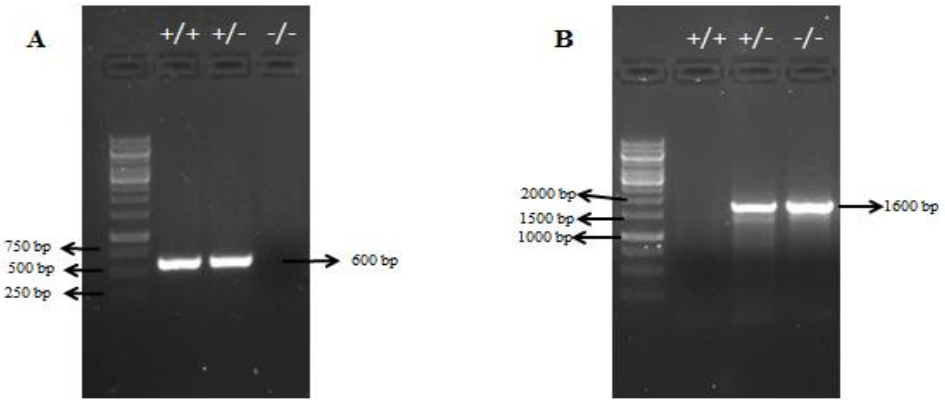

Figure 3.2. Gel images of Galgt1 mice. A. Wild type allele specific PCR product (600bp) and B. Knock out allele specific PCR product (1600bp)

3.2. Thin Layer Chromatography

Thin layer chromatography analyses were performed as described in the materials and methods chapter. Analyses were performed in eight groups of mice in two different ages. For age matched control, Neu4$^{-/-}$, HexA$^{-/-}$, Galgt1$^{-/-}$, Neu4$^{-/-}$HexA$^{-/-}$, HexA$^{-/-}$Galgt1$^{-/-}$, Neu4$^{-/-}$Galgt1$^{-/-}$, Neu4$^{-/-}$HexA$^{-/-}$Galgt1$^{-/-}$, gangliosides were analyzed with thin layer chromatography and orcinol staining. TLC was performed for three (Figure 3.3 and 3.5) and six (Figure 3.7 and 3.9) months of age mice groups for both acidic and neutral gangliosides. As standard, total lipids (LacCer, GM1, GD3, GD1a, GD1b, and Gt1b) and GM3, GM1 and GD3 gangliosides were used. Densitometry analyses of band size were performed using Image J 1.49v.

Figure 3.3 shows Thin Layer Chromatography and orcinol staining for acidic gangliosides for 3-month-old mice. For HexA$^{-/-}$ and Neu4$^{-/-}$HexA$^{-/-}$ mice, as expected, accumulation of ganglioside GM2 occurred (Seyrantepe et al. 2010). Accumulation of GM2 ganglioside was higher in Neu4$^{-/-}$HexA$^{-/-}$ double deficient mice when compared with HexA$^{-/-}$ mice (Figure 3.4 C). As previously shown, in Galgt1$^{-/-}$ mice, only synthesis and accumulation simple gangliosides LacCer, GM3 and GD3 occurs (Liu et al. 1999). As expected, for Galgt1$^{-/-}$, HexA$^{-/-}$Galgt1$^{-/-}$, Neu4$^{-/-}$Galgt1$^{-/-}$ and Neu4$^{-/-}$HexA$^{-/-}$Galgt1$^{-/-}$ mice, there was only accumulation of those simple gangliosides. Accumulation of ganglioside GM3 and GD3 was much higher in HexA$^{-/-}$Galgt1$^{-/-}$ than the rest of the mice (Figure 3.4.B & D).

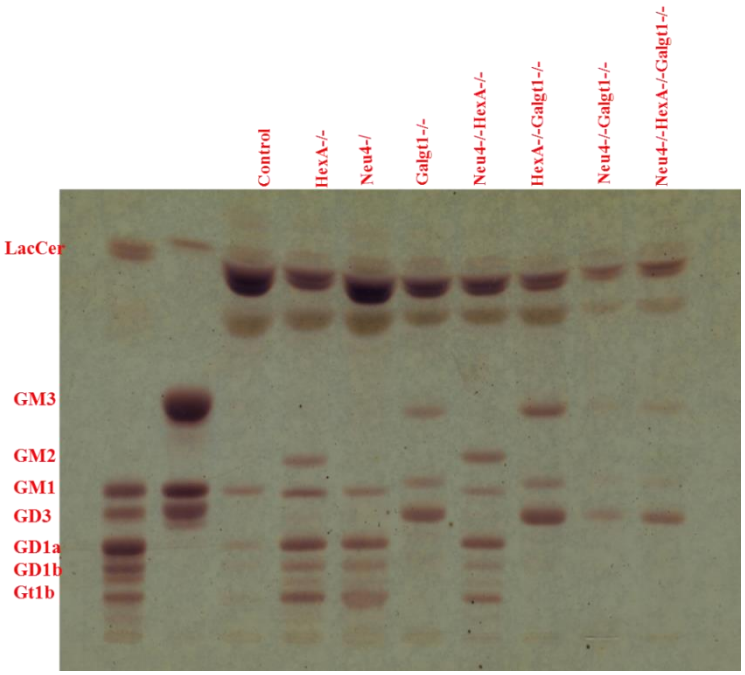

Figure 3.3. Thin layer chromatography and orcinol staining for acidic gangliosides of three-month-old Control, $HexA^{-/-}$, $Neu4^{-/-}$, $Galgt1^{-/-}$, $Neu4^{-/-}HexA^{-/-}$, $HexA^{-/-}Galgt1^{-/-}$, $Neu4^{-/-}Galgt1^{-/-}$ and $Neu4^{-/-}HexA^{-/-}Galgt1^{-/-}$ mice.

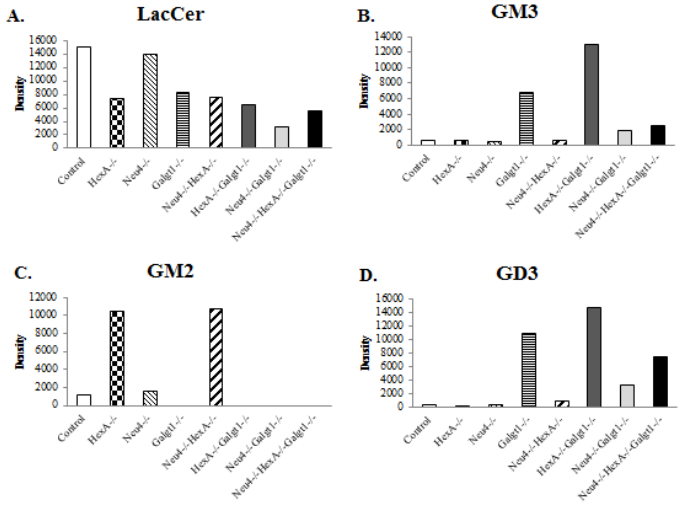

Figure 3.4. Quantification of band density of acidic ganglioisdes in TLC for three-month-old deficient mice with their control littermate. A.Lactosylceramide; B.GM3; C.GM2; D. GD3.

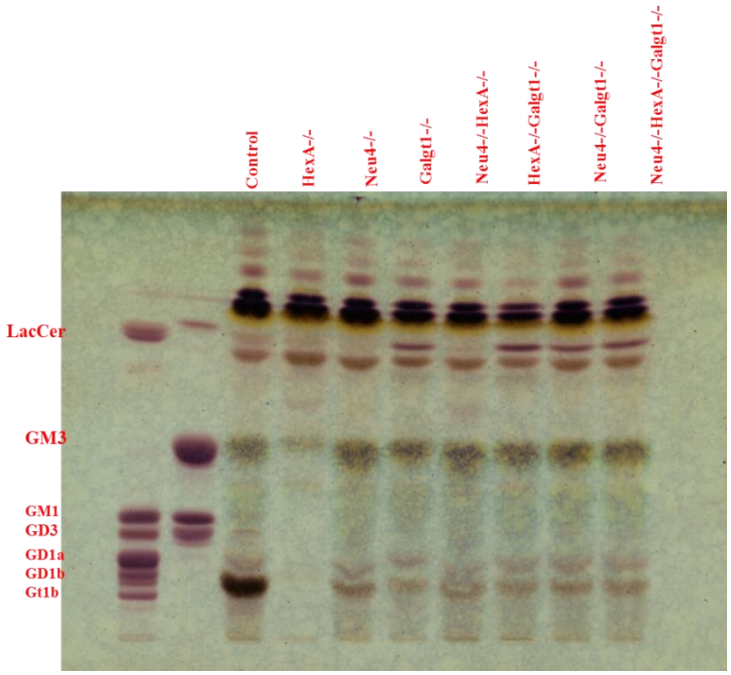

Figure 3.5. Thin layer chromatography and orcinol staining for neutral gangliosides of three-month-old Control, $HexA^{-/-}$, $Neu4^{-/-}$, $Galgt1^{-/-}$, $Neu4^{-/-}HexA^{-/-}$, $HexA^{-/-}Galgt1^{-/-}$, $Neu4^{-/-}Galgt1^{-/-}$ and $Neu4^{-/-}HexA^{-/-}Galgt1^{-/-}$ mice.

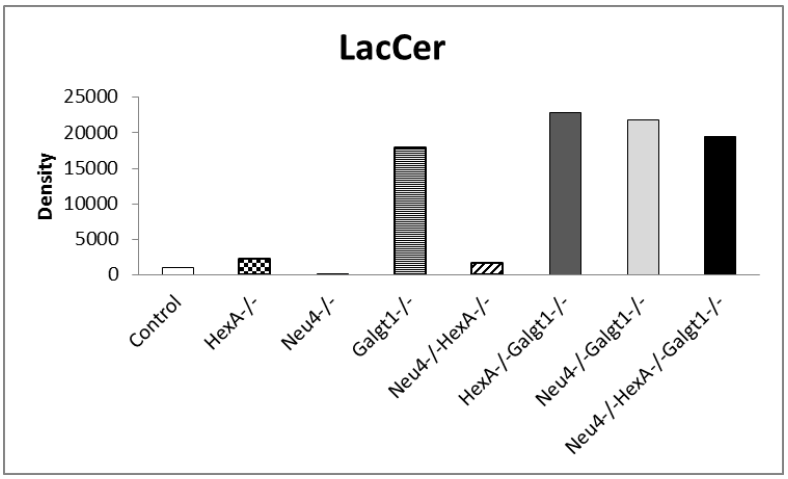

Figure 3.6. Quantification of neutral lactosylceramide band density of TLC for three-month-old deficient mice with their wild-type littermate.

Figure3.7 shows Thin Layer Chromatography and orcinol staining for acidic gangliosides for six months of old mice. Ganglioside GM2 accumulation amount was higher in $HexA^{-/-}$ mice than $Neu4^{-/-}HexA^{-/-}$ double deficient mice (Figure 3.8 C). There was no GM2 ganglioside expression in $Galgt1^{-/-}$, $HexA^{-/-}Galgt1^{-/-}$, $Neu4^{-/-}Galgt1^{-/-}$ and $Neu4^{-/-}HexA^{-/-}Galgt1^{-/-}$ mice. As previously shown, in $Galgt1^{-/-}$ mice only synthesize and accumulate simple gangliosides LacCer, GM3 and GD3 (Liu et al. 1999). As expected for $Galgt1^{-/-}$, $HexA^{-/-}Galgt1^{-/-}$, $Neu4^{-/-}Galgt1^{-/-}$ and $Neu4^{-/-}HexA^{-/-}Galgt1^{-/-}$ mice, there was only accumulation of those simple gangliosides. The accumulation amount of those simple gangliosides was higher for $Galgt1^{-/-}$ and $Neu4^{-/-}Galgt1^{-/-}$ mice when compared to control littermate (Figure 3.4.B & D).

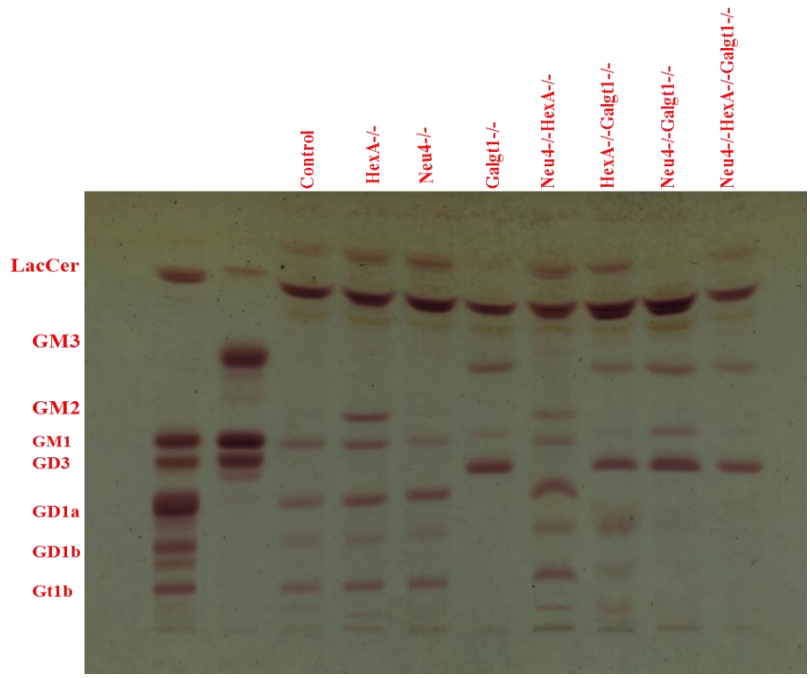

Figure 3.7 Thin layer chromatography and orcinol staining for acidic gangliosides of six-month-old Control, $HexA^{-/-}$, $Neu4^{-/-}$, $Galgt1^{-/-}$, $Neu4^{-/-}HexA^{-/-}$, $HexA^{-/-}Galgt1^{-/-}$, $Neu4^{-/-}Galgt1^{-/-}$ and $Neu4^{-/-}HexA^{-/-}Galgt1^{-/-}$ mice. In the experiment n=1.

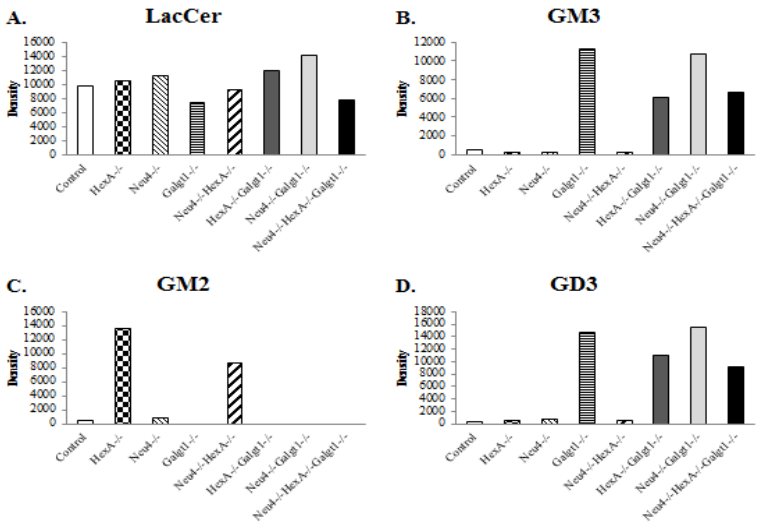

Figure 3.8. Quantification of band density of acidic gangliosides in TLC for six-month-old deficient mice with their wild-type littermates. A. Lactosylceramide; B.GM3; C.GM2; D. GD3.

Figure 3.9 shows Thin Layer Chromatography and orcinol staining for neutral gangliosides for six month of old mice. When general ganglioside pattern of all genotypes were similar, there was only accumulation of LacCer for Galgt1$^{-/-}$, HexA$^{-/-}$ Galgt1$^{-/-}$, Neu4$^{-/-}$Galgt1$^{-/-}$ and Neu4$^{-/-}$HexA$^{-/-}$Galgt1$^{-/-}$ mice. According to figure 3.10 LAcCer accumulations was higher in Galgt1$^{-/-}$ and Neu4$^{-/-}$Galgt1$^{-/-}$ mice when compared with the control littermate.

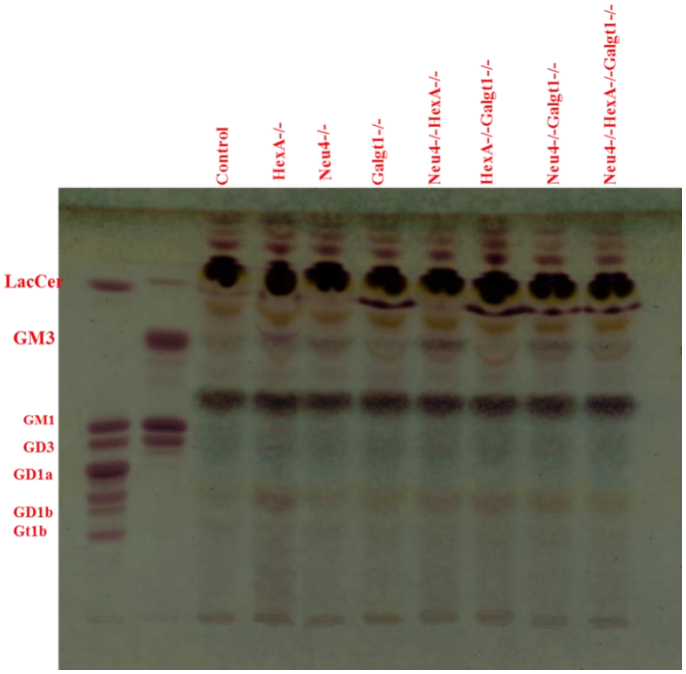

Figure 3.9 Thin layer chromatography and orcinol staining for neutral gangliosides of six-month-old Control, HexA$^{-/-}$, Neu4$^{-/-}$, Galgt1$^{-/-}$, Neu4$^{-/-}$HexA$^{-/-}$, HexA$^{-/-}$ Galgt1$^{-/-}$, Neu4$^{-/-}$Galgt1$^{-/-}$ and Neu4$^{-/-}$HexA$^{-/-}$Galgt1$^{-/-}$ mice.

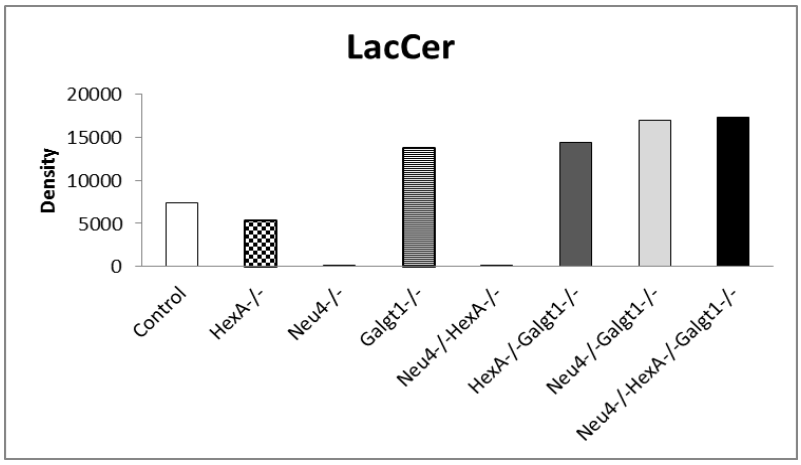

Figure 3.10. Quantification of lactosylceramide band density in TLC for six-month-old deficient mice with their wild-type littermate

3.3. Real Time PCR

Real time PCR analyses has been optimized for our laboratory conditions and then all samples were analyzed in that condition as described in the Material Method chapter. For age matched Control, $HexA^{-/-}$, $Neu4^{-/-}$, $Galgt1^{-/-}$, $Neu4^{-/-}HexA^{-/-}$, $HexA^{-/-}Galgt1^{-/-}$, $Neu4^{-/-}Galgt1^{-/-}$ and $Neu4^{-/-}HexA^{-/-}Galgt1^{-/-}$ mice, expression levels of different synthesis and degradation genes were analyzed with real time PCR. GAPDH was used as internal control since it is a housekeeping gene.

At the beginning, statistical analyses were conducted using two-way ANOVA in Excel. However, sample size used in RT-PCR was not even and small to find significant differences (n=3). According to two-way ANOVA results, there were no significant differences among genotypes and ages. So, it was looked other tests. It was used two-tailed unpaired-t tests. Normally, cut-off 0.05 for an unpaired t-test, but in this experiment, there was seven knock-out and one control conditions in two ages, because of this; it was divided p-value cut-off by 8. In order for to get significant results, new p-values became < .00625. As mentioned in aim, it was aimed to understand the effect of sialidase Neu4 in glycosphingolipid metabolism. So, each group was compared with its control and $Neu4^{-/-}$ littermates. Also, each group was compared with each other.

GM3S enzyme plays role in synthesis of GM3 ganglioside from LacCer by adding sialic acid residue into lactose. For three months of age $Neu4^{-/-}$ mice, expression rate of GM3S was increased (p=0.06) when compared to control littermate. There was no statistically difference between expression rates of GM3S in $HexA^{-/-}$ (p=0.4) and $Galgt1^{-/-}$ (p=0.02) mice when compared with control mice. On the other hand, single deficient $Galgt1^{-/-}$ (p=0.0008), double deficient $Neu4^{-/-}Galgt1^{-/-}$ (p=0.004) and triple deficient $Neu4^{-/-}HexA^{-/-}Galgt1^{-/-}$ (p=0.002) was significantly different from $Neu4^{-/-}$ mice (Figure 3.11A). For six-month-age mice old group, there was no statically difference between $HexA^{-/-}$, $Neu4^{-/-}$ and $Galgt1^{-/-}$ mice, when compared to control littermate. However, in $Neu4^{-/-}HexA^{-/-}Galgt1^{-/-}$ mice, expression level was increased (p=0.03) when compared with single deficient $HexA^{-/-}$, $Neu4^{-/-}$ and $Galgt1^{-/-}$ mice (Figure 3.11B). When three-month-old and six-month-old mice littermates compared with each other, there was an increase in $Neu4^{-/-}HexA^{-/-}Galgt1^{-/-}$ mice by increasing age (Figure 3.11C).

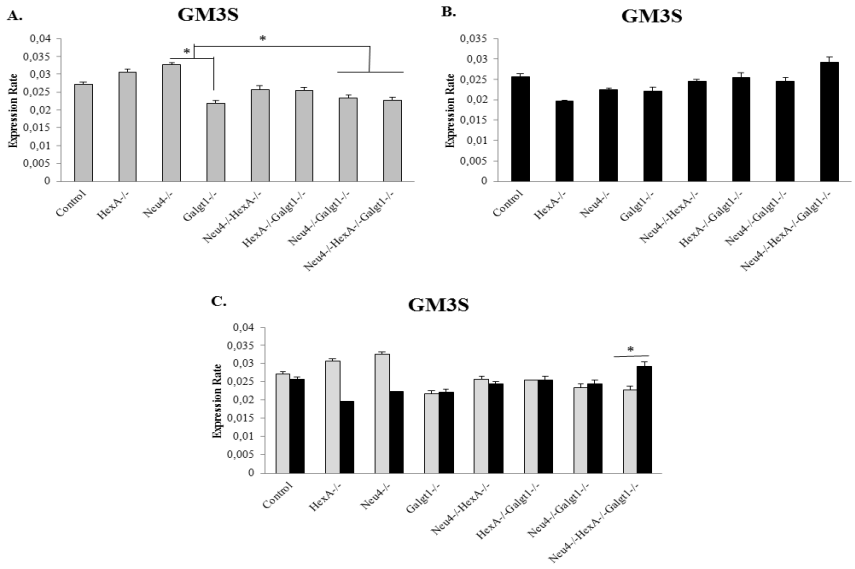

Figure 3.11. Real Time PCR results for expression levels GM3S gene for Control, $HexA^{-/-}$, $Neu4^{-/-}$, $Galgt1^{-/-}$, $Neu4^{-/-}HexA^{-/-}$, $HexA^{-/-}Galgt1^{-/-}$, $Neu4^{-/-}Galgt1^{-/-}$ and $Neu4^{-/-}HexA^{-/-}Galgt1^{-/-}$ mice. A. expression levels in three-month-old mice; B. expression levels in six-month-old mice; C. Together representation of three-and six-month-old mice. In the experiment n=3. p values were calculated using t-test (p*<0.0065). Error bars were calculated as ±SEM.

GD3 Synthase (GD3S) takes role in the synthesis of ganglioside GD3 by adding sialic acid residue to lactose moiety of GM3. When compared to control littermate expression of GD3S gene were increased significantly in $HexA^{-/-}$ mice (p=0.003). Also, expression level of GD3S was significantly increased in $HexA^{-/-}$ mice when compared to $Galgt1^{-/-}$ (p=0.001), $HexA^{-/-}Galgt1^{-/-}$ (p=0.0002), $Neu4^{-/-}Galgt1^{-/-}$ (p=0.0001) and $Neu4^{-/-}HexA^{-/-}Galgt1^{-/-}$ (p=0.0001) mice (Figure3.12A). For six months of age mice, expression levels of GD3S gene were not significantly changed (Figure 3.12 B). When three- and six-month-old mice littermates compared with each other, there was no significant increase or decrease occurred.

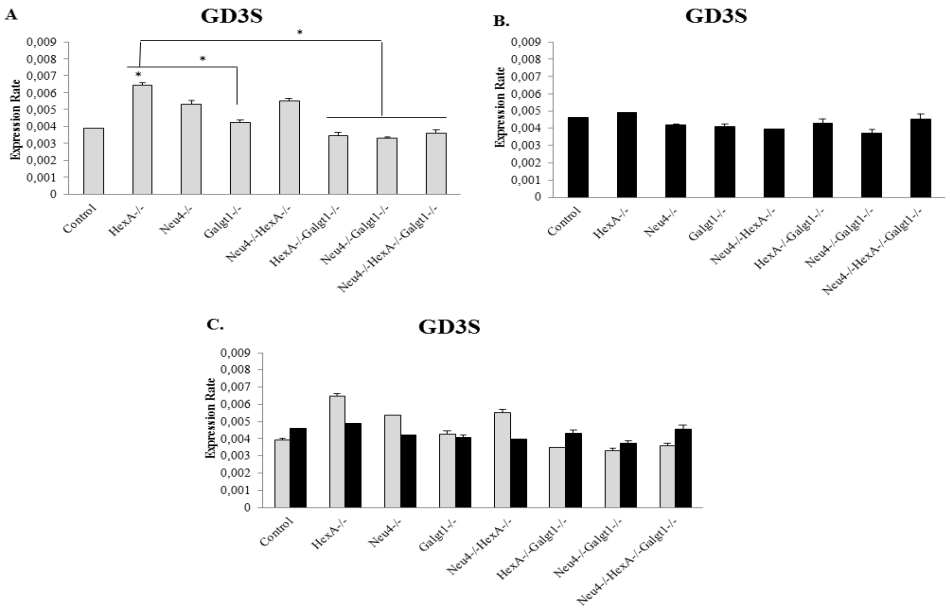

Figure 3.12. Real Time PCR results for expression levels GD3S gene for Control, $HexA^{-/-}$, $Neu4^{-/-}$, $Galgt1^{-/-}$, $Neu4^{-/-}HexA^{-/-}$, $HexA^{-/-}Galgt1^{-/-}$, $Neu4^{-/-}Galgt1^{-/-}$ and $Neu4^{-/-}HexA^{-/-}Galgt1^{-/-}$ mice. Figure representation: A. expression levels in three-month-old mice; B. expression levels in six-month-old mice; C. Together representation of three-and six-month-old mice. In the experiment n=3. p values were calculated using t-test ($p^*<0.0065$). Error bars were calculated as ±SEM.

Galgt1 is a transferase enzyme and plays a role in the synthesis of complex gangliosides by adding N-acetylneuraminic acid residue to GM3, GD3 and GT3 to synthesize ganglioside GM2, GD2 and GT2. In $Galgt1^{-/-}$ mice, it was expected to no expression of Galgt1 gene. As expected, there was no expression of Galgt1 gene in

Galgt1$^{-/-}$, HexA$^{-/-}$Gagt1$^{-/-}$, Neu4$^{-/-}$Galgt1$^{-/-}$ and Neu4$^{-/-}$HexA$^{-/-}$Galgt1$^{-/-}$ mice (Figure 3.13). For three-month-old mice, there was no significant change occurred in expression levels of Galgt1 gene for HexA$^{-/-}$, Neu4$^{-/-}$ and Neu4$^{-/-}$HexA$^{-/-}$ mice when compared with the control littermate (Figure 3.13A). For six-months-old mice, expression rate of Galgt1, increased in Neu4$^{-/-}$ and decreased for HexA$^{-/-}$ mice. HexA works in the opposite direction with the Galgt1 enzyme. Decrease in the expression levels of Galgt1 gene in six-month-old mice (when compared with the three-month-old mice) might be age dependent (Figure 3.13 C).

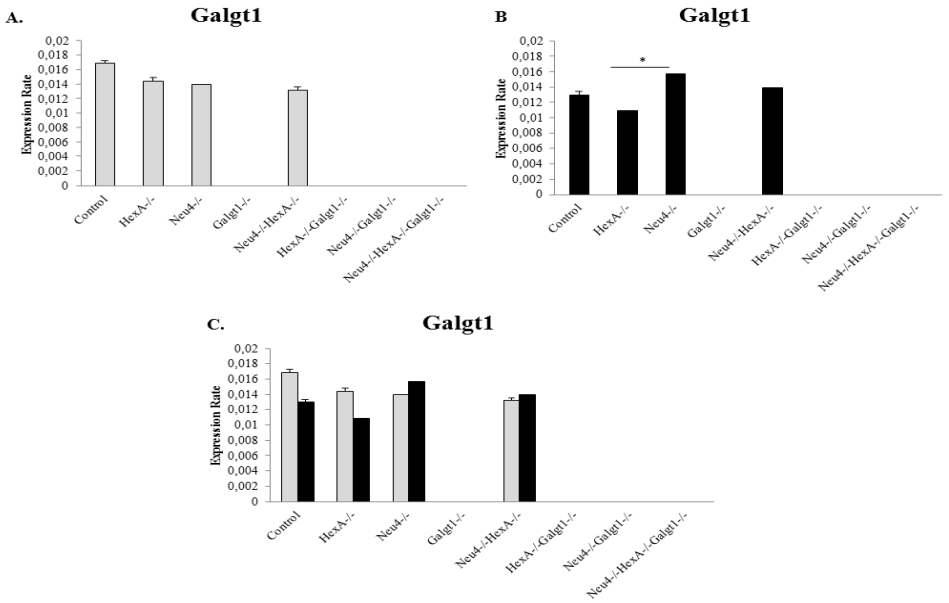

Figure 3.13. Real Time PCR results for expression levels Galgt1 gene for Control, HexA$^{-/-}$, Neu4$^{-/-}$, Galgt1$^{-/-}$, Neu4$^{-/-}$HexA$^{-/-}$, HexA$^{-/-}$Galgt1$^{-/-}$, Neu4$^{-/-}$ Galgt1$^{-/-}$ and Neu4$^{-/-}$HexA$^{-/-}$Galgt1$^{-/-}$ mice. A. expression levels in three-month-old mice; B. expression levels in six-month-old mice; C. Together representation of three-and six-month-old mice. In the experiment n=3. p values were calculated using t-test (p*<0.0065). Error bars were calculated as ±SEM.

B3Galt4 is an enzyme that converts GA2 into GA1 by adding lactose residue into N-acetylneuraminic acid residue. B3Galt4 is one of the key enzymes in the 0-series ganglioside production. In three-month-old mice group mice, expression rate of B3Galt4 gene was decreased in Galgt1$^{-/-}$ mice when compared to Neu4$^{-/-}$ (p=0.05) and HexA$^{-/-}$ (p=0.03) littermates. Also, expression rate of B3Galt4 gene was significantly

decreased in Neu4$^{-/-}$Galgt1$^{-/-}$ mice when compared to Neu4$^{-/-}$ (p=0.006) and HexA$^{-/-}$ (p=0.003) littermates. Decreased expression rate in Galgt1-/- mice, were not compensated (Figure 3.14A). For six-month-old mice group there was no significant change in the expression levels of B3Galt4 gene (Figure 3.14B). Again, between three- and six-month-old mice groups no significant change observe between littermates (Figure 3.14C).

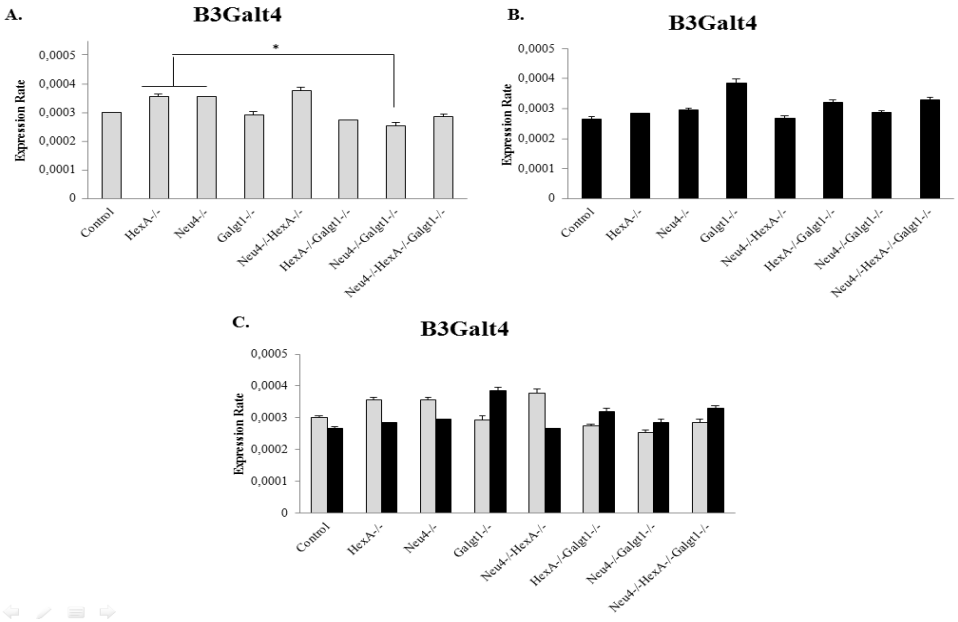

Figure 3.14. Real Time PCR results for expression levels B3Galt4 gene for Control, HexA$^{-/-}$, Neu4$^{-/-}$, Galgt1$^{-/-}$, Neu4$^{-/-}$HexA$^{-/-}$, HexA$^{-/-}$Galgt1$^{-/-}$, Neu4$^{-/-}$ Galgt1$^{-/-}$ and Neu4$^{-/-}$HexA$^{-/-}$Galgt1$^{-/-}$ mice. Figure representation: A. expression levels in three-month-old mice; B. expression levels in six-month-old mice; C. Together representation of three-and six-month-old mice. In the experiment n=3. p values were calculated using t-test (p*<0.0065). Error bars were calculated as ±SEM.

B4Galt6 enzyme converts GlcCer into LacCer by adding lactose moiety into glucose. That enzyme has role in the very beginning of the ganglioside synthesis pathway. In three months of age mice group in the Neu4$^{-/-}$HexA$^{-/-}$Galgt1$^{-/-}$ mice, expression rate of B4Galt6 gene was significantly decreased when compared to control littermates (p=0.004). Also, expression levels of B3Galt4 gene has increased in Neu4$^{-/-}$ Galgt1$^{-/-}$ mice when compared to Neu4$^{-/-}$ mice (p=0.04). Increasing of expression rate in in Neu4$^{-/-}$Galgt1$^{-/-}$ mice and decreasing in Neu4$^{-/-}$HexA$^{-/-}$Galgt1$^{-/-}$ mice were significant

between two genotypes (p=0.002) (Figure 3.15A). For six-month-old mice group there was no significant change in the expression levels of B4Galt6 gene (Figure 3.15B). Again, between three-and six-month-old mice groups there was no significant change between littermates occurred (Figure 3.14C).

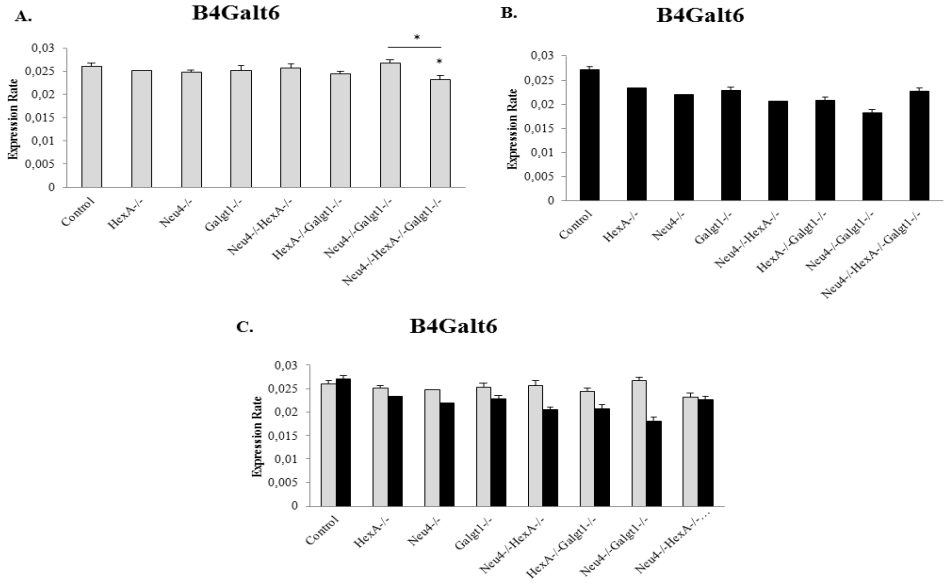

Figure 3.15. Real Time PCR results for expression levels B4Galt6 gene for Control, $HexA^{-/-}$, $Neu4^{-/-}$, $Galgt1^{-/-}$, $Neu4^{-/-}HexA^{-/-}$, $HexA^{-/-}Galgt1^{-/-}$, $Neu4^{-/-}Galgt1^{-/-}$ and $Neu4^{-/-}HexA^{-/-}Galgt1^{-/-}$ mice. Figure representation: A. expression levels in three-month-old mice; B. expression levels in six-month-old mice; C. Together representation of three-and six-month-old mice. In the experiment n=3. p values were calculated using t-test (p*<0.0065). Error bars were calculated as ±SEM.

β-gal is an enzyme that takes role in the a-series of degradation pathway of gangliosides by removing lactose residue linked to N-neuraminic acid residue of GM1. In three-month-old mice, there was no significant change in the expression level of β-gal when compared with control littermate. However, there was a slight decrease in the expression rate of β-gal in $Neu4^{-/-}Galgt1^{-/-}$ mice when compared with $Neu4^{-/-}$ and $Galgt1^{-/-}$ mice (Figure 3.16A). In six-month-old mice group, β-gal expression rate was increased in $HexA^{-/-}$ mice when compared with the $Neu4^{-/-}$ (p=0.0005) and $Galgt1^{-/-}$ (p=0.002) mice. For $Neu4^{-/-}HexA^{-/-}Galgt1^{-/-}$ mice, expression rate of β-gal was significantly decreased when compared with the $HexA^{-/-}$ mice (Figure 3.16B). There

was no significant change in expression level of β-gal between three- and six-month-old mice (Figure 3.16C).

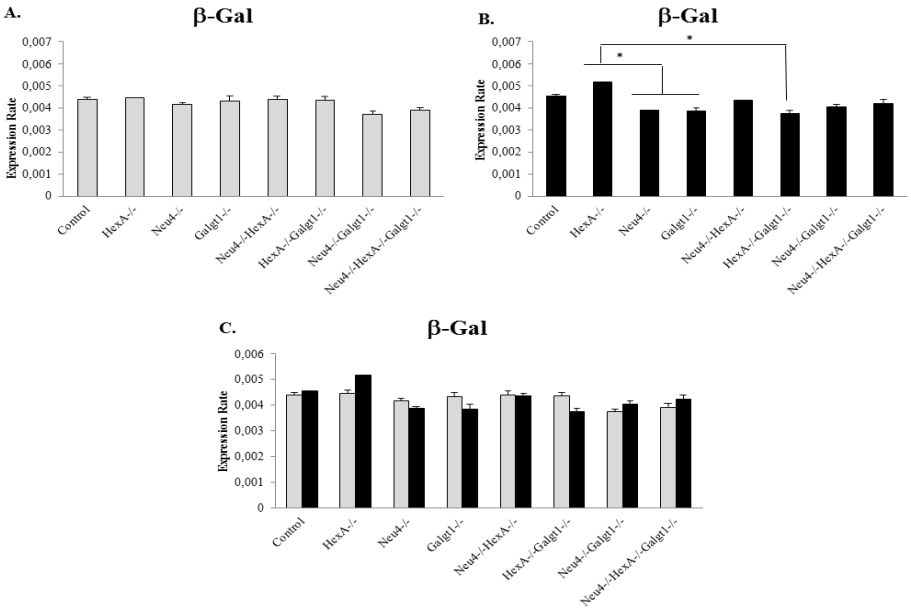

Figure 3.16. Real Time PCR results for expression levels β-galactosidase gene for Control, $HexA^{-/-}$, $Neu4^{-/-}$, $Galgt1^{-/-}$, $Neu4^{-/-}HexA^{-/-}$, $HexA^{-/-}Galgt1^{-/-}$, $Neu4^{-/-}Galgt1^{-/-}$ and $Neu4^{-/-}HexA^{-/-}Galgt1^{-/-}$ mice. Figure representation: A. expression levels in three-month-old mice; B. expression levels in six-month-old mice; C. Together representation of three-and six-month-old mice. In the experiment n=3. p values were calculated using t-test ($p^*<0.0065$). Error bars were calculated as ±SEM.

GM2-Activator Protein (GM2AP) removes mature GM2 from intraendosamal membrane and by making a Michaelis-Menten Complex with HexA protein to further degrade ganglioside GM2 into ceramide. In three-month-old mice, there was an increase in the expression level of GM2AP in $Neu4^{-/-}Galgt1^{-/-}$ mice when compared with control (p= 2,87E+09), $HexA^{-/-}$ (p=0.009) $Neu4^{-/-}$ (p=0.09), $Neu4^{-/-}HexA^{-/-}$ (p=0.005), HexA-/-$Galgt1^{-/-}$ (0.0001) and $Neu4^{-/-}HexA^{-/-}Galgt1^{-/-}$ (p= 1,02E+09) mice (Figure 3.17A). In six-month- old mice group there was no significant change in expression levels of GM2AP when compared to control littermate (Figure 3.17B). There was no significant change in expression level of GM2AP between three- and six-month-old mice (Figure 3.17C).

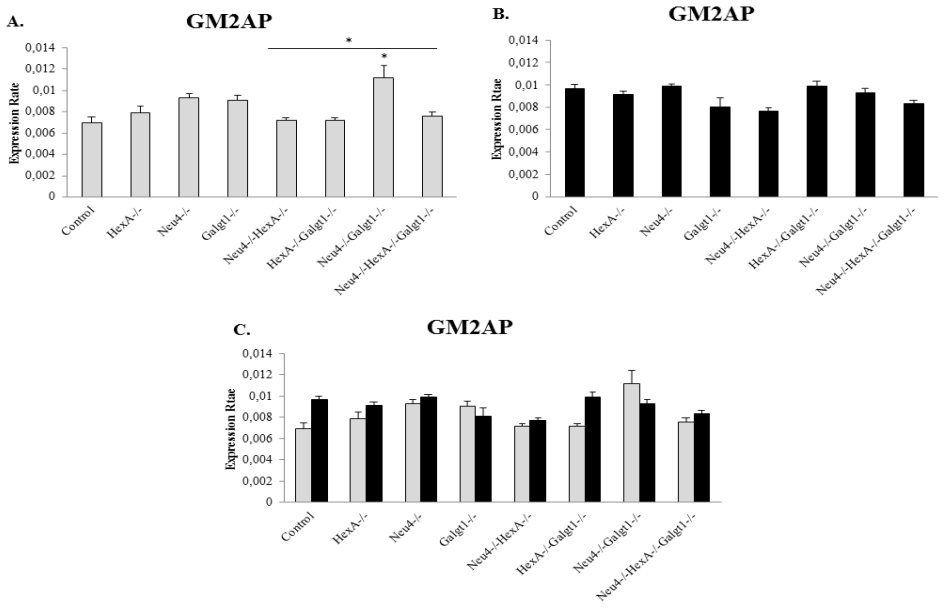

Figure 3.17. Real Time PCR results for expression levels GM2AP gene for Control, $HexA^{-/-}$, $Neu4^{-/-}$, $Galgt1^{-/-}$, $Neu4^{-/-}HexA^{-/-}$, $HexA^{-/-}Galgt1^{-/-}$, $Neu4^{-/-}Galgt1^{-/-}$ and $Neu4^{-/-}HexA^{-/-}Galgt1^{-/-}$ mice. Figure representation: A. expression levels in three-month-old mice; B. expression levels in six-month-old mice; C. Together representation of three-and six-month-old mice. In the experiment n=3. p values were calculated using t-test ($p^*<0.0065$). Error bars were calculated as ±SEM.

β-hexosaminidase B (HexB) is an enzyme that is composed of two β-subunits. β-HexB metabolizes GA2 into LacCer by removing N-acetylneuraminic acid residue linked to lactose residue in O-series ganglioside degradation pathway. In the deficiency of HexB Sandhoff's Disease occurs. For three-month-old mice, expression rate of HexB was significantly increased when compared with the $Neu4^{-/-}$ ($p=0.002$) and $Neu4^{-/-}Galgt1^{-/-}$ ($p=0.0008$) littermates (Figure 3.18A). In six-month- old mice group there was no significant change in expression levels of HexB when compared to control littermate (Figure 3.18B). When three- and six-month-old old mice groups compared no significant change occurred in expression level of HexB among both ages (Figure 3.18C).

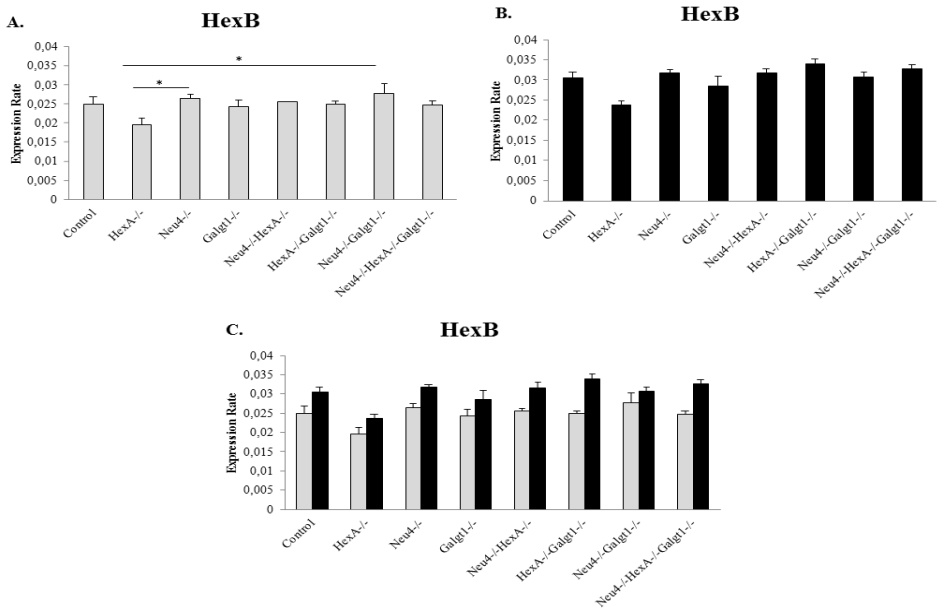

Figure 3.18. Real Time PCR results for expression levels β-HexB gene for Control, $HexA^{-/-}$, $Neu4^{-/-}$, $Galgt1^{-/-}$, $Neu4^{-/-}HexA^{-/-}$, $HexA^{-/-}Galgt1^{-/-}$, $Neu4^{-/-}Galgt1^{-/-}$ and $Neu4^{-/-}HexA^{-/-}Galgt1^{-/-}$ mice. Figure representation: A. expression levels in three-month-old mice; B. expression levels in six-month-old mice; C. Together representation of three-and six-month-old mice. In the experiment n=3. p values were calculated using t-test ($p^*<0.0065$). Error bars were calculated as ±SEM.

Sialidase NEU1 is located mostly in lysosomes and it is associated with a carboxypeptidase protective protein cathepsin A (CathA) and β-galactosidase enzyme. CathA stabilizes active form of sialidase and protects it against rapid proteolytic degradation in the lysosome (D'Azzo et al. 1982). Deficiency and/or malfunction of NEU1 is linked to sialidosis and galactosialidosis which are lysosomal storage diseases with skeletal abnormalities and neurological degeneration (Dridi et al. 2013). In three-month-old mice expression levels of Neu1 were increased in $Neu4^{-/-}Galgt1^{-/-}$ ($p=0.005$) mice when compared with the control littermate (Figure 3.19A). Also, when compared with the $Neu4^{-/-}$ and $Galgt1^{-/-}$ mice, there was a significant increase in the expression rate of Neu1 in $Neu4^{-/-}Galgt1^{-/-}$ mice. This change in expression levels of Neu1 were not observed in six-month-old mice group (Figure 3.19B). There was no significant change in expression level of Neu1 between three- and six-month-old mice (Figure 3.19C).

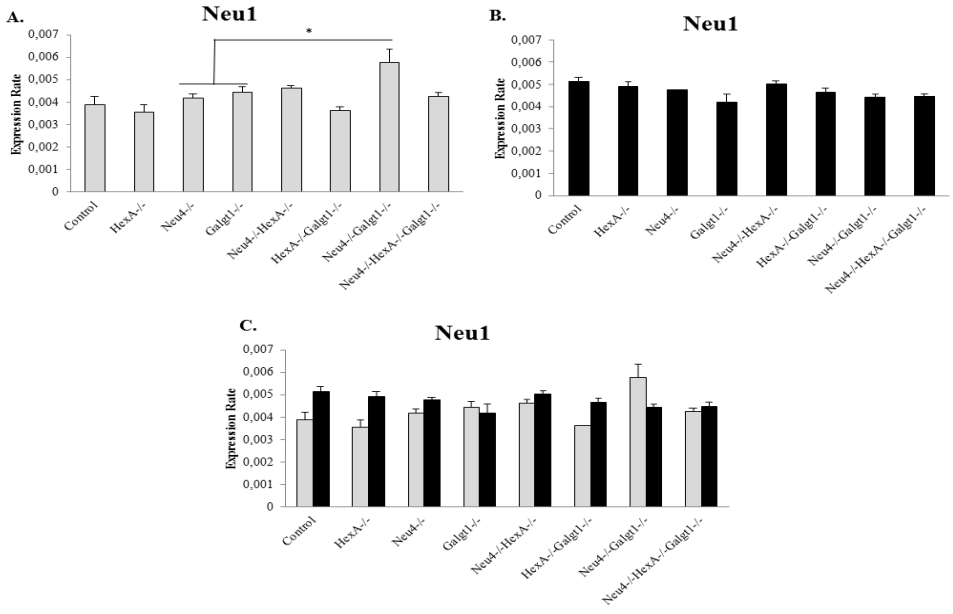

Figure 3.19. Real Time PCR results for expression levels sialidase Neu1 gene for Control, $HexA^{-/-}$, $Neu4^{-/-}$, $Galgt1^{-/-}$, $Neu4^{-/-}HexA^{-/-}$, $HexA^{-/-}Galgt1^{-/-}$, $Neu4^{-/-}Galgt1^{-/-}$ and $Neu4^{-/-}HexA^{-/-}Galgt1^{-/-}$ mice. Figure representation: A. expression levels in three-month-old mice; B. expression levels in six-month-old mice; C. Together representation of three-and six-month-old mice. In the experiment n=3. p values were calculated using t-test ($p^*<0.0065$). Error bars were calculated as ±SEM.

Sialidase NEU2 located in cytoplasm of cells. NEU2 is able to hydrolyze glycoproteins, oligosaccharides and gangliosides. Expression of sialidase Neu2 is 100-fold less than other sialidases. However, even the expression level is too small Neu2 has a many roles in cell as mentioned in introduction part. There was no significant change observed in expression levels of Neu2 in three months of age when compared to control littermate. When compared with the $Neu4^{-/-}$ mice, there was an increase in expression rate of Neu2 in $HexA^{-/-}$ ($p=0.07$) $Neu4^{-/-}HexA^{-/-}$ ($p=0.04$) and $Neu4^{-/-}HexA^{-/-}Galgt1^{-/-}$ ($p=0.04$) mice. Also, when compared with the $HexA^{-/-}$ ($p=0.009$) and $Galgt1^{-/-}$ ($p=0.007$) mice, there was an increase in the expression rate of sialidase Neu2 in $HexA^{-/-}Galgt1^{-/-}$ mice (Figure 3.20A). When six months of age mice were examined, expression levels of Neu2 were increased in $Neu4^{-/-}$ animal when compared with the $Galgt1^{-/-}$ littermate ($p=0.01$). Also, in double knock-out $Neu4^{-/-}Galgt1^{-/-}$ expression level of sialidase Neu2 was decreased when compared with the $Neu4^{-/-}$ littermate. Decreased expression levels of sialidase Neu2 in $Galgt1^{-/-}$ mice, was reduced Neu2 expression in all double and triple knock-outs of $Galgt1^{-/-}$ (figure 3.20B). Overall, between three- and

6-month-old littermates there was a decrease in Neu2 expression of $HexA^{-/-}Galgt1^{-/-}$ mice and an increase in $Neu4^{-/-}HexA^{-/-}Galgt1^{-/-}$ mice with increasing age (Figure 3.20C). However, neither of those changes was significant.

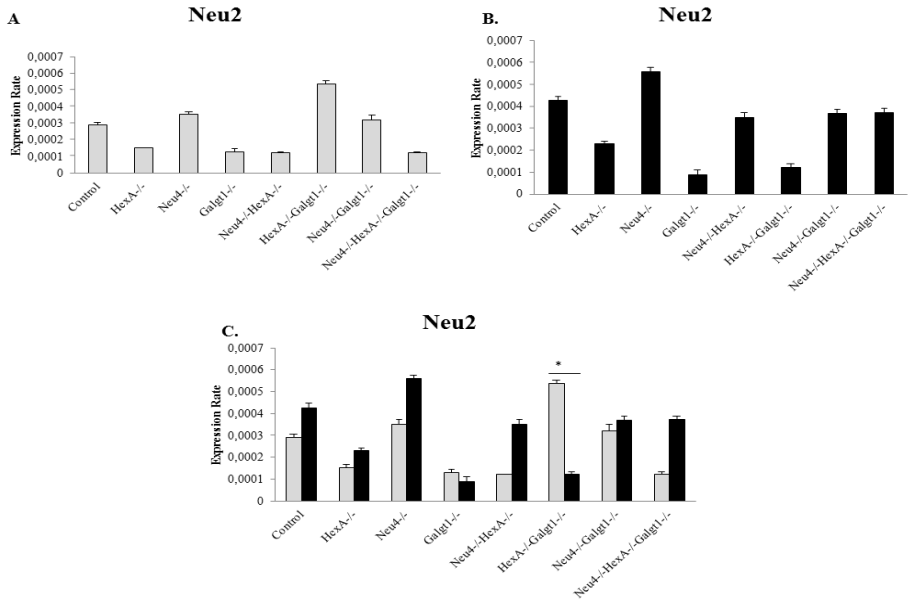

Figure 3.20. Real Time PCR results for expression levels sialidase Neu2 gene for Control, $HexA^{-/-}$, $Neu4^{-/-}$, $Galgt1^{-/-}$, $Neu4^{-/-}HexA^{-/-}$, $HexA^{-/-}Galgt1^{-/-}$, $Neu4^{-/-}Galgt1^{-/-}$ and $Neu4^{-/-}HexA^{-/-}Galgt1^{-/-}$ mice. Figure representation: A. expression levels in three-month-old mice; B. expression levels in six-month-old mice; C. Together representation of three-and six-month-old mice. In the experiment n=3. p values were calculated using t-test ($p^*<0.0065$). Error bars were calculated as ±SEM.

Sialidase NEU3 located on plasma membrane and removes sialic acid residues from gangliosides by the means of modulating cellular activation, differentiation and transformation (Stamatos et al. 2010). Sialidase NEU3 is active towards gangliosides including GM1 and GD1a (Seyrantepe et al. 2008). In three-month-old animal group there was significant increase in the expression level of Neu3 in $Neu4^{-/-}Galgt1^{-/-}$ mice when compared with control (p=0.0001), $HexA^{-/-}$ (p=0.0007),$Neu4^{-/-}$ (p=0.0001) and $Neu4^{-/-}HexA^{-/-}Galgt1^{-/-}$ (p=0.007) littermates (Figure 3.21A). There was decreased expression level of Neu3 in $Neu4^{-/-}HexA^{-/-}$ mice when compared to control and $HexA^{-/-}$ and $Neu4^{-/-}$ littermates for six-month-old mice, but it is not significant as statistically

(Figure 3.21B). Overall, between three- and six-month-old littermates there was no significant change occurred in Neu3 expression with increasing age (Figure 3.21C).

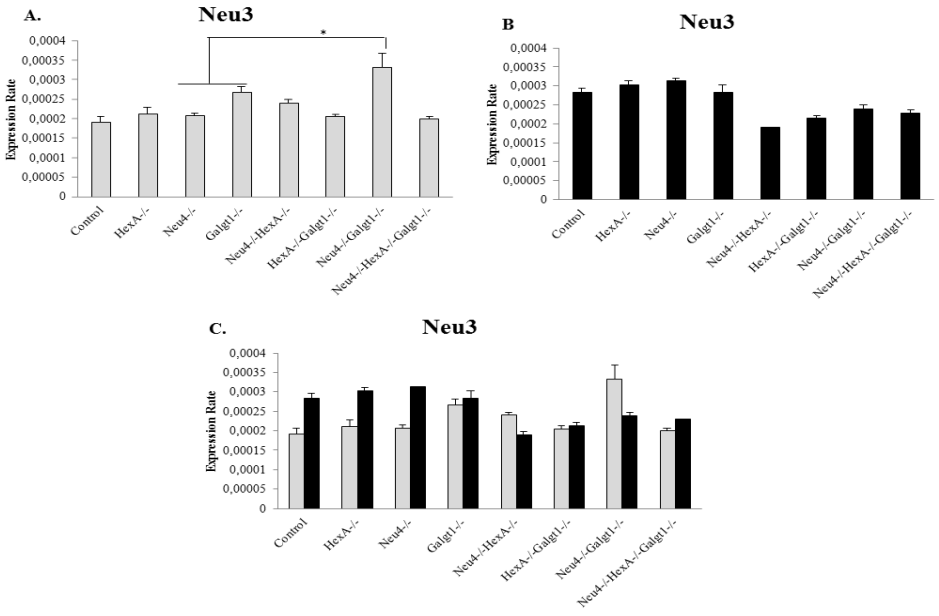

Figure 3.21. Real Time PCR results for expression levels sialidase Neu3 gene for Control, $HexA^{-/-}$, $Neu4^{-/-}$, $Galgt1^{-/-}$, $Neu4^{-/-}HexA^{-/-}$, $HexA^{-/-}Galgt1^{-/-}$, $Neu4^{-/-}Galgt1^{-/-}$ and $Neu4^{-/-}HexA^{-/-}Galgt1^{-/-}$ mice. Figure representation: A. expression levels in three-month-old mice; B. expression levels in six-month-old mice; C. Together representation of three-and six-month-old mice. In the experiment n=3. p values were calculated using t-test ($p^*<0.0065$). Error bars were calculated as ±SEM.

Sialidase NEU4 mostly located in lysosomes of cells. Sialidase Neu4 is responsible degradation of GD1a into GM1 by removing sialic acid residue. So, there was no expression of sialidase Neu4 gene for $Neu4^{-/-}$, $Neu4^{-/-}HexA^{-/-}$, $Neu4^{-/-}Galgt1^{-/-}$ and $Neu4^{-/-}HexA^{-/-}Galgt1^{-/-}$ mice, as expected. There was a decrease in expression rate of sialidase Neu4 in $HexA^{-/-}Galgt1^{-/-}$ mice when compared with the control ($p=0.0004$) and $HexA^{-/-}$ ($p=0.0007$) littermates in three-month-old mice (Figure 3.22A). In $Galgt1^{-/-}$ mice, expression rate of sialidase Neu4 were decreased significantly for six months of age when compared with the control ($p=0.0004$) and $HexA^{-/-}$ ($p=0.001$) littermates (Figure 3.22B). Overall, between three- and six-month-old littermates there was no significant change occurred in Neu4 expression with increasing age (Figure 3.22C).

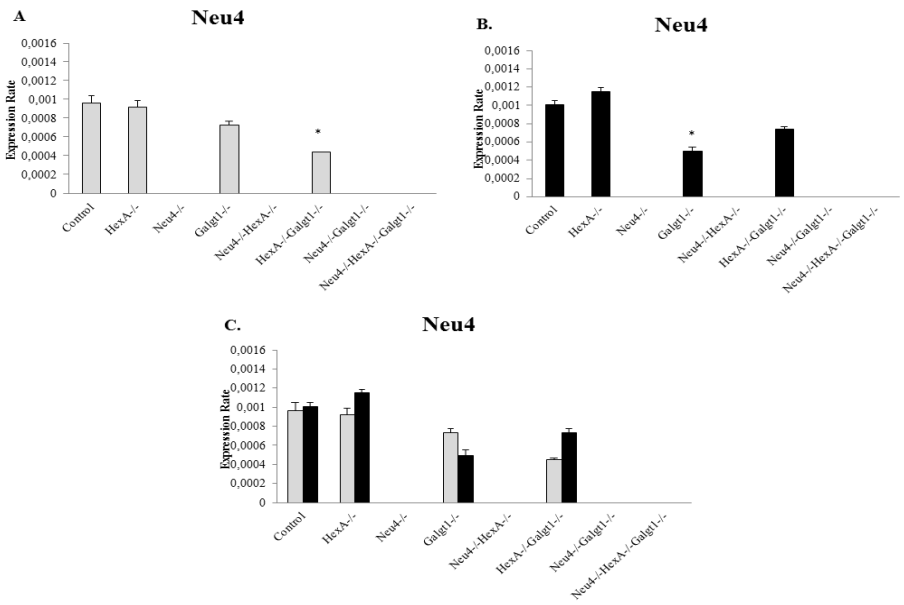

Figure 3.22. Real Time PCR results for expression levels sialidase Neu4 gene Control, $HexA^{-/-}$, $Neu4^{-/-}$, $Galgt1^{-/-}$, $Neu4^{-/-}HexA^{-/-}$, $HexA^{-/-}Galgt1^{-/-}$, $Neu4^{-/-}Galgt1^{-/-}$ and $Neu4^{-/-}HexA^{-/-}Galgt1^{-/-}$ mice. Figure representation: A. expression levels in three-month-old mice; B. expression levels in six-month-old mice; C. Together representation of three-and six-month-old mice. In the experiment n=3. p values were calculated using t-test ($p^*<0.0065$). Error bars were calculated as ±SEM.

3.4. Enzyme Activity Assay

Enzyme activity analyses were optimized in our laboratory conditions and all samples were analyzed in that conditions as described in the material method chapter. For age matched Control, $HexA^{-/-}$, $Neu4^{-/-}$, $Galgt1^{-/-}$, $Neu4^{-/-}HexA^{-/-}$, $HexA^{-/-}Galgt1^{-/-}$, $Neu4^{-/-}Galgt1^{-/-}$ and $Neu4^{-/-}HexA^{-/-}Galgt1^{-/-}$ mice enzyme activity levels of β-galactosidase, β-glucosidase, β-hexosaminidase B and sialidase Neu1 enzymes were analyzed spectrofluorometrically. Enzyme activity assays were conducted for three- and six-month-old age groups for 4 different enzymes. In the experiment for three- and six-month-old control littermates, specific enzyme activity accepted as 100% and the enzyme activity for the rest of animals calculated relatively.

β-galactosidase (β-gal) is an enzyme that takes role in the degradation pathway of gangliosides by removing lactose residue linked to N-neuraminicacid residue of GM1 to convert into GM2. In three-month-old animal group β-gal activity decreased in $Neu4^{-}$

$^{-/-}$ mice (50%). Also, β-gal activity increased in Galgt1$^{-/-}$ (116%) and Neu4$^{-/-}$HexA$^{-/-}$ Galgt1$^{-/-}$ (131%) animal. In the rest of the animals there was not much change occurred in enzyme activities (Figure 3.23A). In six-month-old animal group in HexA$^{-/-}$ and Neu4$^{-/-}$ mice, there was an increase (120%) in the enzyme activity. Again enzyme activity was the same for Neu4$^{-/-}$HexA$^{-/-}$Galgt1$^{-/-}$ (131%) animal (Figure 3.23B). When both ages were compared with each other, the most significant increase occurred in Neu4$^{-/-}$ mice. For the rest of the mice, enzyme activities were not changed much (Figure 3.23C).

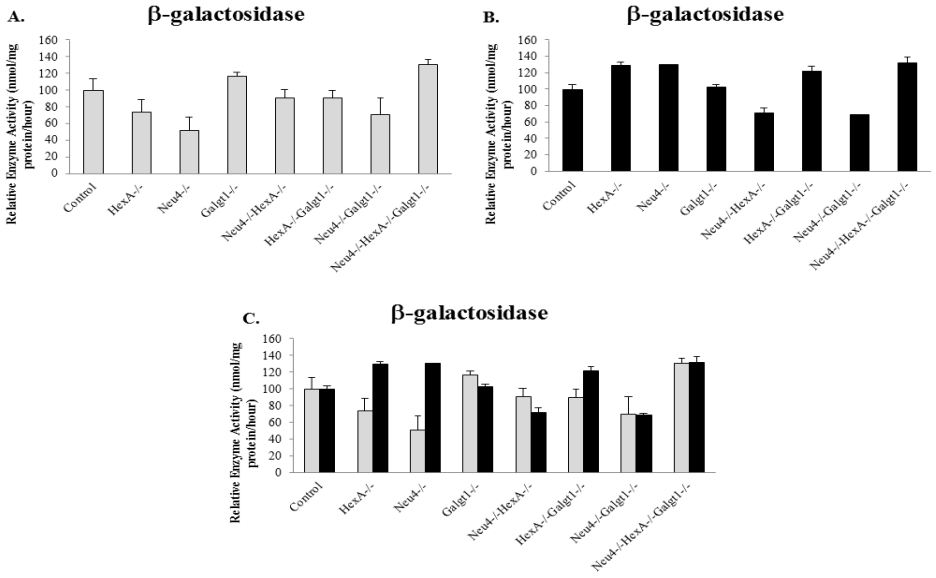

Figure 3.23. Relative enzyme activity measurement of β-galactosidase on Control, HexA$^{-/-}$, Neu4$^{-/-}$, Galgt1$^{-/-}$, Neu4$^{-/-}$HexA$^{-/-}$, HexA$^{-/-}$Galgt1$^{-/-}$, Neu4$^{-/-}$ Galgt1$^{-/-}$ and Neu4$^{-/-}$HexA$^{-/-}$Galgt1$^{-/-}$ mice. Figure representation is: A. relative enzyme activity in three-month-old mice; B. relative enzyme activity in six-month-old mice; C. Together representation of relative enzyme activities of three-and six-month-old mice. In the experiment n=3. Error bars were calculated as ±SEM.

β-glucosidase is an enzyme that is found in lysosomes. That enzyme removes glucose residues by removing glucosidic bonds. This enzyme is a housekeeping enzyme in lysosome and its deficiency causes a lysosomal storage disease; Gaucher disease. For three-month-old animals, β-glucosidase activity much more increased in Neu4$^{-/-}$ mice (160%) when compared with the control littermate. Also, β-glucosidase activity

decreased in Galgt1$^{-/-}$ (49%) animal. In the rest of the animals there was not much change in enzyme activities (Figure 3.24A). In 6-months old animal group of HexA$^{-/-}$ (148%) and HexA$^{-/-}$Galgt1$^{-/-}$ (200%) mice there is an increase in the enzyme activity. Enzyme activity was decreased for Neu4$^{-/-}$ (50%) animal (Figure 3.24B). When both ages were compared with each other, the most significant decrease was occurred in Neu4$^{-/-}$ mice and most significant increase were occurred in HexA$^{-/-}$Galgt1$^{-/-}$ mice. For the rest of the mice, enzyme activities were not changed much (Figure 3.24C).

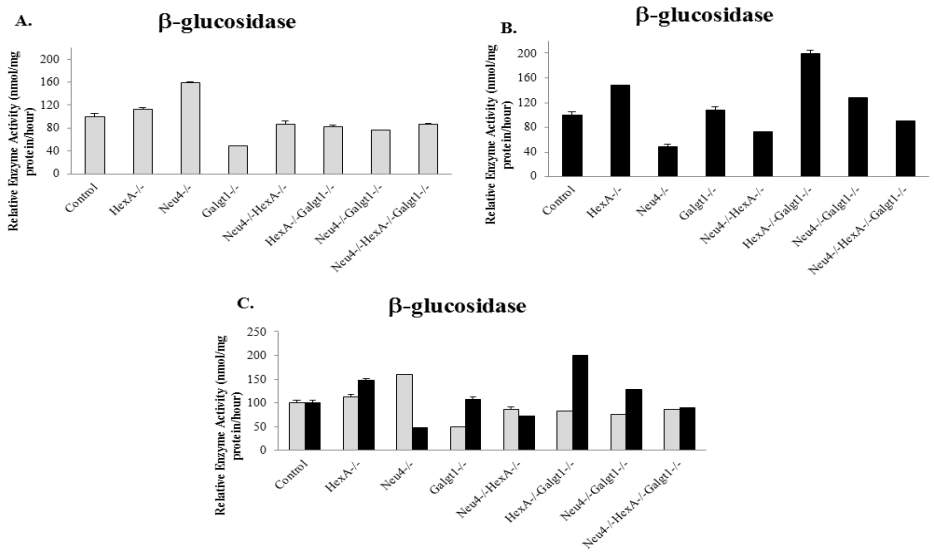

Figure 3.24. Relative enzyme activity measurement of β-glucosidase on three- and six-month-old Control, HexA$^{-/-}$, Neu4$^{-/-}$, Galgt1$^{-/-}$, Neu4$^{-/-}$HexA$^{-/-}$, HexA$^{-/-}$ Galgt1$^{-/-}$, Neu4$^{-/-}$Galgt1$^{-/-}$ and Neu4$^{-/-}$HexA$^{-/-}$Galgt1$^{-/-}$ mice. Figure representation is: A. relative enzyme activity in three-month-old mice; B. relative enzyme activity in six-month-old mice; C. Together representation of relative enzyme activities of three-and six-month-old mice. In the experiment n=3. Error bars were calculated as ±SEM.

β-hexosaminidase B (HexB) is an enzyme that is composed of two β-subunits. β-HexB metabolizes GA2 into LacCer by removing N-acetylneuraminic acid residue linked to lactose residue in o-series ganglioside degradation pathway. In the deficiency of HexB causes Sandhoff's Disease. For three-months-old mice, there was not a significant change in enzyme activities of Neu4$^{-/-}$ (85%) and Galgt1$^{-/-}$ (105%) mice. HexB activity much more increased in HexA$^{-/-}$ mice (170%). Also, HexB activity was

decreased in HexA$^{-/-}$Galgt1$^{-/-}$ (60%) mice. In the rest of the animals there was not much change in enzyme activities (Figure 3.25A). In six-month-old Neu4$^{-/-}$HexA$^{-/-}$ (133%) mice, there was an increase in the enzyme activity. Enzyme activity was decreased for Galgt1$^{-/-}$ (58%) animal (Figure 3.25B). When both ages were compared with each other, the most significant decrease was occurred in HexA$^{-/-}$ mice. For the rest of the mice, enzyme activities were not changed much (Figure 3.25C).

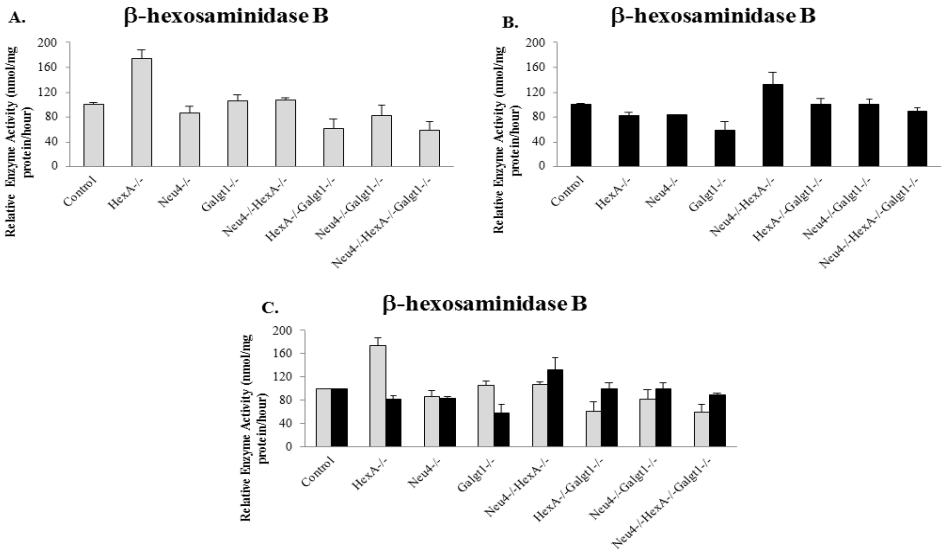

Figure 3.25. Relative enzyme activity measurement of β-hexosaminidase B on three- and six- month-old Control, HexA$^{-/-}$, Neu4$^{-/-}$, Galgt1$^{-/-}$, Neu4$^{-/-}$HexA$^{-/-}$, HexA$^{-/-}$Galgt1$^{-/-}$, Neu4$^{-/-}$Galgt1$^{-/-}$ and Neu4$^{-/-}$HexA$^{-/-}$Galgt1$^{-/-}$ mice. Figure representation is: A. relative enzyme activity in three-month-old mice; B. relative enzyme activity in six-month-old mice; C. Together representation of relative enzyme activities of three-and six-month-old mice. In the experiment n=3. Error bars were calculated as ±SEM.

Sialidase NEU1 is located mostly in lysosomes and it is associated with a carboxypeptidase protective protein cathepsin A (CathA) and β-galactosidase enzyme. CathA stabilizes active form of sialidase and protects it against rapid proteolytic degradation in the lysosome (D'Azzo et al. 1982). Deficiency and/or malfunction of NEU1 is linked to sialidosis and galactosialidosis which are lysosomal storage diseases with skeletal abnormalities and neurological degeneration (Dridi et al. 2013). Neu1 activity was decreased in three-month-old HexA$^{-/-}$Galgt1$^{-/-}$ (46%) mice. In the rest of the

mice there was not much change in enzyme activities (Figure 3.26A). In six-month-old mice group of Neu4$^{-/-}$ (132%), HexA$^{-/-}$ (123%), HexA$^{-/-}$Galgt1$^{-/-}$ (156%) and Neu4$^{-/-}$ Galgt1$^{-/-}$ (140%) there was an increase in the enzyme activities (Figure 3.25B). When both ages were compared with each other, the most significant increase was occurred in HexA$^{-/-}$Galgt1$^{-/-}$mice by increasing age. For the rest of the mice, enzyme activities were not changed much (Figure 3.26C).

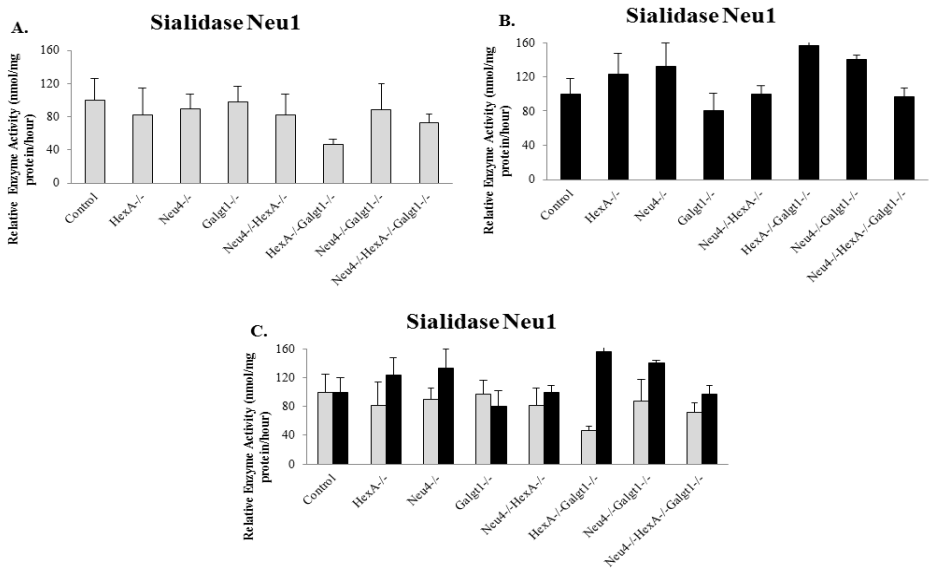

Figure 3.26. Specific enzyme activity measurement of sialidase Neu1 on three- and six-month-old Control, HexA$^{-/-}$, Neu4$^{-/-}$, Galgt1$^{-/-}$, Neu4$^{-/-}$HexA$^{-/-}$, HexA$^{-/-}$ Galgt1$^{-/-}$, Neu4$^{-/-}$Galgt1$^{-/-}$ and Neu4$^{-/-}$HexA$^{-/-}$Galgt1$^{-/-}$ mice. Figure representation is: A. relative enzyme activity in three-month-old mice; B. relative enzyme activity in six-month-old mice; C. Together representation of relative enzyme activities of three-and six-month-old mice. In the experiment n=3. Error bars were calculated as ±SEM.

3.5. Behavioral Analysis

Behavioral experiments were performed as mentioned in material and methods chapter. Along the experiments, ethical issues were applied and there was any damage given to the animals.Used animals are listed below.

Table 3.1. Used animals in Behaviour Experiments

	Passive avoidance		**Rotarod**	
Genotype/Age	3M	6M	3M	6M
Control	7♀, 3♂	3♀, 2♂	4♀, 3♂	7♀, 5♂
$HexA^{-/-}$	4♀	2♀, 2♂	1♀, 5♂	5♀, 3♂
$Neu4^{-/-}$	3♀, 3♂	2♀, 2♂	4♀, 2♂	4♀, 4♂
$Galgt1^{-/-}$	2♀, 2♂	4♀	4♀, 3♂	4♀
$Neu4^{-/-}HexA^{-/-}$	6♀, 5♂	6♀, 1♂	7♀, 9♂	9♀, 4♂
$HexA^{-/-}Galgt1^{-/-}$	4♀, 2♂	2♀, 2♂	2♀, 2♂	2♀, 2♂
$Neu4^{-/-}Galgt1^{-/-}$	4♀, 7♂	4♀, 5♂	6♀, 8♂	4♀, 7♂
$Neu4^{-/-}HexA^{-/-}Galgt1^{-/-}$	3♀, 3♂	6♀, 2♂	3♀, 6♂	5♀, 3♂

3.5.1. Rotarod Experiment

Rotarod test is designed to evaluate motor coordination of mice. Decreased time on rod over repeated testing sessions shows cerebellar learning of mice (Crawley 1999). Among many motor coordination tests rotarod test is suitable for identification of cerebellar deficits in mice and rats (Shiotsuki et al. 2010). In the test, mice stay balanced on rotating rod and time of fall of the rod is recorded.

There was a significant decrease on time of fall of $HexA^{-/-}$, $Galgt1^{-/-}$, Neu4-/-$Galgt1^{-/-}$ and $Neu4^{-/-}HexA^{-/-}Galgt1^{-/-}$ mice when compared with the control littermate in three-month-old. When there was no difference time on rod between control and $HexA^{-/-}$ littermate, with the double deficiency of HexA and Galgt1, there was a significant decrease on the $HexA^{-/-}Galgt1^{-/-}$ mice (Figure 3.27A). That can be result of Galgt1 deficiency. Also in six-month-old mice group, decreasing fall off time for $Galgt1^{-/-}$ mice, were caused decreased time to stay on rod for $HexA^{-/-}Galgt1^{-/-}$ mice (Figure 3.27B). There was a significant decrease in time of rod for the $Neu4^{-/-}HexA^{-/-}Galgt1^{-/-}$ mice when compared with the $HexA^{-/-}$ and $Neu4^{-/-}$ mice. When three- and six-month-old mice compared with each other, time spent on rod was decreased significantly for $Neu4^{-/-}$, $Galgt1^{-/-}$ and $Neu4^{-/-}HexA^{-/-}Galgt1^{-/-}$ mice with increasing age (Figure 3.28C).

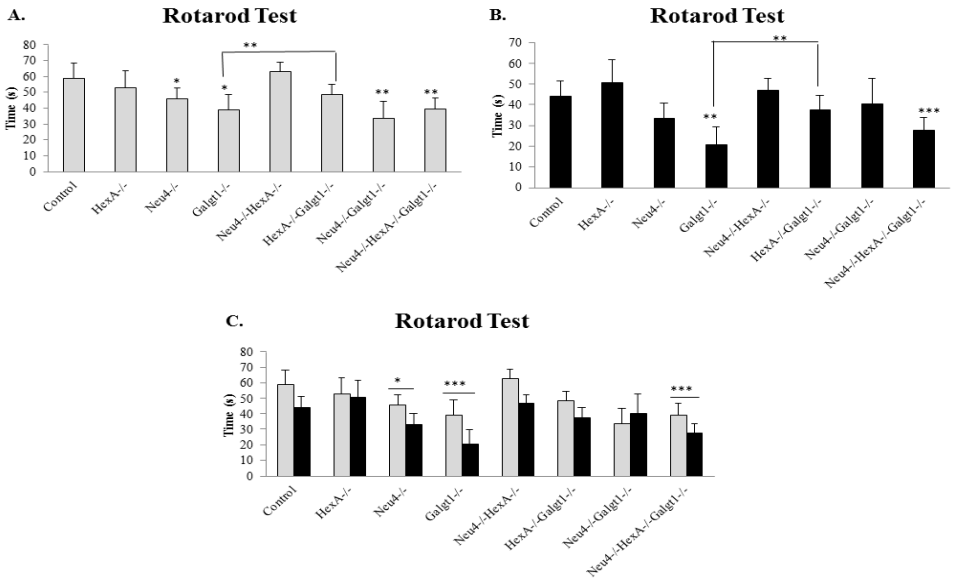

Figure 3.27. Rotarod result of three-and six-month-old Control, $HexA^{-/-}$, $Neu4^{-/-}$, $Galgt1^{-/-}$, $Neu4^{-/-}HexA^{-/-}$, $HexA^{-/-}Galgt1^{-/-}$, $Neu4^{-/-}Galgt1^{-/-}$ and $Neu4^{-/-}HexA^{-/-}Galgt1^{-/-}$ mice. Figure representation is: A. time on rod for three-month-old animals; B. time on rod for six-month-old mice; C. Together representation of three-and six-month- old mice. p values were calculated using t-test (***<0.01<**<0.03<*<0.05). Error bars were calculated as ±SEM

3.5.2. Passive Avoidance Task

Passive avoidance test is fear motivated test and used to detect short term or long term memory in mice. In three-month-old mice group, Control, $HexA^{-/-}$, $Galgt1^{-/-}$ mice were not entered the box with electricity again. However, $Neu4^{-/-}$ mice entered the small-dark-box. $Neu4^{-/-}HexA^{-/-}$ and $Neu4^{-/-}HexA^{-/-}Galgt1^{-/-}$ mice were reentered the box with decreased time (Figure 3.28A). For six month of age mice group, control and $Neu4^{-/-}$Galgt1-/- mice were not entered the small-dark-box. However, $HexA^{-/-}Galgt1^{-/-}$ mice were entered the box in a short time (Figure 3.28B). In this test there was no significant change between animals were observed (Figure 3.28A and B). When three- and six-month-old littermates compared with each other, $Neu4^{-/-}$, $Neu4^{-/-}HexA^{-/-}$ and $Neu4^{-/-}HexA^{-/-}Galgt1^{-/-}$ mice entered the box again in a short time (Figure 3.28C).

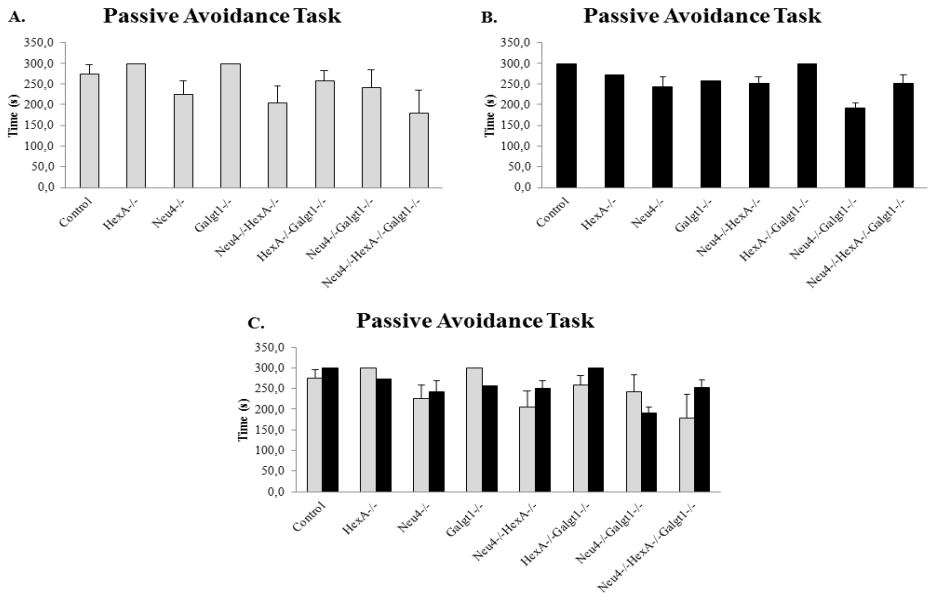

Figure 3.28.Passive avoidance task result shows time as seconds, comparison of three- and six-month-old Control, $HexA^{-/-}$, $Neu4^{-/-}$, $Galgt1^{-/-}$, $Neu4^{-/-}HexA^{-/-}$, $HexA^{-/-}Galgt1^{-/-}$, $Neu4^{-/-}Galgt1^{-/-}$ and $Neu4^{-/-}HexA^{-/-}Galgt1^{-/-}$ mice in test day. Error bars were calculated as ±SEM.

3.6. GM2 Antibody Staining

GM2 is a complex ganglioside that accumulates in Tay-Sachs patients. In Tay-Sachs patients, deficiency of HexA enzyme causes accumulation of GM2 ganglioside. GM2 ganglioside does not metabolize into GM1 and its accumulation occurs. To characterize the accumulation level of GM2 ganglioside in three- and six- month-old mice brain tissues were stained with anti-GM2 antibody (Figure 3.29). Figure 3.29B&E shows hippocampi of both $HexA^{-/-}$ and $Neu4^{-/-}HexA^{-/-}$ mice stained with a GM2 antibody detected by a fluorescence secondary (DyLight488) antibody. These images show no staining in the $Galgt1^{-/-}$, $HexA^{-/-}Galgt1^{-/-}$, $Neu4^{-/-}Galgt1^{-/-}$ and $Neu4^{-/-}HexA^{-/-}Galgt1^{-/-}$ mice when compared to $HexA^{-/-}$ and $Neu4^{-/-}HexA\text{-}^{-/-}$ littermates. In $HexA^{-/-}$ and $Neu4^{-/-}HexA^{-/-}$ mice staining are more intense in older mice, and become more diffuse.

3M **6M**

A.Control

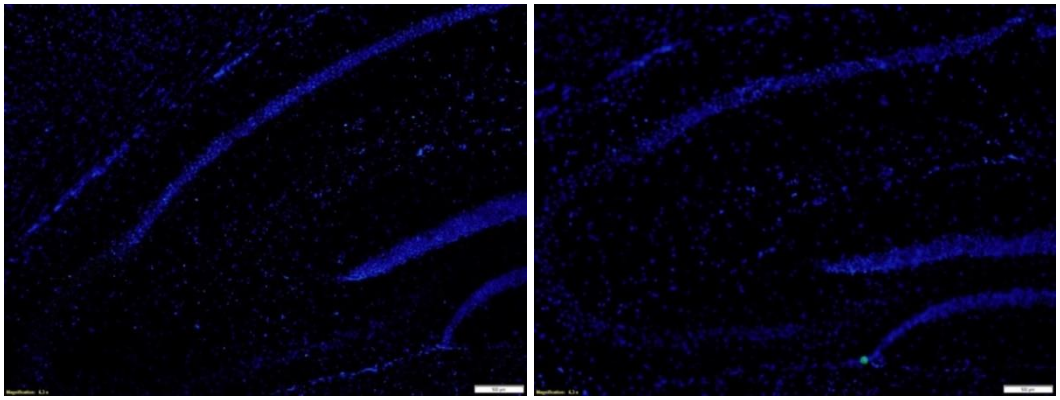

B.HexA$^{-/-}$

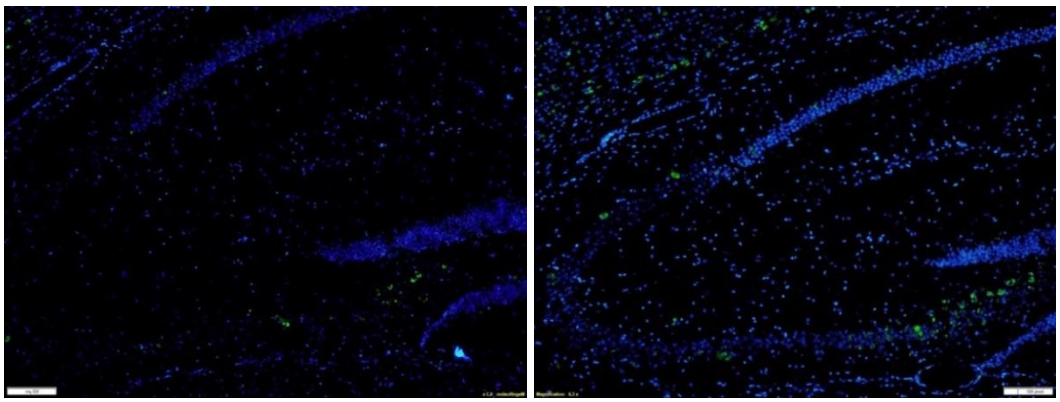

C.Neu4$^{-/-}$

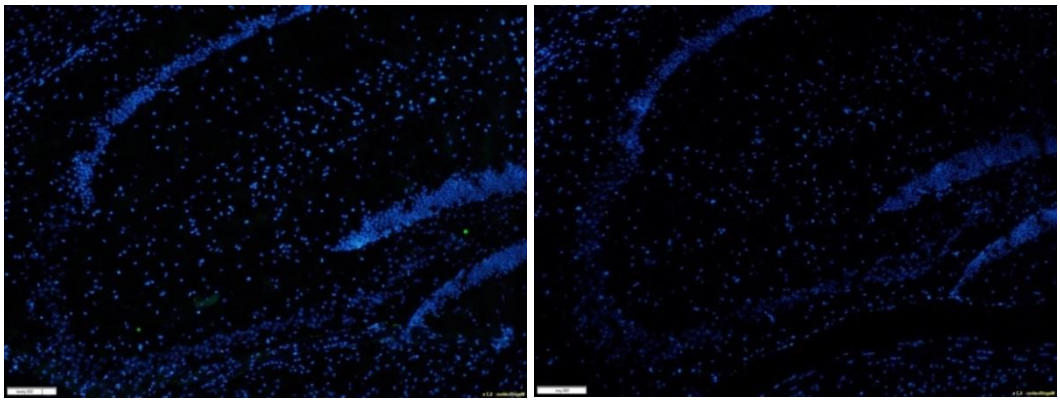

Figure 3.29. Hippocampal GM2 distribution in three- and six-month-old mice after staining with GM2 antibody and DAPI. One animal was shown per genotype. A. Control; B. HexA-/- ; C. Neu4-/- ; D. Galgt1-/- ; E. Neu4-/-HexA-/-; F. HexA-/-Galgt1-/- ; G. Neu4-/-Galgt1-/- ; H. Neu4-/-HexA-/-Galgt1-/-. Images were taken at 20 x magnification. No cells were labeled when the primary antibody was omitted.

(cont. on next page)

3M **6M**

D.Galgt1$^{-/-}$

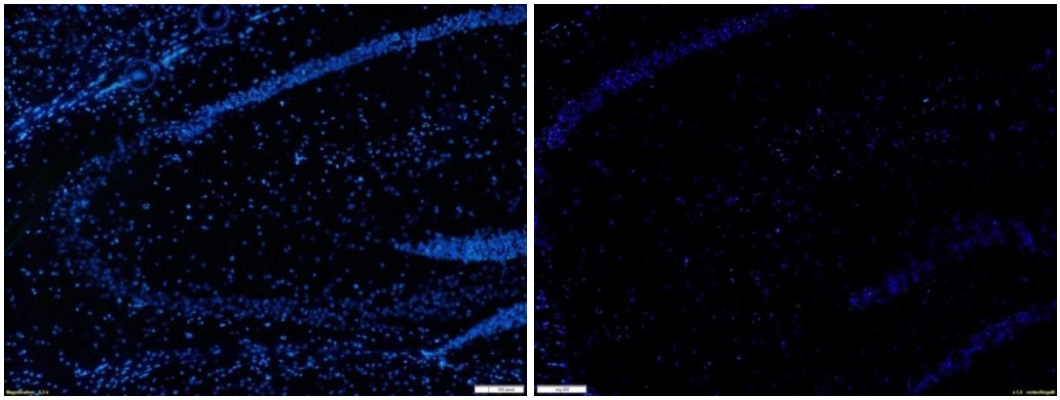

E.Neu4$^{-/-}$HexA$^{-/-}$

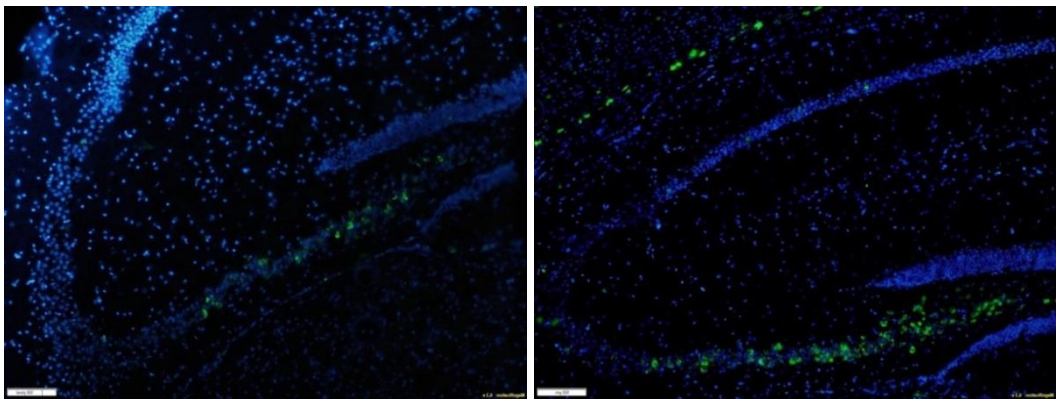

F.HexA$^{-/-}$Galgt1$^{-/-}$

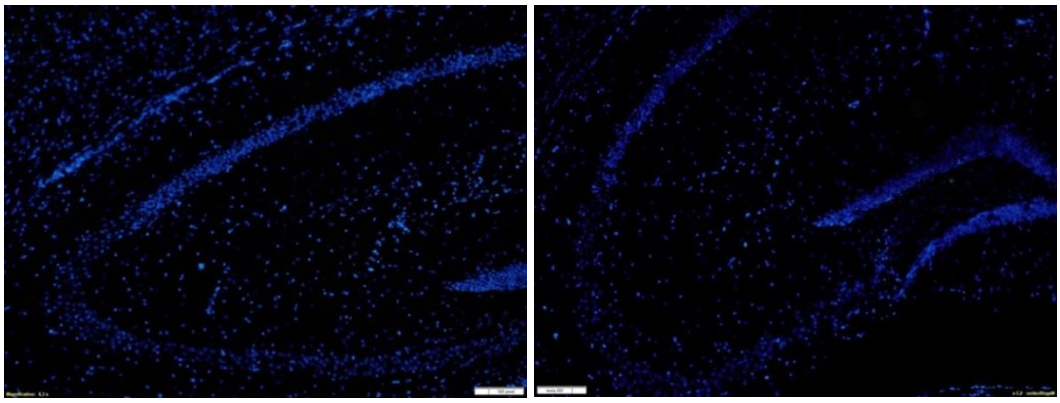

Figure 3.29. (cont.)

(cont. on next page)

3M **6M**

G.Neu4$^{-/-}$Galgt1$^{-/-}$

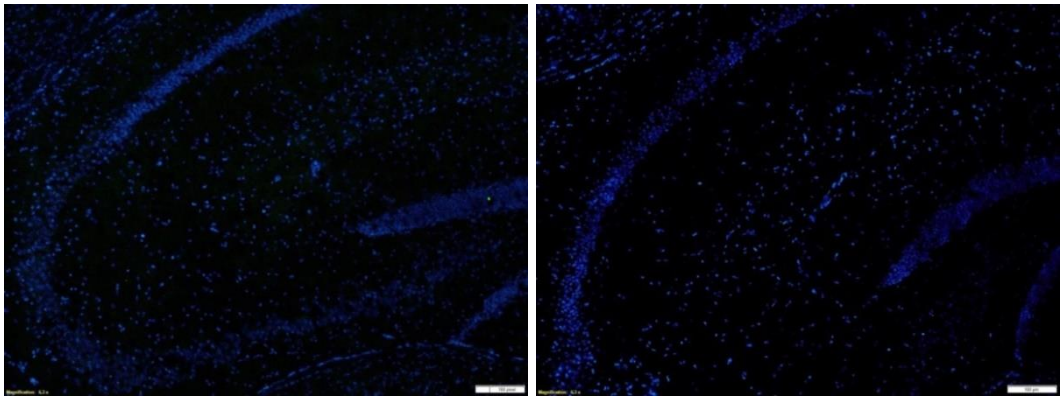

H.Neu4$^{-/-}$HexA$^{-/-}$Galgt1$^{-/-}$

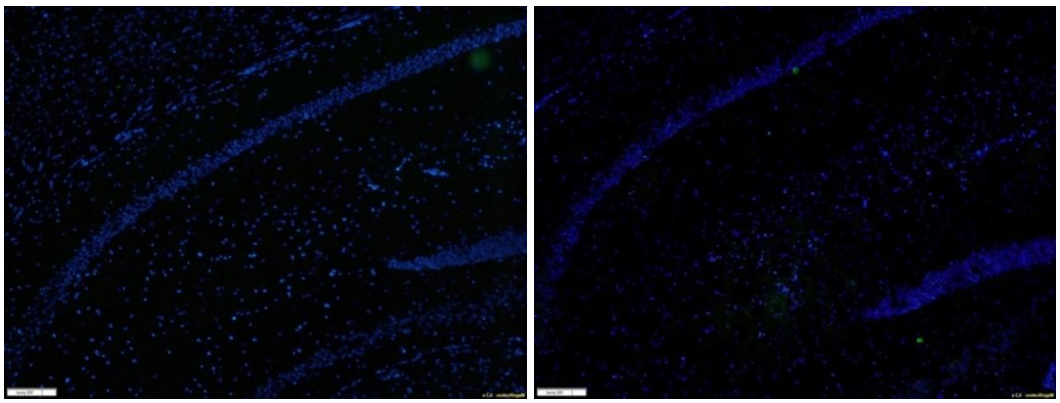

Figure 3.29. (cont.)

CHAPTER 4

DISCUSSION

Tay-Sachs disease is the second most common lysosomal storage disease that is caused by mutation in the HexA gene coding for the alpha subunit of lysosomal β-hexosaminidase A (HexA). HexA is responsible for the removal of N-acetyl-glucosamine residue from GM2 ganglioside to convert it into GM3 in the ganglioside degradation pathway. Deficiency of HexA causes neuronal death with progressive neurological degeneration in human. GM2 derived ganglioside GA2 is present in $HexA^{-/-}$ mice and this ganglioside can be further metabolized into ceramide by HexB (Phaneuf et al. 1996). Because of the metabolic bypass, those mice can escape disease over one years of life (Igdoura et al. 1999).

$Neu4^{-/-}$ mice show different ganglioside pattern compared with wild type mice and there is increased GD1a and decreased GM1 in brains. $Neu4^{-/-}$ mice show lysosomal storage bodies in macrophage cells in the lung, spleen and lymphocytes. There is an increase in gangliosides, ceramide, cholesterol and fatty acids in the brain, lung and spleen (Seyrantepe et al. 2008).

As previously shown Neu4 is a modifier gene. $Neu4^{-/-}HexA^{-/-}$ mice showed a more severe phenotype than in HexA deficiency alone (Seyrantepe et al. 2010). Double mutant mice developed epileptic seizures, motor impairment, tremor and weakness. With the increasing GM2 accumulation, neurological impairment was more severe than HexA deficiency alone.

β-1,4-N-acetylgalactosaminyltransferase (Galgt1) is one of the key enzymes in the synthesis of complex gangliosides and it works in reverse direction of HexA. In the ganglioside synthesis pathway, Galgt1 is responsible for the production of complex gangliosides. In the deficiency of Galgt1, there is only production of simple gangliosides (LacCer, GM3, GD3) occurs. Absence of complex gangliosides causes neurological degeneration.

Mouse models with double knock-out $HexA^{-/-}Galgt1^{-/-}$ and $Neu4^{-/-}Galgt1^{-/-}$ and triple knock out $Neu4^{-/-}HexA^{-/-}Galgt1^{-/-}$ were first time generated in our laboratory for

this study. Brain gangliosides of Neu4$^{-/-}$, HexA$^{-/-}$, Galgt1$^{-/-}$, Neu4$^{-/-}$HexA$^{-/-}$, HexA$^{-/-}$Galgt1$^{-/-}$, Neu4$^{-/-}$Galgt1$^{-/-}$, Neu4$^{-/-}$HexA$^{-/-}$Galgt1$^{-/-}$ were profiled. It was revealed how ganglioside contents were affected from the absence of each enzyme responsible for the biosynthesis and biodegradation of brain gangliosides.

Thin layer chromatography has been used for many years to separate compounds with different molecular weights. Using different solvent systems, it is possible to isolate oligosaccharides, lipids and etc. Thin Layer Chromatography analyses were performed for three- and six-month-old mice. Ganglioside pattern for HexA$^{-/-}$ and Neu4$^{-/-}$HexA$^{-/-}$ (Seyrantepe et al. 2010) and Galgt1$^{-/-}$ (Liu et al. 1999) were as expected from previous studies. It was the first time that double knock-out HexA$^{-/-}$Galgt1$^{-/-}$ and Neu4$^{-/-}$Galgt1$^{-/-}$ and triple knock out Neu4$^{-/-}$HexA$^{-/-}$Galgt1$^{-/-}$ were analyzed in TLC. In three-month-old mice GM3 and GD3 gangliosides accumulated much more in Galgt1$^{-/-}$ and HexA$^{-/-}$Galgt1$^{-/-}$ mice. On the other hand, in six-month-old mice, accumulation levels of GM3 and GD3 increased for Galgt1$^{-/-}$, Neu4$^{-/-}$Galgt1$^{-/-}$ and Neu4$^{-/-}$HexA$^{-/-}$Galgt1$^{-/-}$ and decreased for HexA$^{-/-}$Galgt1$^{-/-}$ mice. As mentioned before, the role of Neu4 on degradation on simple gangliosides is not known yet. Accumulation of simple gangliosides in Neu4$^{-/-}$Galgt1$^{-/-}$ mice might cause the possible role of Neu4 in simple ganglioside degradation. Also, the reason of decrease in the accumulation amount of simple gangliosides in HexA$^{-/-}$Galgt1$^{-/-}$ mice, might be an alternative pathway for the degradation of gangliosides. As previously shown, HexA$^{-/-}$ mice has an alternative pathway to degrade ganglioside GM2 into ceramide. GM2 ganglioside metabolized via GA2 ganglioside to ceramide and HexA deficiency fully corrected (Seyrantepe et al. 2008). There might be a similar or the same bypass mechanism that has a role in the degradation of GM3 and GD3 in HexA$^{-/-}$Galgt1$^{-/-}$ mice. According to previous studies, incidence of disease in Galgt1$^{-/-}$ mice is increases with age (Chiavegatto et al. 2000). Increasing levels of GM3 and GD3 in Galgt1$^{-/-}$, HexA$^{-/-}$Galgt1$^{-/-}$, Neu4$^{-/-}$Galgt1$^{-/-}$ and Neu4$^{-/-}$HexA$^{-/-}$Galgt1$^{-/-}$ mice might be result of increasing age.

In real time PCR, expression levels of different genes were examined. GM3S, GD3S, Galgt1, B3Galt4 and B4Galt6 are involved in synthesis of gangliosides whereas β-gal, HexB, and sialidases responsible for degradation. GM2AP is necessary for the removing of GM2 from endosome membrane to transmit into HexA enzyme protein complex. Low expression rates of the GM3S, GD3S, and B3Galt4 in three-month-old Galgt1$^{-/-}$ mice, caused also decrease in expression rates of those genes in the Neu4$^{-/-}$Galgt1$^{-/-}$ mice. GM3S and GD3S genes are responsible for the synthesis of simple

gangliosides GM3 and GD3, respectively. Those simple gangliosides are further metabolized by Galgt1 to synthesize complex gangliosides. Decreased expression rate of synthesis genes in Galgt1$^{-/-}$ mice caused similar decrease in HexA$^{-/-}$Galgt1$^{-/-}$ and Neu4$^{-/-}$HexA$^{-/-}$Galgt1$^{-/-}$ mice. Expression rates of GM3S, GD3S, and B3Galt4 were decreased for three-month-old mice. These results shows, deficiency of Galgt1 gene may not be compensated. However, expression rate of GM3S gene were increased in in six-month-old Neu4$^{-/-}$HexA$^{-/-}$Galgt1$^{-/-}$ mice when compared with the single deficient counterparts. When three-months-old and six-months-old Neu4$^{-/-}$HexA$^{-/-}$Galgt1$^{-/-}$ mice compared with each other, expression rates of both GM3S and GD3S genes were increased. That might be consequence of deficiency of Galgt1 as well as HexA gene. As seen in figures 3.11C and 3.12C, expression levels of GM3S and GD3S were increase in HexA$^{-/-}$ mice as age dependently. Expression rate of Galgt1 gene was higher in six-month-old Neu4$^{-/-}$ mice when compared with control and HexA$^{-/-}$ mice. We speculate that increase of the expression rate of Galgt1 gene in Neu4$^{-/-}$ mice might be result of possible role of Neu4 gene on simple gangliosides. Also, as seen in figure 3.13C, expression rate of Galgt1 gene in HexA$^{-/-}$ mice were decreased with increasing age. Galgt1 and HexA enzymes work in opposite direction. In the deficiency of HexA, GM2 will not metabolize into GM3 ganglioside. On the other hand, Galgt1 will still continue to synthesize GM2 from GM3 ganglioside. There might be presence of a feedback mechanism, to decrease expression rate of Galgt1 gene, to prevent further increase in the amount of GM2. B4Galt6 gene takes role in the synthesis of LacCer from GlcCer and B3Galt4 takes role in the synthesis of GA2 from GM2 in O-series gangliosides. In three-month-old mice expression rates B4Galt6 and B3Galt4 genes were dramatically changed in Neu4$^{-/-}$Galgt1$^{-/-}$ mice. In all experiments, decreased expression levels of those genes in Galgt1$^{-/-}$ mice were caused decrease of expression rate in Neu4$^{-/-}$Galgt1$^{-/-}$ mice. As previously shown, Neu4 has a role in degradation of GD1a to GM1 (Seyrantepe et al. 2008; Seyrantepe et al. 2010). However it is not known yet, Neu4 has a role in different steps of metabolism pathway. So, Neu4 might have role in degradation part of the simple gangliosides. By this mean, double knock-out mice of Neu4$^{-/-}$Galgt1$^{-/-}$ had more significant changes than single knock-out Neu4$^{-/-}$ and Galgt1$^{-/-}$. In six-month-old mice group, there was not a significant change occurred in B3Galt4 and B4Galt6 expressions. The reason of it might be related to aging. Therefore, expression rate of those genes were not increased much in older mice.

β-gal is an enzyme that metabolizes GM1 into GM2. In deficiency of β-gal, GM1 accumulates in lysosomes (GM1 Gangliosidosis). Although the expression level of β-gal were not significantly changed in $Neu4^{-/-}$ and $Galgt1^{-/-}$ mice, double deficient $Neu4^{-/-}Galgt1^{-/-}$ mice showed decreased β-gal expression. As seen in the Figure 4.1, Neu4 metabolizes GD1a into GM1 and β-gal metabolizes GM1 into GM2. In the deficiency of Neu4 gene, GM1 produced in lower level resulting less expression level of β-gal enzyme. As seen in figure 3.16A, in double knock-out mice expression rate of gene were much more decreased when compared to $Neu4^{-/-}$ single knock-out mice.

β-HexA enzyme is composed of α+β subunits. And β-HexB enzyme is composed of β+β subunits. Deficiency of HexA causes Tay-Sachs and HexB causes Sandhoff's Disease. Mice model with double deficiency of $HexB^{-/-}Galgt1^{-/-}$ were previously generated as a model for substrate deprivation therapy. That mouse has defects in both ganglioside synthesis and degradation, so that mice did not accumulated gangliosides. Lifespan of $HexB^{-/-}Galgt1^{-/-}$ mice were longer than both $HexB^{-/-}$ and $Galgt1^{-/-}$ mice. $HexB^{-/-}Galgt1^{-/-}$ mice had also improved neurologic function. However, in older ages mice developed late-onset neurological disorder with accumulation of oligosaccharides (Liu et al. 1999). We found that significantly decreased expression rate of HexB gene in $HexA^{-/-}$ mice. In $HexA^{-/-}Galgt1^{-/-}$ mice no change on HexB expression were observed when compared with control littermate.

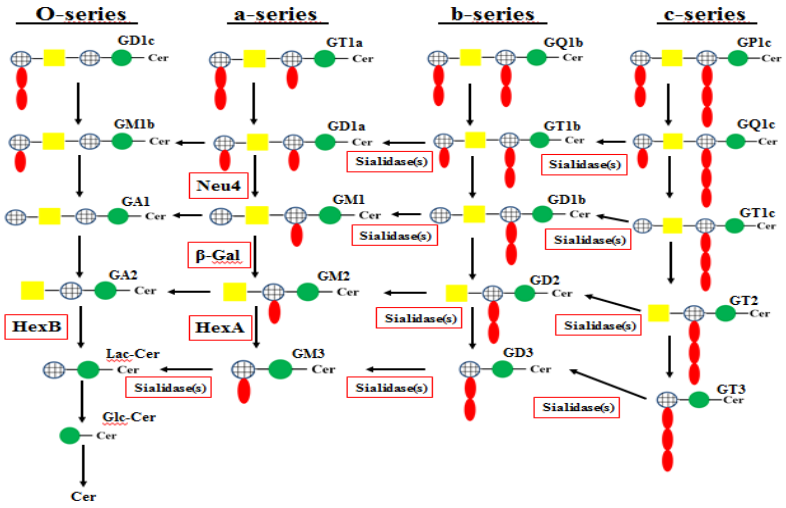

Figure 4.1. Degradation pathway of 0-, a-, b- and c- series gangliosides. (Blue circles with black vertical and horizontal lines represent galactose, red and green spheres represent sialic acids and glucose and yellow squares represents N-acetylgalactosamine residues)

Sialidases are located in different regions of cell with different functions. However, all functions of sialidases in cell is not clear yet (Miyagi and Yamaguchi 2012). Expression levels of Neu1, Neu2, Neu3 and Neu4 were previously analyzed in $HexA^{-/-}$, $Neu4^{-/-}$ and $Neu4^{-/-}HexA^{-/-}$ mice as relative units (Seyrantepe et al. 2010). Expression levels of HexB previously were shown in $HexA^{-/-}$, $Neu4^{-/-}$ and $Neu4^{-/-}HexA^{-/-}$ mice as relative units (Timur et al. 2015) . Our results were consistent with the previously reported expression levels of sialidase and HexB. For Neu1 and Neu3 sialidases, sialidase activity decreased in $Galgt1^{-/-}$ mice. Decreased sialidase activity was also observed in $Neu4^{-/-}Galgt1^{-/-}$ mice. Sialidase Neu2 activity was decreased in $Neu4^{-/-}Galgt1^{-/-}$ mice when compared with the $Neu4^{-/-}$ mice.

Enzyme activities were calculated relatively. β-gal is an enzyme that plays role in the degradation of gangliosides by removing lactose residue linked to N-acetlyneuraminicacid residue of GM1 to convert into GM2. According to that, in three-month-old mice group β-gal activity was decreased in $Neu4^{-/-}$ mice and increased in $Neu4^{-/-}HexA^{-/-}Galgt1^{-/-}$ mice. In six-month-old $HexA^{-/-}$ and $Neu4^{-/-}$ mice there was an increase in the β-gal enzyme activity. There was no difference in β-gal enzyme activity for $Neu4^{-/-}HexA^{-/-}Galgt1^{-/-}$ mice (Figure 3.23B). When both ages were compared with each other, the most significant change occurred in the $Neu4^{-/-}$ mice. Expression rate of the β-gal gene was correlated with the gene expression data (Figure 3.18). According to that, in $Neu4^{-/-}$ mice relative enzyme activity of β-gal was decreased in three-month-old group. Even a small decrease was noted in $Neu4^{-/-}$ mice when compared to control littermates in gene expression levels, littermates showed 50% loss in enzyme activity. In $Neu4^{-/-}Galgt1^{-/-}$ mice relative enzyme activity was about 70%. In double deficiency situation there was a partial recovery of enzyme activity.

For three-month-old mice, β-glucosidase activity was significantly increased in $Neu4^{-/-}$ and decreased in $Galgt1^{-/-}$ mice (Figure 3.24A). In six-month-old mice group of $HexA^{-/-}$ and $HexA^{-/-}Galgt1^{-/-}$ mice there was an increase in the β-glucosidase enzyme activity. Enzyme activity was decreased for $Neu4^{-/-}$ mice (Figure 3.24B). When both ages were compared with each other, the most significant decrease occurred in $Neu4^{-/-}$ mice and the most significant increase occurred in $HexA^{-/-}Galgt1^{-/-}$ mice. For this experiment, data was not consistent with previous study (Timur et al. 2015). In this experiment, $HexA^{-/-}$ mice showed 3 fold-increases in enzyme activity when compared to control littermate at six-months-old. However, Timur et. al. reported that there was no

significant change between $HexA^{-/-}$ and control littermates. This experiment needs further validation.

β-hexosaminidase B (HexB) is an enzyme that is composed of two β-subunits. In the deficiency of HexB, Sandhoff's Disease occurs. For three-month-old mice, HexB activity was much more increased in $HexA^{-/-}$. However, HexB activity decreased in $HexA^{-/-}Galgt1^{-/-}$ mice. In the rest of the mice there was not much change in enzyme activity (Figure 3.25A). We showed only in 6-months old $Neu4^{-/-}HexA^{-/-}$ mice there was an increase in the enzyme activity. Enzyme activity was decreased for $Galgt1^{-/-}$ mice (Figure 3.25B). Enzyme activity of β-hexosaminidase B was related to the expression rate of gene.

Sialidase Neu1 is located mostly in lysosomes. For three-month-old mice, sialidase Neu1 activity was decreased in $HexA^{-/-}Galgt1^{-/-}$ mice (Figure 3.26A). We showed that there was an increase in the enzyme activity in six-month-old $Neu4^{-/-}$, $HexA^{-/-}$, $HexA^{-/-}Galgt1^{-/-}$ and $Neu4^{-/-}Galgt1^{-/-}$ mice (Figure 3.25B). We found that Neu1 enzyme activity is related its gene expression level in $Neu4^{-/-}$ and $Neu4^{-/-}HexA^{-/-}Galgt1^{-/-}$ mice. Our overall data suggest that enzyme activity measurements need further validation.

Rotarod experiment results for $Neu4^{-/-}$ and $Neu4^{-/-}HexA^{-/-}$ mice were similar for both three- and six-month-old mice. For both ages, time spent on rod for $HexA^{-/-}$ and $Neu4^{-/-}HexA^{-/-}$ mice were similar. There was no statistical difference between them. Our data is consistent with the previous results (Seyrantepe et al. 2010). For $Galgt1^{-/-}$ mice, latency to fall was significantly decreased when compared with control littermate (Chiavegatto et al. 2000). In six months of age mice that time on rod was shorter than three months of age mice for $Galgt1^{-/-}$ mice. As age dependent manner, time on rod was significantly decreased for $Neu4^{-/-}$, $Galgt1^{-/-}$ and $Neu4^{-/-}HexA^{-/-}Galgt1^{-/-}$. That decrease on triple knock-out mice, an effect of lack of all complex gangliosides. HexA and Galgt1 genes work in opposite direction. Galgt1 is responsible for the synthesis of complex gangliosides like GM2 (Kolter, Proia, and Sandhoff 2002). HexA gene is responsible or the degradation of GM2 ganglioside into GM3 (Huang et al. 1997). $HexA^{-/-}Galgt1^{-/-}$ mice stayed on rod longer time when compared with the control littermates. As previously shown in mice model of Tay-Sachs, there is an alternative by-pass pathway. There may be the same/or similar pathway has an effect. For that $HexA^{-/-}Galgt1^{-/-}$ mice motor abilities may be fixed when compared to $Galgt1^{-/-}$ mice. By extending subject numbers, experiment might be repeated.

Our study was the first to use passive avoidance task in Neu4$^{-/-}$, HexA$^{-/-}$, Galgt1$^{-/-}$ and Neu4$^{-/-}$HexA$^{-/-}$ mice. On the passive avoidance task, it is expected to mice do not enter the small-dark box after electrical shock. In test day, mice had 300 seconds cut off time. As expected, control littermates were not entered to dark-box for both three and six months of age. However, Neu4$^{-/-}$HexA$^{-/-}$, HexA$^{-/-}$Galgt1$^{-/-}$ and Neu4$^{-/-}$HexA$^{-/-}$ Galgt1$^{-/-}$ littermates were entered the box about 200 seconds after starting of experiment. It shows, short term memory of those mice were not good. This might be result of accumulation of GM2 ganglioside in Neu4$^{-/-}$HexA$^{-/-}$ mice. For HexA$^{-/-}$Galgt1$^{-/-}$ and Neu4$^{-/-}$HexA$^{-/-}$Galgt1$^{-/-}$ littermates, absence of complex gangliosides in brain might cause to short term memory defects.

Immunohistochemistry results showed there was accumulation of GM2 ganglioside in HexA$^{-/-}$ and Neu4$^{-/-}$HexA$^{-/-}$ mice when compared to control littermates. As previously shown GM2 is accumulated in HexA$^{-/-}$ and Neu4$^{-/-}$HexA$^{-/-}$ mice (Seyrantepe et al. 2010). On the other hand, there was no GM2 ganglioside production in Galgt1$^{-/-}$ mice. So, there is no anti-GM2 signal to be developed. This is also true for HexA$^{-/-}$Galgt1$^{-/-}$, Neu4$^{-/-}$Galgt1$^{-/-}$ and Neu4$^{-/-}$HexA$^{-/-}$Galgt1$^{-/-}$ mice. As expected at the beginning of the experiment there is no antibody staining in Galgt1$^{-/-}$, HexA$^{-/-}$Galgt1$^{-/-}$, Neu4$^{-/-}$Galgt1$^{-/-}$ and Neu4$^{-/-}$HexA$^{-/-}$Galgt1$^{-/-}$ since there is no production of complex gangliosides taken together.

Overall, data shows sialidase Neu4 may have a potential role in the degradation and synthesis pathway of simple gangliosides. TLC, gene expression, enzyme activity and behaviour experiments in double deficient Neu4$^{-/-}$Galgt1$^{-/-}$ mice showed different pattern than that of Neu4$^{-/-}$ and Galgt1$^{-/-}$ mice. In single deficient Galgt1$^{-/-}$ mice, expression levels of Neu2 gene were significantly decreased. Neu2 may be a modifier sialidase in the Galgt1 pathway/degradation of simple gangliosides. In single deficiency of Galgt1, some other genetic factors may also play role on gene expression. In younger ages, expression levels of genes were higher than older ages. By aging, expression rates of genes may reaches balance points. So, expression rate of genes were not significantly elevated in old mice. Deficiency of biosynthesis enzyme Galgt1, cause reduced enzyme activities in degradation pathway because of the deficieny of certain substrates. Inhibiton of Galgt1 synthesis pathway migth be used as substrate depriviation therapy in Tay-Sachs patients to increase lifespan. By aging motor coordination and memory of Galgt1$^{-/-}$, HexA$^{-/-}$Galgt1$^{-/-}$, Neu4$^{-/-}$Galgt1$^{-/-}$ and Neu4$^{-/-}$HexA$^{-/-}$Galgt1$^{-/-}$ mice showed

reduction due to absence of complex gangliosides in brain that might be related to short term memory defects.

4.1. Future Perspectives

As mentioned in the introduction part, Galgt1$^{-/-}$ mice has axonal degeneration (Sheikh et al. 1999). So inflammation around the nervous system is possible. As future work, there might be immunohistochemical analysis of double and triple knock mouse with inflammation markers like ED1. Also, there might be examining levels of cytokines and apoptotic markers with RT-PCR.

It is not known whether the sialidase Neu1, Neu2 and Neu3 has a role in the upstream of ganglioside synthesis mechanism, yet. With proper breeding of mice strains (Neu1$^{-/-}$Galgt1$^{-/-}$; Neu2$^{-/-}$Galgt1$^{-/-}$ and Neu3$^{-/-}$Galgt1$^{-/-}$) effects of those sialidases on ganglioside synthesis mechanism can be revealed. So, by focusing only on simple gangliosides (LacCer, GM3, GD3 and GT3) the possible effects of sialidase Neu1, Neu2 and Neu3 on the synthesis mechanism of complex gangliosides can be enlightened.

CHAPTER 5

CONCLUSION

This thesis described the possible role of sialidase Neu4 in degradation pathway of simple gangliosides. Double knock-out $HexA^{-/-}Galgt1^{-/-}$ and $Neu4^{-/-}Galgt1^{-/-}$ and triple knock out $Neu4^{-/-}HexA^{-/-}Galgt1^{-/-}$ mice were generated and analyzed at molecular biological, biochemical, immunohistochemical and behavioural based for the first time.

Our TLC results indicate that there is metabolic by-pass mechanism in $HexA^{-/-}Galgt1^{-/-}$ mice which similiar to $Neu4^{-/-}HexA^{-/-}$ mice. Accumulation of simple gangliosides in $Neu4^{-/-}Galgt1^{-/-}$ mice might also be related the possible role of Neu4 in simple ganglioside degradation.

In this study, the synthesis enzymes were analyzed in $Galgt1^{-/-}$ mice for the first time. Lower expression levels of GM3S, GD3S, B3Galt4 and B6Galt6 genes were detected. In addition, double deficient $Neu4^{-/-}Galgt1^{-/-}$ mice, showed different pattern from single deficient Neu4 and Galgt1 mice. Neu4 may have a role in the Galgt1 synthesis pathway. In $Galgt1^{-/-}$ mice, expression levels of Neu2 gene were decreased. Neu2 may have role in the degradation of complex gangliosides. Decreased expression rate in $Galgt1^{-/-}$ mice, were not compensated. Expression rates of synthesis enzymes GM3S, GD3S, B3Galt4 were decreased in $HexA^{-/-}Galgt1^{-/-}$, $Neu4^{-/-}Galgt1^{-/-}$ and $Neu4^{-/-}HexA^{-/-}Galgt1^{-/-}$ mice. In younger ages, deficencies of Neu4, HexA and Galgt1 has much more effect on expression levels other than older ages.

Motor coordination and memory of $Galgt1^{-/-}$, $HexA^{-/-}Galgt1^{-/-}$, $Neu4^{-/-}Galgt1^{-/-}$ and $Neu4^{-/-}HexA^{-/-}Galgt1^{-/-}$ in aging mice showed reduction resulting short term memory defects.

As a conclusion, Sialidase Neu4 may have a potential role in the degradation and synthesis pathway of simple gangliosides.

REFERENCES

Bernardo, K, R Hurwitz, T Zenk, R J Desnick, K Ferlinz, E H Schuchman, and K Sandhoff. 1995. "Purification, Characterization, and Biosynthesis of Human Acid Ceramidase." *Journal of Biological Chemistry* 270 (19): 11098–102. doi:10.1074/jbc.270.19.11098.

Buitrago, Manuel M., J??rg B. Schulz, Johannes Dichgans, and Andreas R. Luft. 2004. "Short and Long-Term Motor Skill Learning in an Accelerated Rotarod Training Paradigm." *Neurobiology of Learning and Memory* 81 (3): 211–16. doi:10.1016/j.nlm.2004.01.001.

Chen, Hui, Annie Y. Chan, Donald U. Stone, and Nawajes A. Mandal. 2014. "Beyond the Cherry-Red Spot: Ocular Manifestations of Sphingolipid-Mediated Neurodegenerative and Inflammatory Disorders." *Survey of Ophthalmology* 59 (1): 64–76. doi:10.1016/j.survophthal.2013.02.005.

Chiavegatto, S, J Sun, R J Nelson, and R L Schnaar. 2000. "A Functional Role for Complex Gangliosides: Motor Deficits in GM2/GD2 Synthase Knockout Mice." *Experimental Neurology* 166 (2): 227–34. doi:10.1006/exnr.2000.7504.

Crawley, Jacqueline N. 1999. "Behavioral Phenotyping of Transgenic and Knockout Mice: Experimental Design and Evaluation of General Health, Sensory Functions, Motor Abilities, and Specific Behavioral Tests." *Brain Research* 835 (1): 18–26. doi:10.1016/S0006-8993(98)01258-X.

Crawley, Jacqueline N. 2008. "Behavioral Phenotyping Strategies for Mutant Mice." *Neuron* 57 (6): 809–18. doi:10.1016/j.neuron.2008.03.001.

D'Angelo, Giovanni, Serena Capasso, Lucia Sticco, and Domenico Russo. 2013. "Glycosphingolipids: Synthesis and Functions." *FEBS Journal* 280 (24): 6338–53. doi:10.1111/febs.12559.

D'Azzo, A, A Hoogeveen, A J Reuser, D Robinson, and H Galjaard. 1982. "Molecular Defect in Combined Beta-Galactosidase and Neuraminidase Deficiency in Man." *Proceedings of the National Academy of Sciences of the United States of America* 79 (15): 4535–39. doi:10.1073/pnas.79.15.4535.

Dridi, Larbi, Volkan Seyrantepe, Anne Fougerat, Xuefang Pan, Eric Bonneil, Pierre Thibault, Allain Moreau, et al. 2013. "Positive Regulation of Insulin Signaling by Neuraminidase 1." *Diabetes* 62 (7): 2338–46. doi:10.2337/db12-1825.

Gault, Christopher R., Lina M. Obeid, and Yusuf A. Hannun. 2010. "An Overview of Sphingolipid Metabolism: From Synthesis to Breakdown." *Advances in Experimental Medicine and Biology* 688: 1–23. doi:10.1007/978-1-4419-6741-1_1.

Gieselmann, Volkmar. 1995. "Review: Lysosomal Storage Diseases." *Biochimica et Biophysica Acta* 1270 (1995): 103–36. doi:DOI: 10.1146/annurev.bi.60.070191.001353.

Hanada, Kentaro, Keigo Kumagai, Satoshi Yasuda, Yukiko Miura, Miyuki Kawano,

Masayoshi Fukasawa, and Masahiro Nishijima. 2003. “Molecular Machinery for Non-Vesicular Trafficking of Ceramide.” *Nature* 426 (6968): 803–9. doi:10.1038/nature02188.

Hata, Keiko, Koichi Koseki, Kazunori Yamaguchi, Setsuko Moriya, Yasuo Suzuki, Sangchai Yingsakmongkon, Go Hirai, Mikiko Sodeoka, Mark Von Itzstein, and Taeko Miyagi. 2008. “Limited Inhibitory Effects of Oseltamivir and Zanamivir on Human Sialidases.” *Antimicrobial Agents and Chemotherapy* 52 (10): 3484–91. doi:10.1128/AAC.00344-08.

Huang, Jing Qi, Jacquetta M Trasler, Suleiman Igdoura, Jean Michaud, Nobuo Hanai, and Roy A Gravel. 1997. “Apoptotic Cell Death in Mouse Models of G(M2) Gangliosidosis and Observations on Human Tay-Sachs and Sandhoff Diseases.” *Human Molecular Genetics* 6 (11): 1879–85. doi:10.1093/hmg/6.11.1879.

Igdoura, Suleiman A, Carmen Mertineit, Jacquetta M Trasler, and A Roy. 1999. “Sialidase-Mediated Depletion of G M2 Ganglioside in Tay – Sachs Neuroglia Cells” 8 (6): 1111–16.

Jeyakumar, M., T. D. Butters, R. a. Dwek, and F. M. Platt. 2002. “Glycosphingolipid Lysosomal Storage Diseases: Therapy and Pathogenesis.” *Neuropathology and Applied Neurobiology* 28 (5): 343–57. doi:10.1046/j.1365-2990.2002.00422.x.

Jeyakumar, M., R. Thomas, E. Elliot-Smith, D. A. Smith, A. C. Van der Spoel, A. D'Azzo, V. Hugh Perry, T. D. Butters, R. A. Dwek, and F. M. Platt. 2003. “Central Nervous System Inflammation Is a Hallmark of Pathogenesis in Mouse Models of GM1 and GM2 Gangliosidosis.” *Brain* 126 (4): 974–87. doi:10.1093/brain/awg089.

Kaye, Edward M. 2001. “Lysosomal Storage Diseases.” *Current Treatment Options in Neurology* 3 (3): 249–56. doi:10.1007/s11940-001-0006-9.

Kolter, Thomas. 2012. “Ganglioside Biochemistry.” *ISRN Biochemistry* 2012: 1–36. doi:10.5402/2012/506160.

Kolter, Thomas, Richard L. Proia, and Konrad Sandhoff. 2002. “Combinatorial Ganglioside Biosynthesis.” *Journal of Biological Chemistry*, 1–22.

Kolter, Thomas, and Konrad Sandhoff. 2006. “Sphingolipid Metabolism Diseases.” *Biochimica et Biophysica Acta* 1758 (12): 2057–79. doi:10.1016/j.bbamem.2006.05.027.

Lahiri, S., and A. H. Futerman. 2007. “The Metabolism and Function of Sphingolipids and Glycosphingolipids.” *Cellular and Molecular Life Sciences* 64 (17): 2270–84. doi:10.1007/s00018-007-7076-0.

Ledeen, Robert, and Gusheng Wu. 2011. “New Findings on Nuclear Gangliosides: Overview on Metabolism and Function.” *Journal of Neurochemistry* 116 (5): 714–20. doi:10.1111/j.1471-4159.2010.07115.x.

Liu, Y, A Hoffmann, A Grinberg, H Westphal, M P McDonald, K M Miller, J N Crawley, K Sandhoff, K Suzuki, and R L Proia. 1997. “Mouse Model of GM2 Activator Deficiency Manifests Cerebellar Pathology and Motor Impairment.” *Proceedings of the National Academy of Sciences of the United States of America*

94 (15): 8138–43. doi:10.1073/pnas.94.15.8138.

Liu, Y, R Wada, H Kawai, K Sango, C Deng, T Tai, M P McDonald, et al. 1999. “A Genetic Model of Substrate Deprivation Therapy for a Glycosphingolipid Storage Disorder.” *The Journal of Clinical Investigation* 103 (4): 497–505. doi:10.1172/JCI5542.

Lloyd, Kenneth O., and Koichi Furukawa. 1998. “Biosynthesis and Functions of Gangliosides: Recent Advances.” *Glycoconjugate Journal* 15 (7): 627–36. doi:10.1023/A:1006924128550.

Manna, Moutusi, Tomasz Róg, and Ilpo Vattulainen. 2014. “The Challenges of Understanding Glycolipid Functions: An Open Outlook Based on Molecular Simulations.” *Biochimica et Biophysica Acta - Molecular and Cell Biology of Lipids* 1841 (8). Elsevier B.V.: 1130–45. doi:10.1016/j.bbalip.2013.12.016.

Martinez, Zak, Min Zhu, Shubo Han, and Anthony L Fink. 2007. “GM1 Specifically Interacts with α-Synuclein and Inhibits Fibrillation †.” *Biochemistry* 46 (7): 1868–77. doi:10.1021/bi061749a.

Miklyaeva, Elena I, Weijia Dong, Alexandre Bureau, Roya Fattahie, Yongqin Xu, Meng Su, Gordon H Fick, et al. 2004. “Late Onset Tay-Sachs Disease in Mice with Targeted Disruption of the Hexa Gene: Behavioral Changes and Pathology of the Central Nervous System.” *Brain Research* 1001 (1–2): 37–50. doi:10.1016/j.brainres.2003.11.067.

Miyagi, Taeko, and Kazunori Yamaguchi. 2012. “Mammalian Sialidases: Physiological and Pathological Roles in Cellular Functions.” *Glycobiology* 22 (7): 880–96. doi:10.1093/glycob/cws057.

Miyagi, T, and S Tsuiki. 1984. “Rat-Liver Lysosomal Sialidase. Solubilization, Substrate Specificity and Comparison with the Cytosolic Sialidase.” *European Journal of Biochemistry / FEBS* 141 (1): 75–81. http://www.ncbi.nlm.nih.gov/pubmed/6723666.

Phaneuf, Daniel, Nobuaki Wakamatsu, Jing Qi Huang, Anita Borowski, Alan C. Peterson, Sheila R. Fortunato, Gerd Ritter, et al. 1996. “Dramatically Different Phenotypes in Mouse Models of Human Tay-Sachs and Sandhoff Diseases.” *Human Molecular Genetics* 5 (1): 1–14. doi:10.1093/hmg/5.1.1.

Platt, Frances M, Barry Boland, and Aarnoud C van der Spoel. 2012. “The Cell Biology of Disease: Lysosomal Storage Disorders: The Cellular Impact of Lysosomal Dysfunction.” *The Journal of Cell Biology* 199 (5): 723–34. doi:10.1083/jcb.201208152.

Risher, W. Christopher, Sagar Patel, Il H wan Kim, Akiyoshi Uezu, Srishti Bhagat, Daniel K. Wilton, Louis Jan Pilaz, et al. 2014. “Astrocytes Refine Cortical Connectivity at Dendritic Spines.” *eLife* 3: 1–24. doi:10.7554/eLife.04047.

Róg, Tomasz, and Ilpo Vattulainen. 2014. “Cholesterol, Sphingolipids, and Glycolipids: What Do We Know about Their Role in Raft-like Membranes?” *Chemistry and Physics of Lipids* 184: 82–104. doi:10.1016/j.chemphyslip.2014.10.004.

Sandhoff, Roger, Rudolf Geyer, Richard Jennemann, Claudia Paret, Eva Kiss, Tadashi

Yamashita, Karin Gorgas, et al. 2005. “Novel Class of Glycosphingolipids Involved in Male Fertility.” *Journal of Biological Chemistry* 280 (29): 27310–18. doi:10.1074/jbc.M502775200.

Schengrund, Cara-Lynne. 2015. “Gangliosides: Glycosphingolipids Essential for Normal Neural Development and Function.” *Trends in Biochemical Sciences* 40 (7): 397–406. doi:10.1016/j.tibs.2015.03.007.

Schnaar, Ronald L, Akemi Suzuki, and Pamela Stanley. 2009. “Glycosphingolipids.” In *Essentials of Glycobiology*. http://www.ncbi.nlm.nih.gov/pubmed/20301240.

Schneider Gasser, Edith M, Carolin J Straub, Patrizia Panzanelli, Oliver Weinmann, Marco Sassoè-Pognetto, and Jean-Marc Fritschy. 2006. “Immunofluorescence in Brain Sections: Simultaneous Detection of Presynaptic and Postsynaptic Proteins in Identified Neurons.” *Nature Protocols* 1 (4): 1887–97. doi:10.1038/nprot.2006.265.

Schultz, Mark L., Luis Tecedor, Michael Chang, and Beverly L. Davidson. 2011. “Clarifying Lysosomal Storage Diseases.” *Trends in Neurosciences* 34 (8). Elsevier Ltd: 401–10. doi:10.1016/j.tins.2011.05.006.

Schulze, Heike, Thomas Kolter, and Konrad Sandhoff. 2009. “Principles of Lysosomal Membrane Degradation. Cellular Topology and Biochemistry of Lysosomal Lipid Degradation.” *Biochimica et Biophysica Acta - Molecular Cell Research* 1793 (4). Elsevier B.V.: 674–83. doi:10.1016/j.bbamcr.2008.09.020.

Senn, H J, M Orth, E Fitzke, H Wieland, and W Gerok. 1989. “Gangliosides in Normal Human Serum. Concentration, Pattern and Transport by Lipoproteins.” *European Journal of Biochemistry / FEBS* 181 (3): 657–62. doi:10.1111/j.1432-1033.1989.tb14773.x.

Seyrantepe, Volkan, Maryssa Canuel, Stéphane Carpentier, Karine Landry, Stéphanie Durand, Feng Liang, Jibin Zeng, et al. 2008. “Mice Deficient in Neu4 Sialidase Exhibit Abnormal Ganglioside Catabolism and Lysosomal Storage.” *Human Molecular Genetics* 17 (11): 1556–68. doi:10.1093/hmg/ddn043.

Seyrantepe, Volkan, Karine Landry, Stéphanie Trudel, Jacob A. Hassan, Carlos R. Morales, and Alexey V. Pshezhetsky. 2004. “Neu4, a Novel Human Lysosomal Lumen Sialidase, Confers Normal Phenotype to Sialidosis and Galactosialidosis Cells.” *Journal of Biological Chemistry* 279 (35): 37021–29. doi:10.1074/jbc.M404531200.

Seyrantepe, Volkan, Pablo Lema, Aurore Caqueret, Larbi Dridi, Samar Bel Hadj, Stephane Carpentier, Francine Boucher, et al. 2010. “Mice Doubly-Deficient in Lysosomal Hexosaminidase A and Neuraminidase 4 Show Epileptic Crises and Rapid Neuronal Loss.” *PLoS Genetics* 6 (9): e1001118. doi:10.1371/journal.pgen.1001118.

Seyrantepe, Volkan, Helena Poupetova, Roseline Froissart, M. T. Zabot, Irène Maire, and Alexey V. Pshezhetsky. 2003. “Molecular Pathology of NEU1 Gene in Sialidosis.” *Human Mutation* 22 (5): 343–52. doi:10.1002/humu.10268.

Sheikh, K a, J Sun, Y Liu, H Kawai, T O Crawford, R L Proia, J W Griffin, and R L

Schnaar. 1999. “Mice Lacking Complex Gangliosides Develop Wallerian Degeneration and Myelination Defects.” *Proceedings of the National Academy of Sciences of the United States of America* 96 (June): 7532–37. doi:10.1073/pnas.96.13.7532.

Shiotsuki, Hiromi, Kenji Yoshimi, Yasushi Shimo, Manabu Funayama, Yukio Takamatsu, Kazutaka Ikeda, Ryosuke Takahashi, Shigeru Kitazawa, and Nobutaka Hattori. 2010. “A Rotarod Test for Evaluation of Motor Skill Learning.” *Journal of Neuroscience Methods* 189 (2): 180–85. doi:10.1016/j.jneumeth.2010.03.026.

Shiozaki, Kazuhiro, Koichi Koseki, Kazunori Yamaguchi, Momo Shiozaki, Hisashi Narimatsu, and Taeko Miyagi. 2009. “Developmental Change of Sialidase Neu4 Expression in Murine Brain and Its Involvement in the Regulation of Neuronal Cell Differentiation.” *Journal of Biological Chemistry* 284 (32): 21157–64. doi:10.1074/jbc.M109.012708.

Stamatos, Nicholas M, Ivan Carubelli, Diantha van de Vlekkert, Erik J Bonten, Nadia Papini, Chiguang Feng, Bruno Venerando, et al. 2010. “LPS-Induced Cytokine Production in Human Dendritic Cells Is Regulated by Sialidase Activity.” *Journal of Leukocyte Biology* 88 (6): 1227–39. doi:10.1189/jlb.1209776.

Stiedl, Oliver, and Sven Ögren. 2014. “Passive Avoidance.” *Encyclopedia of Psychopharmacology*. Berlin, Heidelberg: Springer Berlin Heidelberg, 1–10. doi:10.1007/978-3-642-27772-6_160-2.

Takahashi, Kohta, Masahiro Hosono, Ikuro Sato, Keiko Hata, Tadashi Wada, Kazunori Yamaguchi, Kazuo Nitta, Hiroshi Shima, and Taeko Miyagi. 2015. “Sialidase NEU3 Contributes Neoplastic Potential on Colon Cancer Cells as a Key Modulator of Gangliosides by Regulating Wnt Signaling.” *International Journal of Cancer. Journal International Du Cancer* 137 (7): 1560–73. doi:10.1002/ijc.29527.

Takamiya, K., A. Yamamoto, K. Furukawa, S. Yamashiro, M. Shin, M. Okada, S. Fukumoto, et al. 1996. “Mice with Disrupted GM2/GD2 Synthase Gene Lack Complex Gangliosides but Exhibit Only Subtle Defects in Their Nervous System.” *Proceedings of the National Academy of Sciences* 93 (20): 10662–67. doi:10.1073/pnas.93.20.10662.

Tettamanti, Guido, R. Bassi, P. Viani, and L. Riboni. 2003. “Salvage Pathways in Glycosphingolipid Metabolism.” *Biochimie* 85 (3–4): 423–37. doi:10.1016/S0300-9084(03)00047-6.

Timur, Z.K., S. Akyildiz Demir, C. Marsching, R. Sandhoff, and V. Seyrantepe. 2015. “Neuraminidase-1 Contributes Significantly to the Degradation of Neuronal B-Series Gangliosides but Not to the Bypass of the Catabolic Block in Tay–Sachs Mouse Models.” *Molecular Genetics and Metabolism Reports* 4. Elsevier B.V.: 72–82. doi:10.1016/j.ymgmr.2015.07.004.

Valaperta, Rea, Vanna Chigorno, Luisa Basso, Alessandro Prinetti, Roberto Bresciani, Augusto Preti, Taeko Miyagi, and Sandro Sonnino. 2006. “Plasma Membrane Production of Ceramide from Ganglioside GM3 in Human Fibroblasts.” *The FASEB Journal : Official Publication of the Federation of American Societies for Experimental Biology* 20 (8): 1227–29. doi:10.1096/fj.05-5077fje.

Wu, Gusheng, Zi Hua Lu, Neil Kulkarni, Ruchi Amin, and Robert W. Ledeen. 2011. “Mice Lacking Major Brain Gangliosides Develop Parkinsonism.” *Neurochemical Research* 36 (9): 1706–14. doi:10.1007/s11064-011-0437-y.

Yamanaka, S, M D Johnson, A Grinberg, H Westphal, J N Crawley, M Taniike, K Suzuki, and R L Proia. 1994. “Targeted Disruption of the Hexa Gene Results in Mice with Biochemical and Pathologic Features of Tay-Sachs Disease.” *Proceedings of the National Academy of Sciences of the United States of America* 91 (21): 9975–79. doi:10.1073/pnas.91.21.9975.

Yamashita, Tadashi, Yun-Ping Wu, Roger Sandhoff, Norbert Werth, Hiroki Mizukami, Jessica M Ellis, Jeffrey L Dupree, Rudolf Geyer, Konrad Sandhoff, and Richard L Proia. 2005. “Interruption of Ganglioside Synthesis Produces Central Nervous System Degeneration and Altered Axon-Glial Interactions.” *Proceedings of the National Academy of Sciences of the United States of America* 102 (8): 2725–30. doi:10.1073/pnas.0407785102.

Yao, Denggao, Rhona McGonigal, Jennifer a Barrie, Joanna Cappell, Madeleine E Cunningham, Gavin R Meehan, Simon N Fewou, et al. 2014. “Neuronal Expression of GalNAc Transferase Is Sufficient to Prevent the Age-Related Neurodegenerative Phenotype of Complex Ganglioside-Deficient Mice.” *The Journal of Neuroscience : The Official Journal of the Society for Neuroscience* 34 (3): 880–91. doi:10.1523/JNEUROSCI.3996-13.2014.

Yu, Robert K., and Robert W. Ledeen. 1972. “Gangliosides of Human, Bovine and Rabbit Retina.” *Biochimica et Biophysica Acta (BBA)/Lipids and Lipid Metabolism* 280 (2): 356–64. doi:10.1016/0005-2760(72)90104-X.

Yu, Robert K., Yi-Tzang Tsai, Toshio Ariga, and Makoto Yanagisawa. 2011. “Structures, Biosynthesis, and Functions of Gangliosides-an Overview.” *Journal of Oleo Science* 60 (10): 537–44. doi:10.5650/jos.60.537.

Yu, Robert K, Yi-Tzang Tsai, and Toshio Ariga. 2012. “Functional Roles of Gangliosides in Neurodevelopment: An Overview of Recent Advances.” *Neurochemical Research* 37 (6): 1230–44. doi:10.1007/s11064-012-0744-y.

Zhang, Xinbo, and Frederick L. Kiechle. 2004. “Review: Glycosphingolipids in Health and Disease.” *Annals of Clinical and Laboratory Science* 34 (1): 3–13.

Zhao, Jinmin, Keiko Furukawa, Satoshi Fukumoto, Masahiko Okada, Heiko Furugen, Hiroshi Miyazaki, Kogo Takamiya, et al. 1999. “Attenuation of Interleukin 2 Signal in the Spleen Cells of Complex Ganglioside-Lacking Mice.” *Journal of Biological Chemistry* 274 (20): 13744–47. doi:10.1074/jbc.274.20.13744.